Republic of Iraq
Ministry of Higher Education and Scientific Research
University of Kerbala-College of Science
Chemistry Department

Synthesis and Investigation of Hybrid Polyoxometalate (POM) -Dopamine Nano-Structures as Drug Delivery System

A Thesis

Submitted to the Council of the College of Science/ University of Kerbala

In a Partial Fulfillment of the Requirements for the Degree of Master of Science in Chemistry

By

Saja Mohammed Hussein Ali

B.Sc. Chemistry (2016) /University of Kerbala

Supervisor

Prof. Dr. Luma Majeed Ahmed

Dr. Muqdam Mahdi Mohammed Ali

2021AD ***1442AH***

"بِسْمِ اللهِ الرَّحْمَـٰنِ الرَّحِيمِ"

﴿ ً وَجَعَلْنَا اللَّيْلَ وَالنَّهَارَ آيَتَيْنِ فَمَحَوْنَا آيَةَ اللَّيْلِ وَجَعَلْنَا آيَةَ النَّهَارِ مُبْصِرَةً لِتَبْتَغُواْ فَضْلاً مِّن رَّبِّكُمْ وَلِتَعْلَمُواْ عَدَدَ السِّنِينَ وَالْحِسَابَ وَكُلَّ شَيْءٍ فَصَّلْنَاهُ تَفْصِيلا ً﴾

صَدَقَ اللهُ العَلِيُّ العَظيم

« سورة الإسراء » الآية 12

Supervisor Certification

I certify that this thesis " **Synthesis and Investigation of Hybrid Polyoxometalate (POM) -Dopamine Nano-Structures as Drug Delivery System"** was conducted under my supervision at the department of chemistry, College of science, University of Kerbala, as a partial fulfillment of the requirements for the degree of Master of Science in Chemistry**.**

Signature:

Name: **Dr. Luma Majeed Ahmed**
Title: Professor
Address: University of Kerbala, College of Science, Department of Chemistry.
Date: / / 2021

Signature:

Name: **Dr. Muqdam Mahdi Mohammed Ali**
Title: Instructor
Address: University of Kerbala, College of pharmacy
Date: / / 2021

Report of the Head of Chemistry Department

According to the recommendation presented by the Chairman of the Postgraduate Studies Committee, I forward this thesis **" Synthesis and Investigation of Hybrid Polyoxometalate (POM)-Dopamine Nano-Structures as Drug Delivery System "** for examination.

Signature:

Asst. Prof. Dr. Adnan Ibrahim Mohammed

Head of Chemistry Department

Address: University of Kerbala, College of Science, Department of Chemistry.

Date: / / 2021

Report of Linguistic Evaluator

"I certify that the linguistic evaluation of this thesis "**Synthesis and Investigation of Hybrid Polyoxometalate (POM) -Dopamine Nano-Structures as Drug Delivery System** " was assessed by myself and it is linguistically accepted.

Signature:
Name**: Dhiya Khaleel Nile**
Title: Instructor
Address: University of Kerbala, College of Education for the Humanities, Department of English
Date: / /2021

Report of Scientific Evaluator

I certify that the scientific evaluation of this thesis "**Synthesis and Investigation of Hybrid Polyoxometalate (POM) -Dopamine Nano-Structures as Drug Delivery System** " was assessed by myself and it is scientifically accepted.

Signature:

Name**: Abbas Jassim Attia**
Title: Professor
Address: University of Babylon, College of Science, Department of Chemistry

Date: / /2021

Signature:

Name**: Oraas Adnan Hatem**
Title:Assistant Professor
Address: University of Al-Qadisiyah, College of Science, Department of Chemistry

Date: / /2021

Examination Committee Certification

We, the examining committee, certify that we have read this thesis and examined the student (**Saja Mohammed Hussein Ali**) in its contents and that in our opinion; it is adequate as a thesis for the degree of Master of Science in chemistry.

Signatur :
Name: **Dr. Ayad Fadhil Mohammed Al-Kaim**
Title: Professor
Address: Babylon university- college of science , Department of Chemistry.

Date: / /2021
(**Chairman**)

Signature:
Name: **Dr. Lekaa Hussain Khdaim**
Title: Assistant Professor
Address: University of Kufa, College of Education for Girls, Department of Chemistry.
Date: / /2021
(**Member**)

Signature :
Name: **Ahmed Hadi Al-Yasari**
Title: Assistant Professor
Address: University of Kerbala, College of Science, Department of Chemistry.
Date: / /2021
(**Member**)

Signature:
Name: **Dr. Luma Majeed Ahmed**
Title: Professor
Address: University of Kerbala, College of Science, Department of Chemistry.
Date: / / 2021

Signature:
Name: **Dr. Muqdam Mahdi Mohammed Ali**
Title: Instructor
Address: University of Kerbala, College of pharmacy
Date: / / 2021

(**Member & Supervisor**)
Approved by the council of the College of Science

Signature:
Name: **Dr. Jasem Hanoon Hashim Al-Awadi**
Title: Assistant Professor
Address: **Dean of College of Science, University of Kerbala.**

Date: / /2021

Dedication

To the one who reached the message and led the trust, the Prophet of mercy,

Our master Muhammad…

To those who carry his name to those who planted me and witnessed the time of my giving to the dearest of my heart,

My father…

To the smile of life, to whom was my support and prayers, my companion to my warm life,

My beloved mother…

To those with their presence, I gain infinite strength and love,

My close friends are heart {Amani, Nidhal, shahada, Qamar, Mayasim, Yasa, and all the friends}

Finally, I thank my family and friends for their continual support throughout this journey. They were my source of encouragement along the way.

Saja Mohammed

Acknowledgments

I begin with immeasurable gratitude to Almighty Allah who has sustained me, gave me strength, guided and spared my life to the present level of my educational attainment, Thankful I ever remain.

This thesis would not have been possible without the guidance and the help of several individuals for whom I would like to extend my gratitude:

First and foremost, I pay my heartfelt tribute to my supervisor **Prof. Dr. Luma Majeed Ahmed** and **Dr. Muqdam Mahdi Mohammed** For their support and encouragement, as well as valuable advice and support for me to complete this work.

It is a matter of loyalty that I extend my thanks and appreciation to **Assistant Prof. Dr. Ahmed Hadi Al-Yasari**, **Prof. Dr. Ali Abdul-Kazem,** and **Dr. Samir Ramadhan**.

Also, I want to thank all faculty members of the Department of Chemistry in the College of Science at the University of Kerbala, for their worthless support of the work.

Saja M. Hussein

Abstract

This thesis consists of three practical parts. The **first part** is interested in the construction of 3D hierarchical nanostructures via a simple and versatile strategy of self-assembly of two components (Dopamine (DA) and Polyoxometalate (POM)) as an organic-inorganic hybrid. The morphology and size of the prepared 3D hierarchical nanostructures could be easily controlled by varying in the ratio of the two components, the pH of the initial Tris-HCl solution, aging, its duration, and their concentrations. SEM technique was used to diagnose the aforementioned nanostructure, and the shape was flower-like hierarchical nanostructures, also, through the (XRD) analysis, it was confirmed that the dimensions are within the nanoscale. The (FTIR) measuring demonstrated the association between dopamine and phosphotungstic acid (PTA).

The **second part** deals with the as-prepared hierarchical nanostructures used to load two drugs [Furosemide(Furo) and Capecitabine(Capi)], and the amount of drugs that loaded on the prepared nanostructure of PTA-DA was determined using UV/Vis spectroscopy. Different loaded times such as (4, 6, 8, 10, and 12h) of the furosemide were done on the nanostructure of PTA-DA surface. The loading percentages of these drugs were found to be (8%, 21%, 25%, 31%, 58%) for furosemide, and (3%, 10%, 31%, 39%, 64%) for Capecitabine, respectively.

Part three is concerned with the releasing process of the two drugs from hierarchical nanostructures in the presence of two buffer solutions, organized with different pH (7.4 of PBS, 2.8 for glycine-HCl). The release process was successful verified by using UV/Vis spectroscopy. The as-prepared flower-like Nanostructure of PTA-D loaded with furosemide showed promising pH-dependent release behavior, suggesting that a nanostructure of PTA-D is a good candidate for the oral delivery of furosemide. The release behavior of the as-prepared flower-like nanostructure of PTA-D loaded with furosemide at pH 7.4 showed a higher release profile than at pH 2.8. While the Nanostructure of PTA-DA loaded with Capecitabine shows a convergent shoot in both media.The nanostructures illustrated an intriguing pH-dependent release behavior, indicating that they could be useful in biomedical research.The releasing reaction for both drugs from prepared flower-like nanostructure surface obeys the pseudo-first-order kinetics in both buffer solutions.

Contents Table

List of Tables

List of Figures

List of Schemes

List of Abbreviations and Symbols

List of Abbreviations and Symbols	
Abbreviations and Symbols	**The Meaning**
Cape	**Capecitabine**
C_{DA}	**Concentration of Dopamine**
CDDS	**Controlled drug delivery system**
C_t	**releasing at time t**
C_T	**Total liberation in time ∞**
D	**Dynamic self-assembly**
d	**the interplanar spacing**
DA	**Dopamine**
DDS	**Drug delivery system**
DOPA	**3,4-dihydroxy-1-phenylalanine**
FT-IR	**Fourier Transformation Infrared**
Furo	**Furosemide**
FWHM	**Full width half – maximum**
ISA	**Ionic self-assembly**
k	**The Scherrer's constant**
k_1	**Rate constant for 1st order**
k_2	**Rate constant for the 2nd order**
L	**Crystallite Size, Mean Crystallite Size**

MOF	**Metal-organic framework**
Oc	**Corner oxygen's**
Oe	**Edge oxygen's**
Ot	**Terminal oxygen's**
PBS	**Phosphate buffered saline**
POM	**Polyoxometalate**
PTA	**Phosphotungstic acid**
S	**Static self-assembly**
SEM	**Scanning Electron Microscopy**
SEM-EDX	**Energy Dispersive X-Ray Spectroscopy**
t	**time of release**
TP	**Thymidine phosphorylase**
Tris	**tris(hydroxymethyl)aminomethane**
UV-Vis	**Ultra Violet light in the range from 315 to 380 nm**
W_{np}	**weight of the nanoparticles**
XRD	**X-Ray Diffraction**
β	**Full Half-Maximum Intensity Width in Degrees**
θ	**Bragg Angle**
λ	**Wavelength**

Chapter One
Introduction

1.1 General Introduction

The development of controlled release dosage forms has resulted in medical significance advancements in the field of drug delivery over the last few decades. There are two types of release patterns: those that release drug at a slow zero or first-order ratio and those that include an initial rapid dose followed by slow zero or first-order sustained component release [1]. The purpose of controlled release systems is to keep drug concentrations in the blood or target tissues as consistent as possible for as long as possible [2]. This can be accomplished by employing nanotechnology as a tool for creating new nanostructures with diverse and improved properties. Nanostructures are getting more attention in recent years because of their unique properties and a wide range of potential applications, Electronic, magnetic, opto-electronic, and catalytic materials, as well as biomedical materials [3,4]. By manipulating the properties of materials such as polymers and fabricating nanostructures, nanotechnology can provide superior drug delivery systems for better disease control and treatment. Nanostructures used as drug delivery systems have several advantages that make them superior to traditional delivery systems. The advantages of nanostructures in drug delivery have been outlined. These benefits are the result of extensive research into the production of nanostructures for drug delivery, such as liposomes, nanocapsules, nanoemulsions, solid lipid nanoparticles, dendrimers, and polymeric nanoparticles. The materials used in the fabrication of nanostructures determine the type of nanostructures obtained, and these nanostructures, in turn, determine the various properties obtained and the release characteristics of incorporated drugs [5]. Self-assembly is gaining traction as a viable bottom-up method for creating new usable nanomaterials by linking various components as advanced nanotechnology [6, 7].

Indeed, the Ionic self-assembly (ISA), or electrostatic interactions between cations and anions, is ubiquitous and plays a key role in the formation of unique nanostructures. [8,9]. Hybrid nanomaterials have been widely researched and used in drug and gene delivery due to their well-controlled shapes, well-defined sizes, and promising properties, electro-optical materials, nano-reactors, and catalysis science. [10,11]. Because of their numerous electronic, magnetic, photochemical, biomedical, and catalytic properties, they have attracted attention as suitable inorganic building blocks and are frequently used in the design of hybrid materials [12,13], controlled drug release systems have several advantages over

compared to commercial or traditional systems such as a developed efficiency drug, reduced toxicity, improved patient suitability, the primary goal of drug release management is to give the best treatment efficacy [14].

1.2 Drug Delivery Systems

A drug delivery system (DDS) is defined as a formulation or device that allows a therapeutic substance to be introduced into the body and improves its effectiveness and safety by controlling the rate, time, and location of drug release in the body [15]. This process involves the management of the therapeutic product, the release of the active components by the product, and the consequent transport of the active ingredients through the biological membranes to the site of action [15]. The drug delivery tools of modern times are just 60 years old [16]. All of the drugs were turned into pill or capsule forms before 1950, which instantly released the loaded drug upon connection with water without any the ability to control the kinetics of drug release [17]. During this period, many drug delivery systems have been developed, according to the below [18-20]:

i. The first-generation (1950–1980), was very successful in evolving many oral and transdermal controlled release formulations for clinical applications.

ii. The second-generation (1980–2010), has not been as successful in producing clinical yields. This is due in large part to the problems nature to overcome. The first-generation drug delivery technologies deal with physicochemical problems, while the second-generation struggled with biological barriers. Controllable physicochemical properties can be used to create controlled drug delivery systems, but it is not possible to overcome the biological barriers.

iii. The third-generation drug delivery systems (after 2010), need to overcome both physicochemical and biological delivery systems. Indeed, Drugs with low water solubility cause physicochemical issues, large peptide and protein drugs molecular weight, and difficulty in regulating the kinetics of drug release. The biological barriers to be solved include the distribution by the body of drug delivery systems rather than the formulation properties, limiting delivery to a specific body target. Besides, in vivo, the response of the body to formulations

restricts their roles. The prosperous future of drug delivery systems depends on whether new delivery systems can resolve the limits imposed by human physiology, and new ways of thinking can accelerate the development process. The history of drug delivery technology from 1950 to the present is listed in Table (1.1).

(Table 1.1). History of technology for drug delivery from (1950) to today's technology and the technology that will be required in the future [21].

The First Generation (1950)	The Second Generation (1980)	The third generation (2010-2040)
Controlled Release Fundamentals	Smart Delivery Systems	Modulated Delivery Systems
Oral delivery Twice-a-day, once-a-day	Zero-order release First-order vs zero-order	Poorly soluble drug delivery Non-toxic excipients
Transdermal delivery Once-a-day, once-a-week	Peptide and protein delivery Long-term storage facility polymers that are biodegradable Pulmonary delivery	Peptide and protein delivery Delivery for >6 months Control of release kinetics Non-invasive delivery
Drug release mechanisms Dissolution Diffusion Osmosis Ion-exchange	Smart polymers and hydrogels Environment-sensitive Self-regulated release (working only in vitro)	Smart polymers and hydrogels Signal specificity and sensitivity Fast response kinetics (working in vivo)
	Nanoparticles Tumor-targeted delivery Gene delivery	Targeted drug delivery Non-toxic to non-target cells Overcoming blood-brain Barrier
Controlling the physicochemical properties of delivery systems successfully	To overcome biological barriers, nobility is required.	Both physicochemical and biological barriers must be overcome.

Generally, there are two types of drug delivery systems:

i. Delayed released: It uses one to more repeated doses for immediate release [22].
ii. Sustained released: It includes any regimen that accomplishes a gradual release of a drug over long periods [23].

iii. Site-directed or receptor systems: It delivers the active component administered directly to the target region in the vital system [24, 25].

1.3 Devices for delivering drugs

Placing the drug in a delivery device and inserting the system into body tissue is one of the most obvious ways to provide sustained-release medication. Table 1 shows the classification of drug delivery devices (1.2). The idea of drug delivery devices is ancient, New technologies on the other hand, are being implemented. Implantation may necessitate the use of surgical techniques and specialized injection devices. These implants must be made of biocompatible materials [26, 27].

(Table 1.2). Drug delivery device classification [28].

Devices for delivering drugs
❖ Surgically implanted devices for lengthy sustained drug release Drug reservoirs.
❖ Devices for controlled/intermittent drug delivery that are surgically implanted.
❖ Pumps and channels.
❖ Implants for controlled release of drugs (non-biodegradable).
❖ Implantable biosensor-drug delivery system.
❖ Microfluidics device for drug delivery.
❖ Controlled-release microchip.
❖ Implants that could benefit from local drug release.
❖ Stents for coronary, carotid, and peripheral arteries.
❖ Ocular transplants.
❖ Dental transplants.
❖ Orthopedic implants.

1.4 Modified drug delivery systems

The anticancer drugs now used in chemotherapy exhibit cytotoxicity that is nonspecific, affecting normal cells. Due to the unpredictable cytotoxic properties, treatment has been shown to cause several side effects in cancer patients [29]. For this reason, various experiments have been carried out to establish specific drug delivery systems capable of restricting the drug's toxicity to specifically target its effects directly on the tumor as much as possible. The use of these drug delivery systems is continuously being tested and improved to enhance the effectiveness, selectivity, and overall impact of the anti-neoplastic drugs [30,31]. Current drug delivery systems that explain a great promise include drugs that are entrapped in polymeric drug carriers such as liposomes, hydrogels, nanoparticles [32], surfactant, colloidal cellular, and viral drug delivery systems [33].

1.5 Drug loading techniques

Ideally, a successful nano particulate system should have a high drug-loading capacity reducing the number of matrix materials that must be administered. There are two methods for loading drugs:

1. Incorporating at the time of nanoparticle production (incorporation method).

2. Absorbing the drug after the formation of nanoparticles by incubating the carrier with a concentrated drug solution (adsorption/absorption technique).

Drug loading and entrapment efficiency depend on the solid-state drug solubility in the matrix material or polymer (solid dissolution or dispersion) [34][35]. High drug-loading nanomedicines can be classified into four categories based on their fabrication strategies [36]:

- **i.** Nanomedicines based on inert carriers, such as inorganic porous carriers and absorption/desorption-type metal-organic framework (MOF)-based nanomedicines.
- **ii.** Nanomedicines containing drugs in the carrier, such as linear and branched PDCs.
- **iii.** Carrier-free nanomedicines, counting drug nanocrystals (DNCs).
- **iv.** Specialized and complex strategies for nanomedicines, such as aqueous noncovalent assembly and multiple drug assembly.

1.6 Controlled drug delivery system (CDDS)

Controlled release dosage forms cover a wide range of prolonged action formulations that provide continuous release of their active ingredients at a predetermined rate and for a predetermined time. The majority of these formulations are designed for oral administration; however recently such devices have also been introduced for parenteral administration, ocular insertion, and transdermal application. The most important objective for the development of this system is to furnish an extended duration of action and thus assure greater patient compliance [37].

A controlled drug delivery system has various advantages over conventional drug delivery as discussed below [38,39]:

i. Decreased occurrence and intensity of adverse effects and toxicity.
ii. Better drug utilization and reduced dosing frequency.
iii. Controlled rate and site of release.
iv. More uniform drug concentration in the systemic circulation.
v. Improved patient compliance.
vi. More reliable and prolonged therapeutic effect.
vii. A greater selectivity of pharmacological action.

So, the drug is only active in the targeted area in which the drug should be released. In comparison to conventional DDSs, targeted DDSs have some characteristics that physicians find appealing. They have poor solubility and stability, in addition to having a shorter half-life than drugs in traditional routes, and absorption. Moreover, when compared to targeted DDSs, drugs in conventional DDSs have low specificity and therapeutic index [40,41]. Controlled drug to achieve more effective treatment by the constant concentration of the drug in the blood plasma and eliminating the possibility of both ineffective dose (Under dose) and Overdose [42,43] and Figure (1.1) It shows the concentration of the drug in the blood plasma By using conventional and controlled drug release systems.

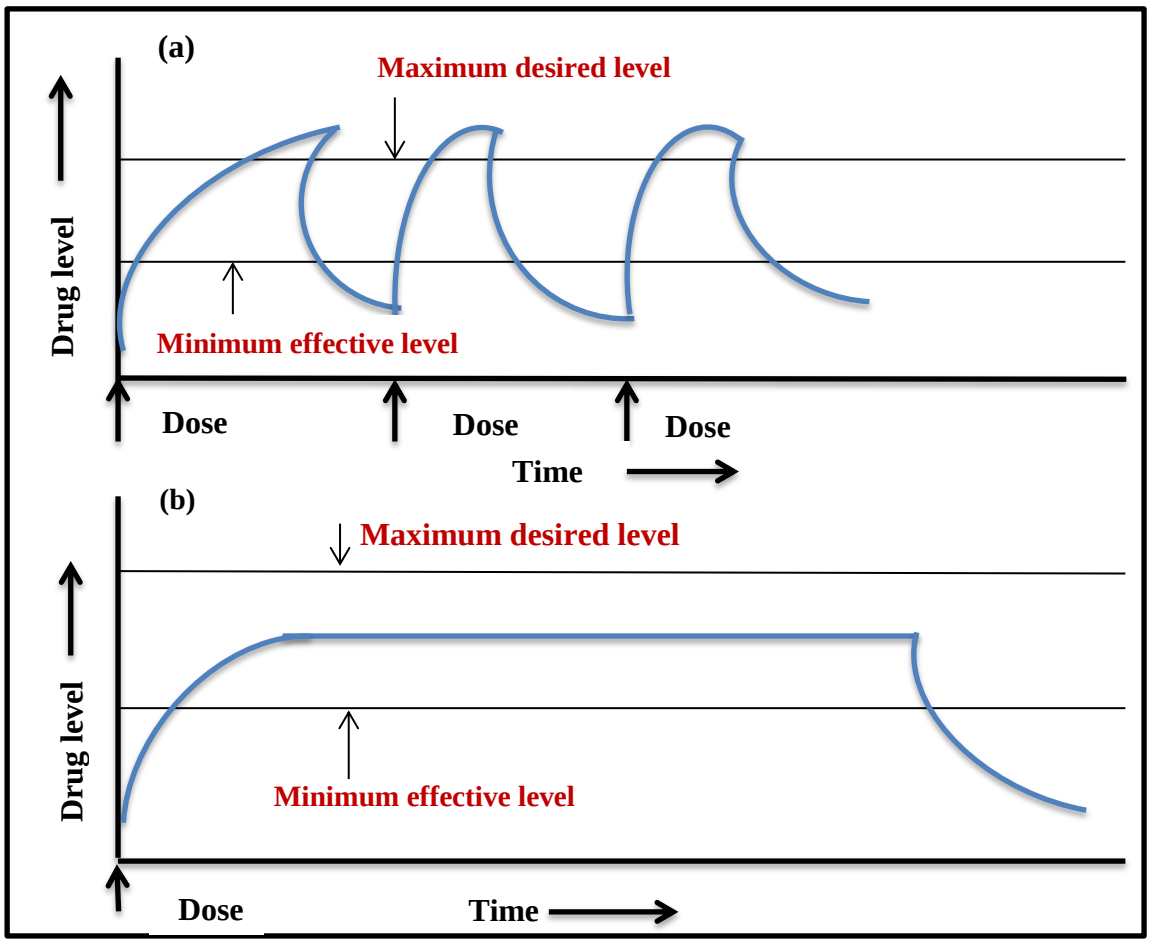

Figure (1.1). Drug level in blood with (a) Traditional drug dosing, (b) Controlled delivery dosing[44,45].

1.7 Applications in drug delivery

Because of their limitless potential to improve human health, drug delivery, and tissue engineering research has seen tremendous progress in recent years. Meanwhile, advances in nanotechnology enable systematic characterization, manipulation, and organization of matter at the nanometer scale. Controlled release reservoirs for drug delivery and artificial matrices for tissue engineering have both been used with biomaterials with the nano-scale organization. The composition, shape, size, and morphology of drug-delivery systems can all be controlled [46,47]. To increase solubility, immunocompatibility, and cellular uptake, their surface properties can be tweaked. Current drug delivery systems have flaws such as low bioavailability, ineffective targeting, and the potential for cytotoxicity.

Nanoparticles, nanocapsules, nanotubes, nanogels, and dendrimers are all promising and versatile nano-scale drug delivery systems [48].

Designing biomaterials with controlled organizations at the nanometer scale can dramatically improve the biological functions of encapsulated drugs and cells. The most recent advancement in the use of nanostructured materials for drug delivery and tissue engineering applications [49].

1.7.1 Nanotechnology

Nanotechnology is the science and technology concerned with the precise adaptation of a material's composition at the molecular level, i.e., the material's subduction to a very small scale that has one or more dimensions in nanoscale, which causes a change in the size of the substances (atoms and molecules), leading them to have different distinctive properties compared with the bulk substances (materials with a micrometric scale or greater), resulting in new uses and applications for these materials [50,51]. The term nano refers to the (Greek) word, which means "dwarf" and generally refers to the materials whose dimensions range from (1-100) nm [52].

1.7.2 Classical approaches for the synthesis of nanoparticles

Nanoparticles can be made in a variety of ways :

1. **Top-down approach:** In this approach, the bulk materials with micro size can be transferred to the nanostructure using mostly a physical method. Because, the top-down approaches will reveal imperfections in the product's surface structure, which is a major limitation [53].

2. **Bottom-up approach:** Nanoparticles are made up of smaller atoms or in less nanoscale, which is first formulated and then assembled to build a block of a particle in nanosize [53, 54].

(Figure 1.2) explains the various methods for making metal nanoparticles. Nanoparticles are made by reducing the size of a suitable starting material (precursor). Various physical and chemical treatments can be used to achieve this size reduction.

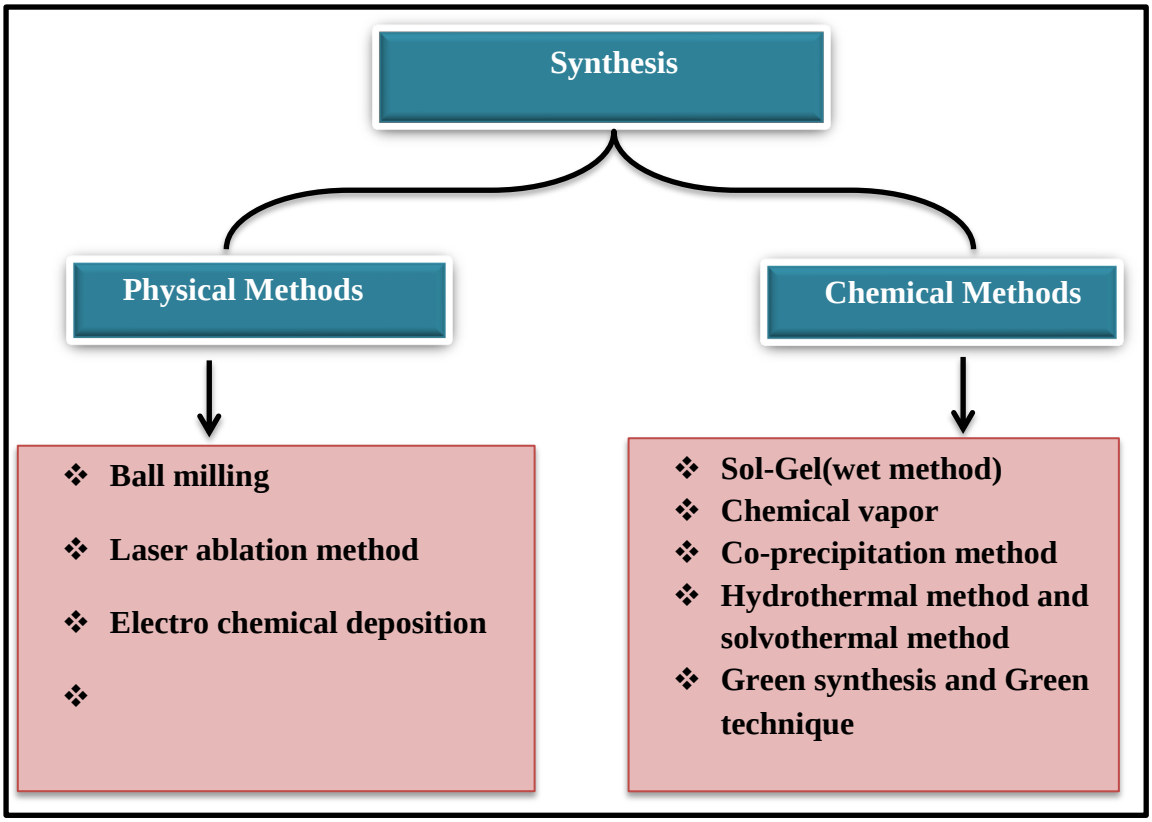

Figure (1.2). Some methods for the synthesis of nanoparticles[55].

1.7.3 Nanopharmacology

Nanopharmacology can be known as the application of nanotechnology in the development and/or discovery of methods to deliver drugs and medical materials and reduce their sizes to the nanoscale level, which leads to improving the pharmaceutical properties of these materials, especially in treating diseases [56]. The benefits of nanotechnology in the pharmaceutical field are shown in Figure (1.3).

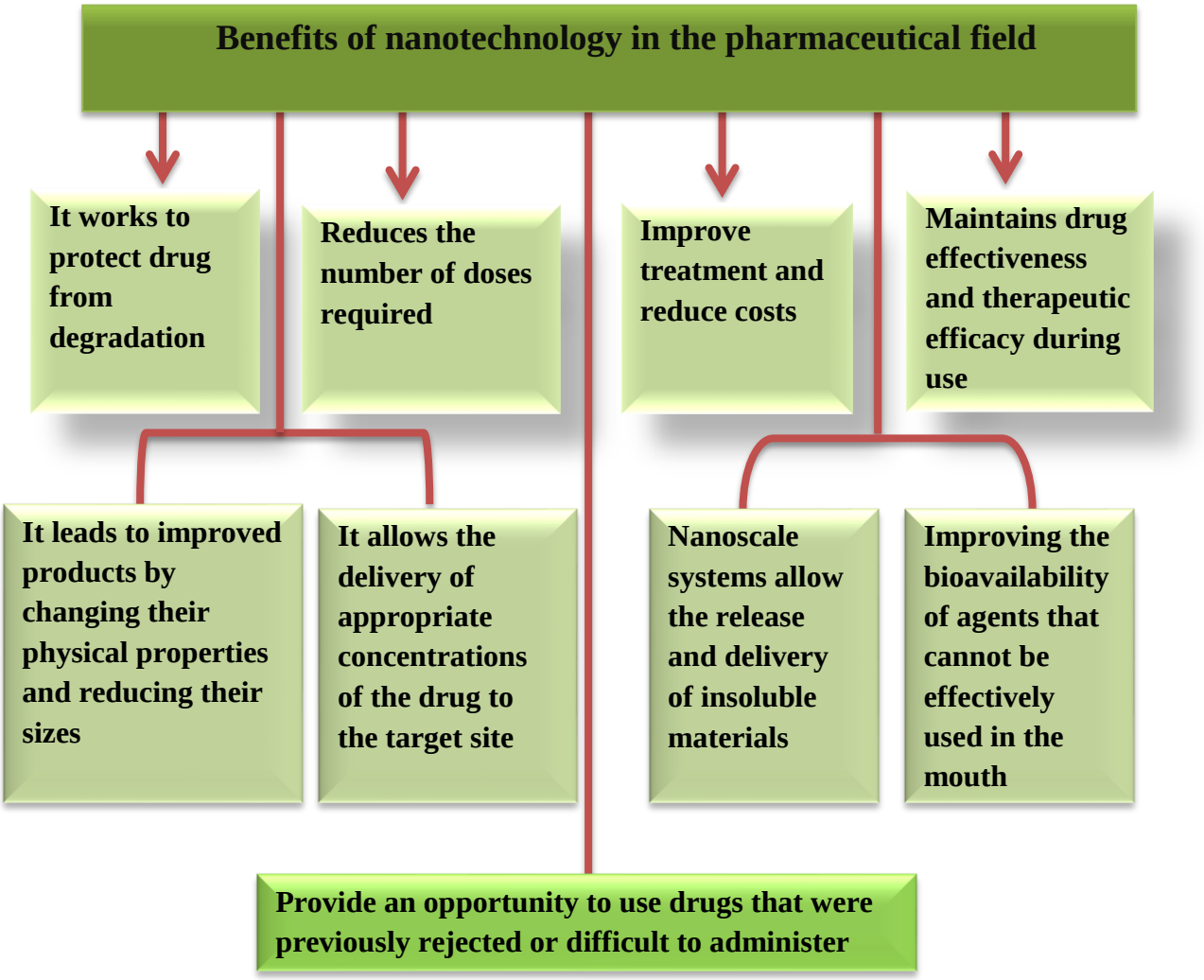

Figure (1.3). Schematic diagram of benefits of nanotechnology in the pharmaceutical field.

1.7.4 Nanocarriers

Nanotechnology has recently are getting more attention because of its ability to diagnose and treat efficiently to variety of tumors. Nanocarriers have been used to avoid the drawbacks of traditional antitumor drug delivery systems, such as non specificity, intense side effects, blast release, and damage to cells that are normal [57]. Antitumor drugs' bioavailability and therapeutic efficacy are improved by nanocarriers, which provide preferential cumulatio at the target site. Although several nanocarriers have

been developed, Just a handful have received clinical approval for delivering antitumor drugs to their target sites [58].

Among the most important nanocarriers that have been tested in drug release systems are: Liposomes, solid lipid nanoparticles, dendrimers, carbon, silicon, polymers, and magnetic nanoparticles are all examples of nanoparticles [58], the figure (1.4) demonstrates the diameters of these materials [59].

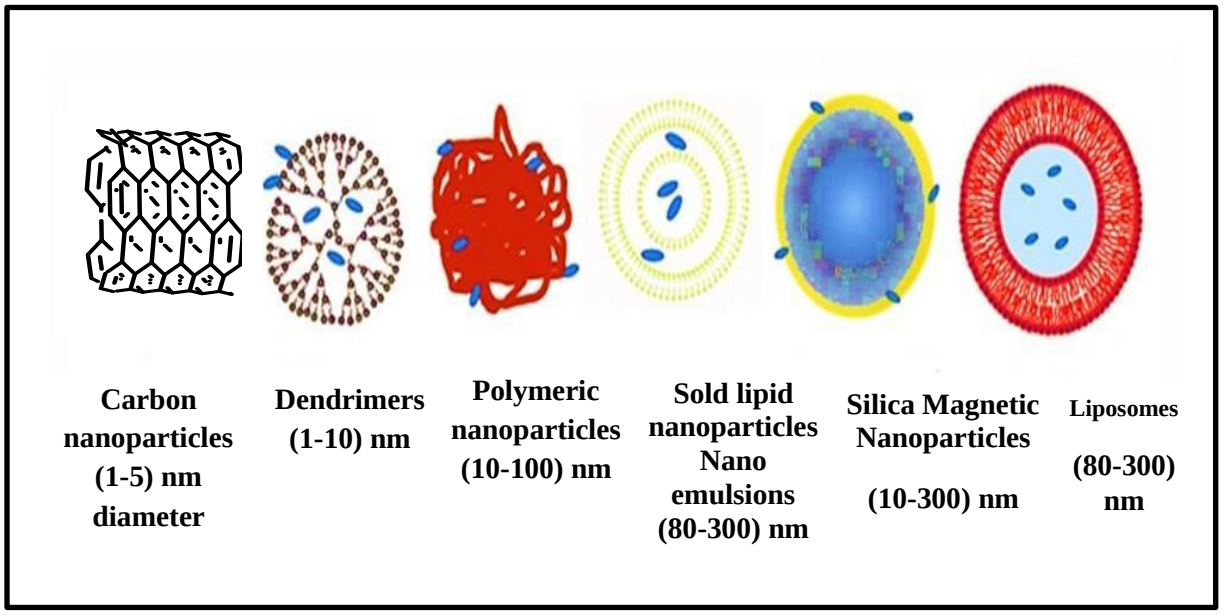

Figure (1.4). Nano systems to drug delivery systems[60].

1.7.5 Drug delivery strategies

For targeted therapy, the route taken to conjugate the drug to the nanocarrier, as well as the technique used to target it, are critical. A medication can either be adsorbed or covalently bound to the surface of the nanocarrier, or it can be encapsulated inside it. Covalent linkage has an advantage over other methods of attachment in that it allows the number of drug molecules bound to the nanocarrier to be regulated , i.e., precise control of the amount of therapeutic compound delivered[61,62]. Active or passive mechanisms may be used to target individual cells with nanocarriers.

The first strategy is based on attracting drug, in which nanocarriers conjugate to the affected site using recognition ligands on the surface of

conjugate antibodies, low molecular ligands like folic acids, peptides, and so on. Physical stimuli (such as temperature, pH, and magnetism) can also be manipulated to achieve the active strategy [63].

The advantages of nanocarriers can be summarized with the following[64]:

- **i.** Nanoparticulate material uptake is simple and can be mediated by a variety of cellular or paracellular processes.
- **ii.** Targeted drug delivery can be accomplished by attaching targeting ligands to particle surfaces or by using magnetic guidance.
- **iii.** Increase the solubility of poorly water-soluble drugs.
- **iv.** Increases the amount of soluble drug at the absorption site to increase the rate of absorption.
- **v.** Reduce immunogenicity to extend the half-life of drugs in the systemic circulation.
- **vi.** Release drugs at a steady rate, reducing the number of times they must be administered.
- **vii.** Target drug delivery to reduce systemic side effects.
- **viii.** Deliver two or more drugs at the same time for combination therapy.
- **ix.** Synergistic effects.

1.8 Nanoparticle Based Approaches for Solubility Enhance - ment

Nanoparticles of poorly water-soluble molecules can be made in a variety of ways [65]. For poorly soluble drugs, there are two main methods for producing drug nanoparticles:

- **i.** The first method is the disintegration method, which involves the reducing size of particles (top-down processes). Attrition is used in top-down processes, while molecular deposition is used in bottom-up processes. High-pressure homogenization is an example of a top-down process [66, 67]. Or high-energy wet-milling in a primarily water-based fluid phase [68, 69], resulting in drug particles in the nanometer range.

ii. The second method is particle nucleation from the molecular state (bottom-up processes) [70, 71]. The Hydrosol method is an example of a bottom-up process [72,73] or sprays freezing into liquid, or supercritical fluid technology, which includes rapid expansion from a liquefied gas solution, gas antisolvent recrystallization, or controlled crystallization during freeze-drying, or drug molecule self-assembly or precipitation. Nanoparticles with a size range of (10–50) nm have shown many advantages as a delivery vehicle when compared to traditional drug delivery methods [74].

1.9 Some medicines used in delivery systems and their importance

Biotechnology advancements are resulting in better medications that can more effectively and precisely target diseases. Drugs are being reformulated by researchers so that they can be used safely in specific conditions. The use of broad-spectrum antibiotics raises the cautionary question that the more selective a drug is, the lower its risk of triggering drug resistance [75].

1.9.1 Capecitabine

Capecitabine(Cape) is an anti-cancer chemotherapy drug marked under the brand name (Xeloda) (also known as "antineoplastic" or "cytotoxic"). Capecitabine is classified as antimetabolite by the world health organization [76]. Its having a formula ($C_{15}H_{22}FN_3O_6$) and IUPAC name (N-[1-(5-deoxy-f~-D-ribofuranosyl)-5-fluoro-1,2-dihydro-2-oxo-4-pyridinyl]-n-pentyl carbamate) is a crystalline substance with a molecular weight of 359.35 (Figure 1.5)[77]. It's also having a highly soluble in water and lasts at least 9 months in tablet form [78].

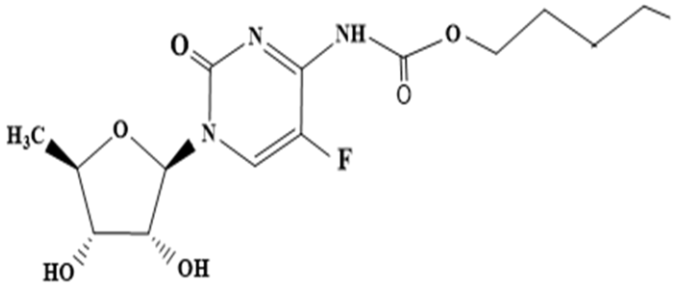

Figure (1.5). Chemical structures of the prodrug capecitabine.

1.9.2 Mechanism of Action to capecitabine

Capecitabine is an oral fluoropyrimidine that is activated by elevated intratumoral thymidine phosphorylase concentrations (TP) in tumor tissue. It was specifically created for reducing fluorouracil exposure in normal tissues while increasing fluorouracil concentrations in tumor cells [79]. Capecitabine is converted to fluorouracil through a three-step enzymatic cascade (Figure 1.6).

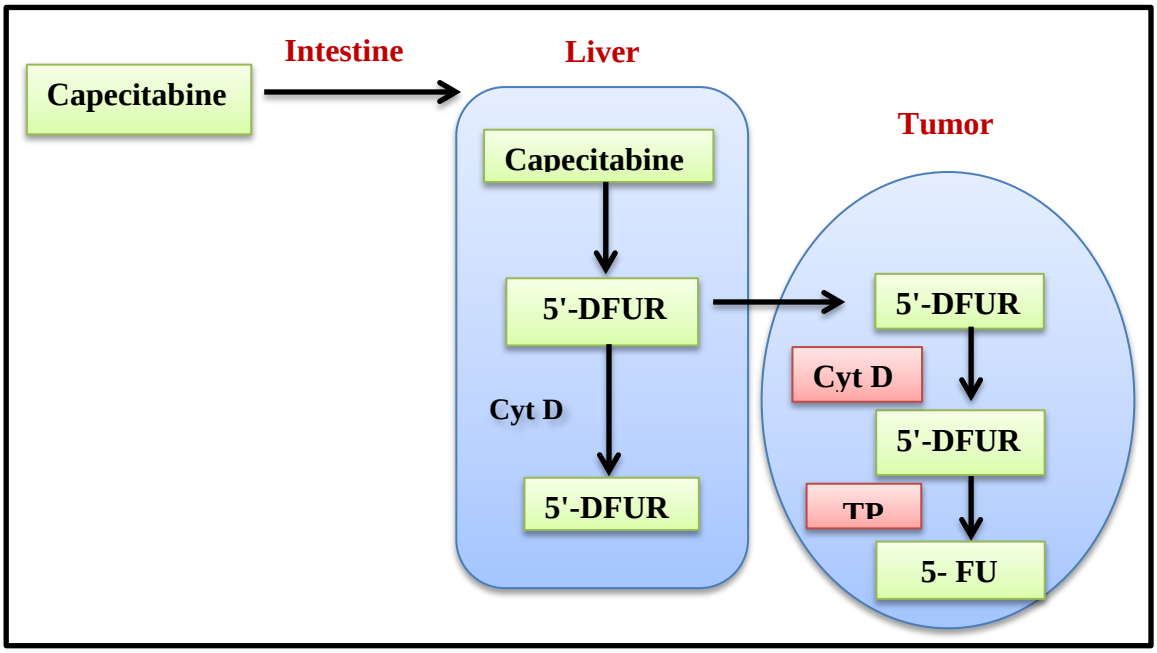

Figure (1.6). Mechanism of Action to capecitabine through a three-step enzymatic cascade[81].

Capecitabine is first absorbed as an intact molecule through the gastrointestinal mucosa. In the liver, it is metabolized to 5′-deoxyfluorocytidine (5′-dFCR) by carboxylesterase, which can then be converted to 5′-deoxyfluorouridine (5′-dFUR) in the presence of hepatic or tumor cytidine, which is present in higher concentrations in tumor tissue than in healthy tissue, resulting in fluorouracil release into the tumor [77,80]. It has two potential pharmaceutical benefits: increased tumor activation and decreased drug accumulation in healthy tissues, and lowering systemic toxicity [82].

1.9.3 Furosemide

Furosemide(Furo), sold under the brand name (Lasix), is a diuretic that is derived from anthranilic acid. The active ingredient in LASIX tablets for oral administration is furosemide, and the inactive ingredients are lactose monohydrate NF, magnesium stearate NF, starch NF, talc USP, and colloidal silicon dioxide NF [83]. LASIX is available in dosage strengths of 20, 40, and 80 mg as white tablets for oral administration. Furosemide is a crystalline powder that is white to off-white and has no odor. It is practically water-insoluble, sparingly soluble in alcohol, freely soluble in dilute alkali solutions, and insoluble in dilute acids[83,84]. Furosemide (4-chloro-N-furfuryl-5-sulfamoylanthranilic acid) is having a molecular formula($C_{12}H_{11}CI\ N_2O_5S$), Molecular weight (330.75 g/mol), and structure, as shown in figure 1.7 [85,86].

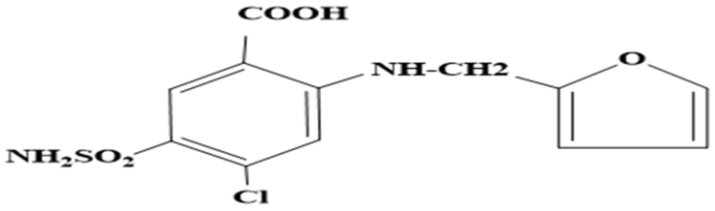

Figure (1.7). Chemical structures of the Furosemide.

Edema is excess fluid in the body, which is caused by heart failure, liver disease, and kidney disease, it is treated by Furosemide that used as a diuretic. Shortness of breath and swelling in your arms, legs, and abdomen may be reduced as a result of this. This medication is also employed to treat hypertension. Strokes, heart attacks, and kidney problems can all be prevented by lowering blood pressure [87].

1.9.4 Mechanism action of furosemide

In the thick ascending limb of the loop of Henle in the renal tubule, the sodium-potassium-2 chloride (Na+-K+-2 Cl-) co-transporter (symporter) is inhibited . 'Jackson' is a (1996) [88].

Furosemide is given orally or intravenously. It has a quick onset of action (less than an hour), and its effects can last up to eight hours. Up to 80% of a given dose of furosemide is excreted in the urine unchanged. It's employed to treat edematous conditions like congestive heart failure and liver cirrhosis, as well as hypertension, as a monotherapy or in combination with other antihypertensive drugs [89].

Furosemide's side effects are caused by:

The elevated excretion of electrolytes is often linked to the negative effects of furosemide. Hypokalemia is serious toxicity that can, for example, enhance digitalis' cardiac effects. Long-term employ of furosemide can cause ototoxicity, hyperglycemia, and elevated LDL cholesterol and triglyceride levels in the blood [90, 91].

1.10 Polyoxometalate (POM)

Polyoxometalate is a common type of discrete inorganic clusters with biomedical properties such as antiviral, anti-tumor, anti-bacterial, and anti-HIV activities [92]. It is a large group of anionic polynuclear metal-oxo nanoclusters, which are recognized as addenda atoms with general formula $[M_xO_y]n$. Generally, this formula consists of two or more high oxidation states (either a d^0 or d^1 electronic configuration) transition metals (M) such as preferably tungsten (W) or molybdenum (Mo), and less frequently niobium (Nb), tantalum (Ta) and vanadium (V), or mixture from these mention metals, bonding together through oxo-ligands (O) in coordination (y) ranged from 4 to 7[93-95]. The coordination number of addenda ions in monomeric MO_4 fragments can be elevated from four to be six in polyanions when acidified, and the terminal O_2 ligands can form pπ–dπ interactions with the metals as double bonds [94]. In 1826, Poly-oxometalates discovered the first POM species by Berzelius [96].

Poly-oxometalates are classified into three families based on their structure and composition. The first class includes the heteropolyanionic compounds, which are made up of a metal-oxide matrix with one or more p-, d- or f-block hetero atoms. They are made up of heteroanions like PO_4^{3-}, SO_4^{2-}, and SiO_4^{2-}etc. that are incorporated with vanadium-,

tungsten-, or molybdenum-based metal oxide framework. This category is widely used as a mono-, di-, and trilacunary clusters that attitude to the intrinsic stability of the resulting stable building block libraries, which is a construction of a larger aggregate by the incorporation of heteroecious [97].

1.10.1 Covalent interactions in POM-based materials

POM clusters are composed of metal ions (M = W, Mo, V,Nb, etc.) and oxo ligands. Organic moieties can be grafted via addenda organometallic compounds on lacunary POM clusters[98] For example, the reaction of Keggin- and Dawson-based lacunary clusters with organotin, organosilicon and organogermanium compounds leads to the formation of stable covalent bonds between the POMs and organic moieties.15,16 Anderson clusters and Dawson clusters of formula $[P2W15V3O62]^{-9}$ can be modified with trisalkoxo ligands by substituting the oxo ligands with alkoxo moieties[99] .Taking H2N-Anderson-R clusters as an example: by tethering a highly delocalized aromatic pyrene moiety covalently to the Mn-Anderson cluster through a Tris [Tris = tris(hydroxymethyl) aminomethane] linker.

cluster nanostructuer successfully prepared a covalently modified Anderson-based framework by grafting pyrene moieties onto the Anderson cluster. The resulting material:

(1) shows physical properties that are fundamentally different from those of the parent POM cluster.

(2) has a nanoporous framework with nanoscale solvent-accessible one-dimensional butterfly-shaped channels, which selectively absorb chlorobenzene.

(3) is stable up to 240 °C, despite being constructed with very weak hydrogenbonding interactions.

1.11 Self-assembly Method

The self-assembly of amphiphilic compounds distributed in water will generate core-shell nanoparticles structures . Due to the presence of a hydrophobic core and a hydrophilic shell, amphiphilic NPs can be employed as a carrier for both hydrophobic and hydrophilic drugs at the same time. Using a hydrophilic shell has the benefit of reducing macrophage

phagocytosis. As a consequence, amphiphilic NPs have are getting more attention [100].

Generally, Self-assembly is gaining traction as a viable bottom-up method for creating new functional nanomaterials by integrating different components as advanced nanotechnology [101]. Ionic self-assembly (ISA), or the self-assembly of cations and anions by electrostatic interactions, is ubiquitous and plays a vital role in the creation of special nanostructures . Due to their well-controlled shapes, well-defined sizes, and promising properties, hybrid nanomaterials have been widely explored and used in electro-optical materials, drug or gene delivery, nanoreactors, and catalysis science [102]. Bio-inspired materials at the micro- and nanoscale have been proposed as a breakthrough in the design of advanced functional materials, and have sparked a lot of interest among various self-assembled hybrid nanomaterials in recent years. Self-assembly can be divided into two types [103]:

1.11.1 Static self-assembly (S):

Figure (1.8) demonstrates this type, which is in a state of global or local equilibrium and does not dissipate energy For example, molecular crystals [104] and most folded, globular proteins are produced by static self-assembly. The formation of the ordered structure in static self-assembly may require energy (for example, stirring), but once formed, it is stable. The majority of self-assembly research has been focused on this static type.

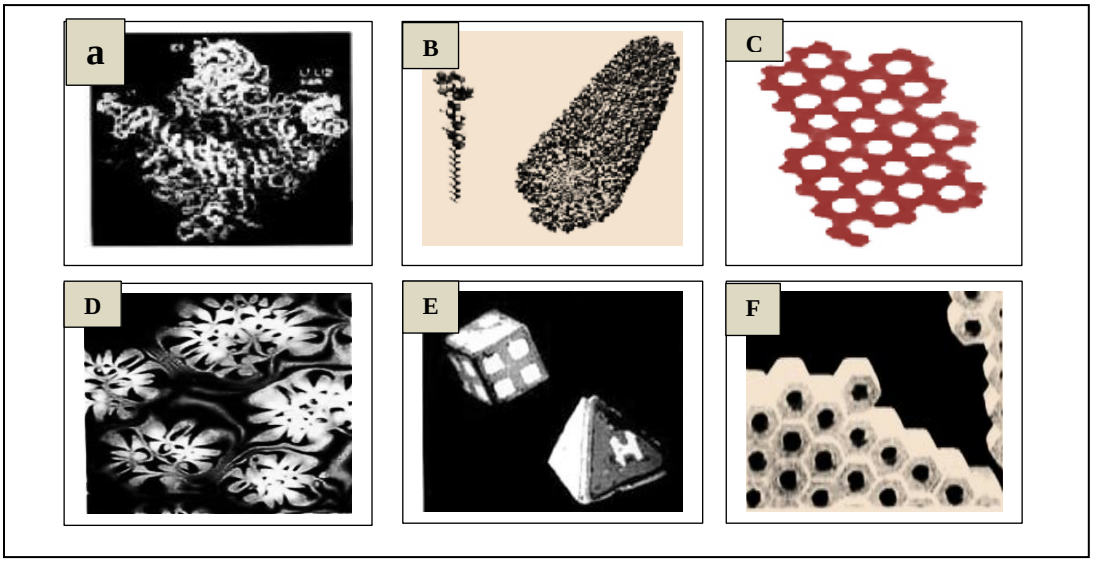

Figure (1.8). Examples of static self-assembly. (A) ribosome's crystal structure. (B) Peptideamphiphile nanobers . (C) Capillary interactions assemble an array of millimeter-

sized polymeric plates at a water/perßuorodecalin interface. (D) Nematic liquid crystal thin lm on isotropic substrate. (E) Planar substrates are folded into micrometer-sized metallic polyhedra. (F) Capillary forces assemble a three-dimensional aggregate of micrometer plates. . Image credits: (A) from [104]; (B) from [105]; (C) from [106]; (D) from [107]; (E) from [108]; (F) from [109].

1.11.2 In dynamic self-assembly (D):

This type of self-assembly sample displayed in Figure 1.9, and only when the system is dissipating energy do the interactions that lead to the formation of structures or patterns between components. Simple examples include patterns formed by reaction and diffusion competition in oscillating chemical reactions [110]; biological cells are much more complex.

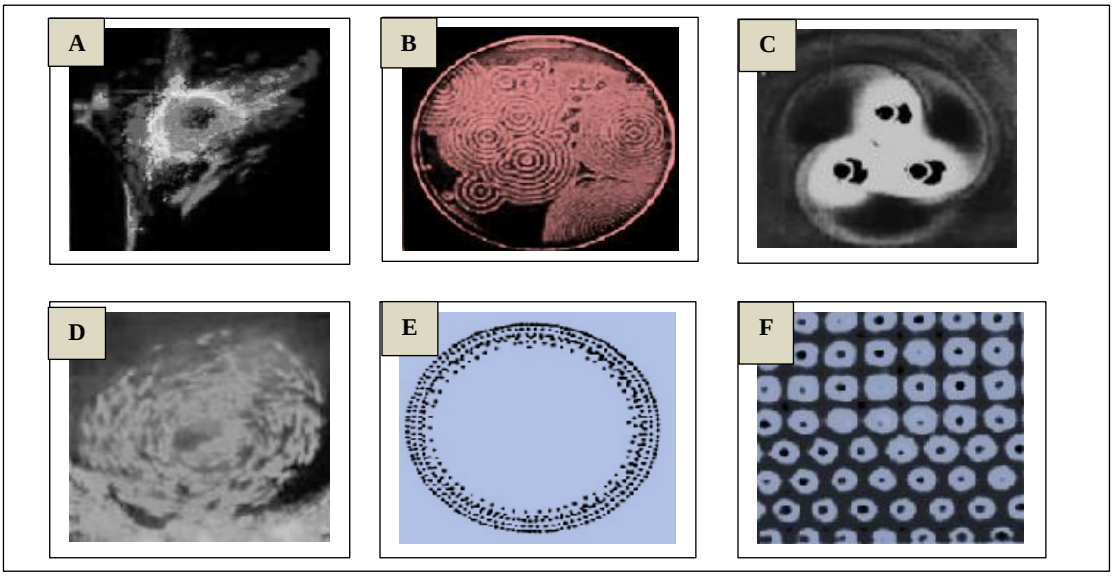

Figure (1.9). Examples of dynamic self-assembly. (A) Microtubules (24 nm in diameter) are colored red . (B) In a 3.5-inch Petri dish, reaction-diffusion waves in a Belousov-Zabatinski reaction. (C) A simple assemblage of three rotating, magnetized disks interacting with one another via vortex-vortex interactions. (D) A school of (Þsh). (E) Charged metallic beads 1 mm in diameter rolling in circular paths on dielectric support from concentric rings. (F) Above a micropatterned metallic support, convection cells formed. The cells' centers are separated by 2 millimeters. Image credits: (A) from [111]; (B) from [105]; (C) from [112].

Through a simple ISA strategy, a Weakley-type POM (a europium ion sandwiched between two Lindquist-type POMs) EuW10 was used as a polyoxoanion to assemble with the cationic DA into a well-ordered nanoflowers structure. The assembled morphologies, fluorescence quenching

mechanisms, and catalytic performance were estimated in detail, and the sizes and morphologies of the 3D nanostructures were based on the concentration and ratio of the anionic and cationic components. The method in scheme 1described here could provide a new route to fabricating multifunctional 3D hierarchical nanostructures [113]. POM clusters are generally proton acceptors for hydrogen bonds; a $[P2W15V3O62]^{-9}$, POM cluster, grafted with a proton donor moiety of an –NH2 group, shows intercluster interactions via N–H_ _ _O hydrogen bonds. this strategy exploited and applied to the construction of self-assembled nanostructures.

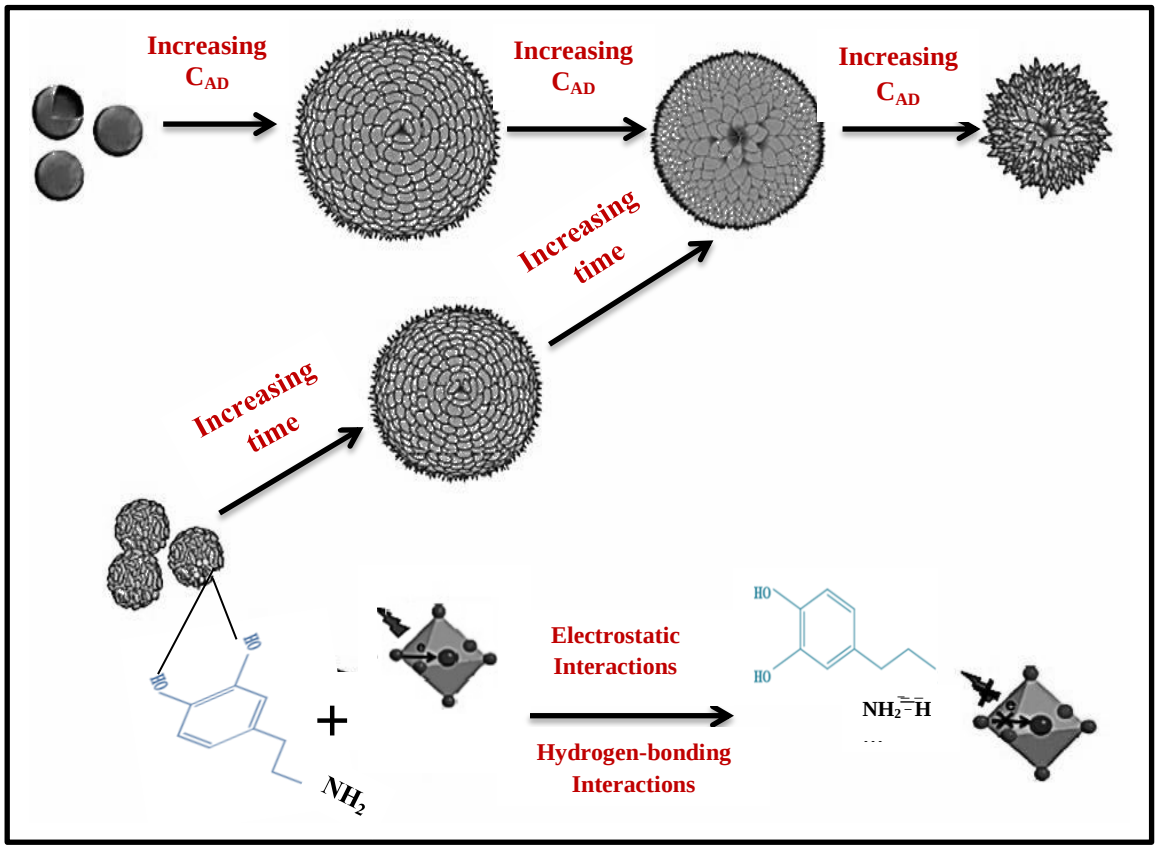

Scheme 1. The schematic illustration of the assembly process[114].

1.12 Dopamine (DA)

Dopamine (DA) is a neurotransmitter that is present in a mammal's central nervous system [108] and has been widely employed in fields such as surface modification, biomedicine, and Li-ion battery technology [115]. The chemical structure of the neurotransmitter dopamine is explained in figure (1.10).

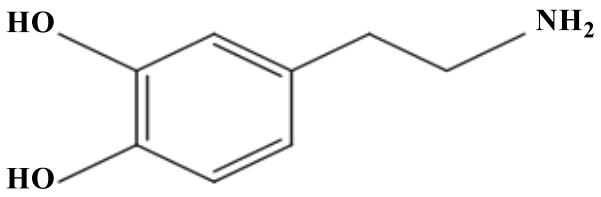

Figure (1.10). The chemical structure of the neurotransmitter dopamine.

In the last decade, there has been a lot of interest in it as a bioinspired surface coating building block. It's a 3,4-dihydroxy-l-phenylalanine structural clone (DOPA) , has been attributed to mussel adhesive versatility, which can polymerize and deposit on a variety of organic and inorganic substrates [116]. Dopamine-based materials are emerging as novel biomaterials with piqued interest in the fields of biosensing, bioimaging, and cancer therapy. due to their unusual physicochemical properties, such as flexible adhesion property, high chemical reactivity, excellent biocompatibility and biodegradability, and good photothermal conversion capacity.

The dopamine system and its projections sites, which include the striatum and the prefrontal cortex (PFC), play crucial roles in modulating motivated behavior, emotion, and high-order cognitive functions related to reward processing. The functions of reward include approach and consummatory behavior as well as the ability to predict the outcomes of potentially rewarding situations, serving goal-directed behavior and providing an evolutionary advantage for creatures facing unpredictable environments. The integrity of the dopamine system is important for efficient processing of reward information. Dysfunction of this system is involved in a variety of disorders, including schizophrenia, Parkinson's disease, pathological gambling, and drug addiction. Although there are clear individual genetic differences regarding susceptibility to and manifestation of these neuropsychopathologies, the influence of genetic predispositions and variations on activation of the human reward system remains poorly understood.

Two important proteins contribute to terminating the action of intra-synaptic:

- Dopamine in the brain: Catechol-O-methyltransferase (COMT), which catabolizes released dopamine.

- dopamine transporter (DAT), which plays a crucial role in determining the duration and amplitude of dopamine action by rapidly recapturing extracellular dopamine into presynaptic terminals after release.

1.13 Hierarchical nanostructures

The 3D hierarchical nanostructures have gotten a lot of attention recently [117] due to their unique properties and a broad variety of possible potential applications ranging from electronic, magnetic, optoelectronic, and catalytic to biomedical fields. The shortest synthetic route for 3D hierarchical nanostructures [118] is possible self-assembly or the autonomous organization of components into ordered aggregations. However, developing easy and reliable methods for the preparation of hierarchically self-assembled architectures with controlled chemical components, sizes, and morphologies, on the other hand, remains a major challenge [119]. The formation of hierarchical nanostructure may have proceeded with the following [120,121]:

- Nucleation.
- Agglomeration of nuclei under the influence of high surface energy and electrostatic interactions.
- Nanocrystal formation from aggregated nuclei reduces surface energy even more.
- Due to the lower energy barrier, anisotropic crystal growth along a preferred crystal axis seeded from nanocrystals is possible.
- Ostwald ripening, in which unstable smaller particles dissolve and larger particles grow by adsorbing monomers from the dissolved particles, driven by surface energy minimization.

1.14 Literature review for hybrid Polyoxometalate (POM)-Dopamine

Messersmith and co-workers[122] in 2007, used dopamine self-polymerization to form thin, surface-adherent polydopamine films onto a wide range of inorganic and organic materials, including noble metals, oxides, polymers, semiconductors, and ceramics. As a 3,4 dihydroxy-l-phenylalanine structural clone (DOPA), it has been linked to mussel

adhesive versatility and has been shown to polymerize and deposited on a variety of organic and inorganic substrates.

Xin and co-workers [123] in 2016, In this work, through the aqueous phase self-assembly of an Eu-containing polyoxometalate (POM), Na9[EuW10O36]·32H2O (EuW10) and different amino acids, we obtained spontaneously formed vesicles that showed luminescence enhancement for EuW10 and arginine (Arg), lysine (Lys), or histidine (His) complexes. The concept of combining POMs with amino acids extends the research category of POM-based functional materials and devices.

Xin and co-workers[124] in 2017, New inorganic-organic hybrid nanoflowers with a Weakley-type structure were created. Surprisingly, the calcinated nanoflower had a high decomposition efficiency against organic pollutants like methyl orange (MO) and rhodamine B dyes (RhB). Furthermore, the catalyst for MO can be reused at least six times with only a slight loss in catalytic efficiency, indicating that it has potential applications in wastewater treatment.

Peng and co-workers [125] in 2018, preparation method of PDA, a rapid increase of research reports concerning new fabrication strategies, functionalization, and applications of dopamine-based materials has been witnessed, using oxidative self-polymerization and other assembly methods based on dopamine.

Al-Yasari and co-workers[126] in 2019, have reported the self-assembly of DA and polyoxometalate; PWA resulting in hierarchical nanostructures form for the oral drug delivery of Doxorubicin.

Khoshnavazi and co-workers [127] in 2020, synthesized Sponge-like inorganic-organic nanohybrid consisting of sandwich-type polyoxometalate of $[P_2W_{18}Ce_3\ (H_2O)_2O_{71}]_{12}$ ($P_2W_{18}Ce_3$) and dopamine (DA) was fabricated by a simple procedure. The DA/$P_2W_{18}Ce_3$ sponge-like nanohybrid is turned into a nanoflower by calcination at 300 ^oC.

Peng and co-workers [128] in 2021, A template for in situ loading of nanoparticles was synthesized by Keggin-type phosphotungstic acid and triazine melamine spontaneously self-assemble into hybrid nanostructures in aqueous media, which can act as an excellent template for the synthesis of nanostructured silver.

1.15 Aim of this work

This study is aimed to:

1. Preparation POM-Dopamine nanostructure.

2. Study the characterizations of the as-prepared nanostructure by X-ray diffraction (XRD), Scan Electronic Microscope (SEM), Infrared spectroscopy (FT-IR).

3. Investigation the possibility of loading different drugs into the as-prepared nanostructure such as furosemide and capecitabine for drug delivery purposes.

4. Study the effect of component ratio Different concentrations of Tris-HCl, and changes in stirring time on the morphology of the nanostructure.

5. Investigation the possibility of releasing different drug loading on the as-prepared nanostructure in different period times within acidic and basic medium by using (UV-Vis) spectroscopy.

Chapter Two Experimental part

2.1 Chemicals

In this work, the chemicals used as tabulated in Table (2.1), used without further purification.

Table (2.1). Used chemicals

No.	Chemicals	Company supplied	Origin	Purities or percentage
1.	Capecitabine	Biotang lncsupplier	America	99%
2.	Dopamine hydrochloride (DA)	Thermo Fisher (TMO)	America	99%
3.	Furosemide	TCl Tokyo	Japan	99%
4.	Glycine	THOMAS BAKER	India	99%
5.	Hydrochloric acid (HCl)	J.K. Baker, Netherlands	India	(36.5-38.0)%
6.	Phosphate buffered saline (PBS)	HiMedia M1452-100G	India	99%
7.	Phosphotungstic acid (PTA)	HiMedia GRM398-100G	India	99%
8.	tris(hydroxymethyl)aminomethane (Tris)	HiMedia TC072-500G	India	99%

2.2 Instruments

Table (2.2). shows the instruments that used in this study with thier companies.

Table (2.2). Employed instruments.

No.	Instruments	Companies	Places
1.	Centrifuge	Hettich- Universal II-Germany	University of Kerbala, College of Science
2.	Digital pH meter	OAICTON-2100, Singapore	University of Kerbala, College of Science
3.	Double –beam UV-Visible-spectrophotometer	AA-1800, Shimadzu, Japan	University of Kerbala, College of Science
4.	Fourier-transform infrared spectroscopy (FTIR)	FT-IR-8400S, Shimadzu ,Japan	University of Kerbala, College of Science
5.	Hotplate Magnetic Stirrer	Heido-MrHei-Standard, Germany	University of Kerbala, College of Science
6.	Oven	Memmert, Germany	University of Kerbala, College of Science
7.	Scan electron Microscopy (SEM)	FESEM FEI Nova Nano SEM 450 device	University of Tehran
8.	Sensitive balance	BL 210 S, Sartorius-Germany	University of Kerbala, College of Science
9.	Ultrasonic	DAIHAN Scientific, Korea	University of Kerbala, College of Science
10.	X-Ray Diffraction instrument	Rigaku Ultima IV	University of Tehran

2.3 Methodologies:

2.3.1 Preparation of Chemical Solutions

2.3.1.1 (Tris-HCl) buffer solution

According to literature method for Junbai Li [124], (Tris-HCl) buffer solution was prepared by dissolving tris(hydroxymethyl) aminomethane (Tris) concentrated (10 mM) With a volume of 1 liter of deionized water then the pH adjusted to be equal (9.5-10.5) using HCl due to pH elevation and then store at 37 ^{o}C.

2.3.1.2 Dopamine solution

This solution was prepared by dissolving exact (5 mg) from dopamine in (5mL) Tris-HCl solution.

2.3.1.3 Phosphotungstic acid (PTA) solution

Exact 5mg of PTA was dissolved in (5mL) of Tris-HCl solution.

2.3.2 Synthesis of the hierarchical nanostructures (Host or carrier)

In a standard procedure, separately, 1 mg of DA and 1 mg of PTA were dissolved in a 10 mM Tris-HCl solution (pH 10.5, 0.5 mL). The PTA solution was added to the DA solution as soon as possible, and after 30 seconds, the produced solution was visible yellowing. Following a 2-hour aging period, the as-synthesised product was collected using three cycles of centrifugation (5000 rpm, 5 min) and water washing [129,130]. Figure (2.1) shows the synthesis process of the hierarchical nanostructures.

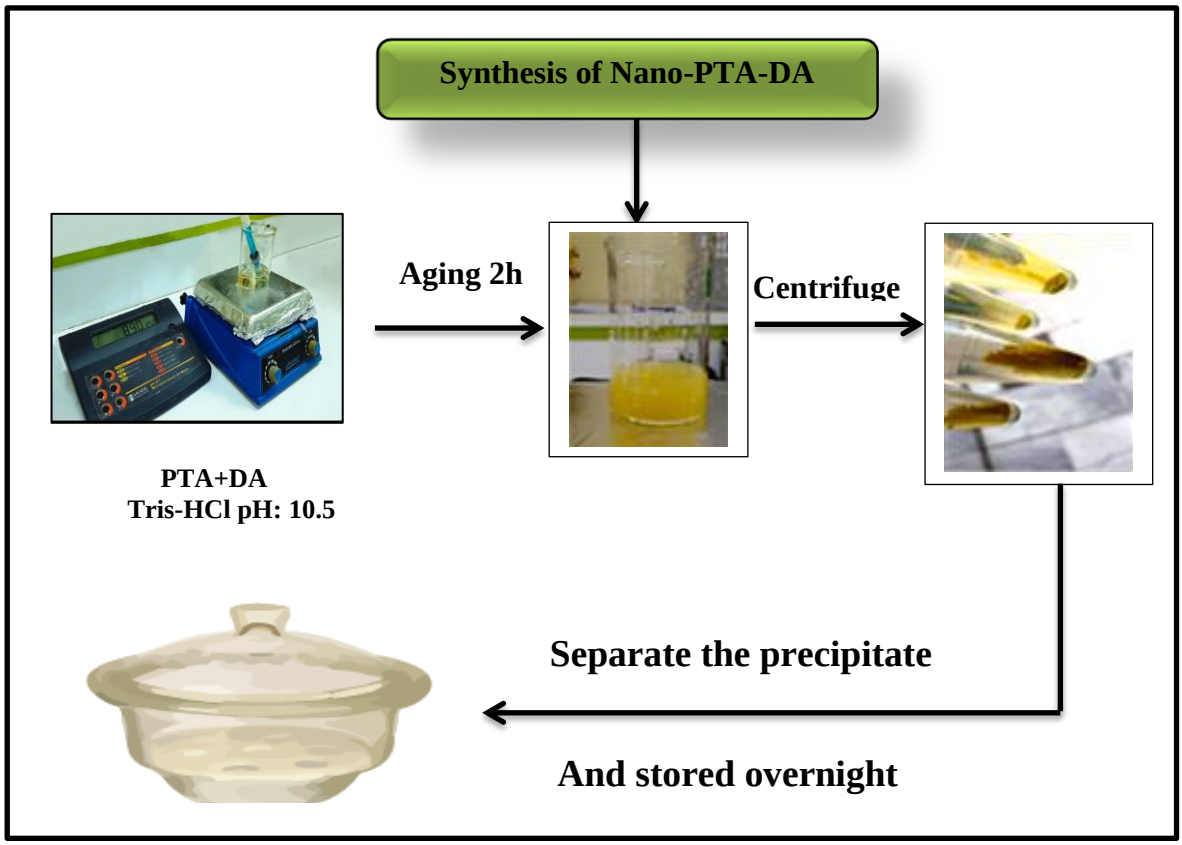

Figure (2.1). The schematic diagram for the synthesis process of the hierarchical nanostructures.

2.3.3 Drug loading into the flower-like hierarchical nanostructures

The model drugs in this study were furosemide and capecitabine. In a 10mM Tris-HCl solution, DA (1 mg/mL) and PTA (1 mg/mL) were combined to make a powder of flowerlike microspheres (10 mg) (pH 9.5), and then immersed in an aqueous solution of drug (1 mg/mL) for Capecitabine and (0.02 mg/mL) for Furosemide[131,132].The mixture was shaken for different times (4,6,8,10, 12) hours at 37 ^{o}C. Following this, the sample was washed three times with ultrapure water before being centrifuged for five minutes at 5000 rpm to remove any unbound drug. The amount of drug adsorbed on the flowe-rlike microspheres was calculated by determining the supernatant's absorbance at 270 nm for Furosemide and

340nm for Capecitabine and study the percentage of drug loading on hybrid nanoparticles by using this equation [132]:

$$Loading\ content = \frac{(Wt-Wf)}{Wnp}\ x\ 100 \qquad \ldots\ldots (2.1)$$

Where: Wt is the total weight of drug fed, Wf is the weight of non-encapsulated free drug, and Wnp is the weight of the nanoparticle.

2.4 Characterizations

2.4.1 Diagnosis using the FT-IR spectrum

The infrared spectrum was studied for each of the nanoparticles hybrid under study, as well as the drug-loaded on the nanocomposite. A tablet of each of these compounds was made with potassium bromide (KBr) after grinding it well. The infrared spectrum was measured in a range of wavelengths (400-4000) cm^{-1}.

2.4.2 X-Ray Diffraction (XRD)

X-ray diffraction analysis is an essential method to detect the complex types in crystalline or amorphous states [133]. The prepared nanostructures were diagnosed before and after drug loading using this analysis, which shows the different angles before and after the intercalation. Based on XRD data, the mean crystallite size (L) is calculated employing Scherrer's equation [134, 135].

$$L = \frac{k\lambda}{\beta \cos\theta} \qquad \ldots(2.2)$$

Here: k is the Scherrer's constant based on the dimensionless shape in ranged 0.94-0.85, λ is the wavelength of Cu kα (used 0.15406 nm) as irradiation source, 2θ a Bragg diffraction angle and β is (FWHM) the full half-maximum intensity width in degrees, which must convert to radians by multiplying it by (π/180).

Depending on Bragg's equation (2.3), a calculation made the interplanar spacing (d) was calculated before and after the preparation of the as prepared flower-like hierarchical nanostructures of the main components

Dopamine(DA) and phosphotungstic acid (PTA), it was also calculated for the drugs before and after the loading process[136].

$$n\lambda = 2d\ sin\,\theta \qquad \ldots (2.3)$$

Where n is an integer = 1, and $\boldsymbol{\lambda}$ is the wavelength of the X-rays = 1.540 Å, $\boldsymbol{\theta}$ is the diffraction angle.

2.4.3 Scanning Electron Microscopy (SEM)

The shape and surface characteristics of flowerlike hierarchical nanostructures before and after drug loading were analyzed by scanning electron microscopy. The Nova NanoSEM scanning electron microscope delivers best in class imaging and analytical performance in a single, easy-to-use instrument, High resolution imaging – low voltage [1kV] resolution is 1.8 nm in low vacuum mode and 1.4 nm in high vacuum mode.

2.5 Study drug release

2.5.1 Designation Calibration Curve for Furosemide

The calibration curve of Furosemide was done by preparing six sequential concentrations within the range (0.00078-0.05)mg/mL. This drug solution was read its absorbance for these concentrations at the wavelength (λ_{max}) 270 nm. A calibration curve of Furosemide was drawn between absorption verse concentration with treatment by Least Squar method as shown in figure (2.2).

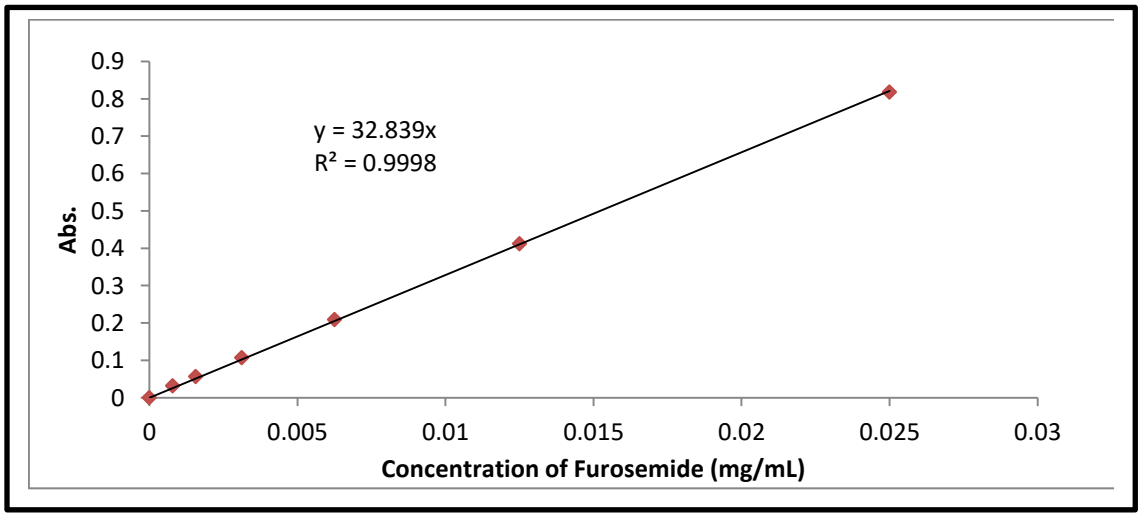

Figure (2.2). Calibration curve for Furosemide.

2.5.2 Designation Calibration Curve for Capecitabine

The calibration curve of Capecitabine was performed by preparing seven sequential concentrations within the range (0.000078-0.14) mg/mL, and then read the absorbance of this drug solution at the maximum wavelength(λ_{max}) equal to 340nm. This calibration curve was drawn between absorption verse concentration with treating by Least Squar method as explained in figure (2.3).

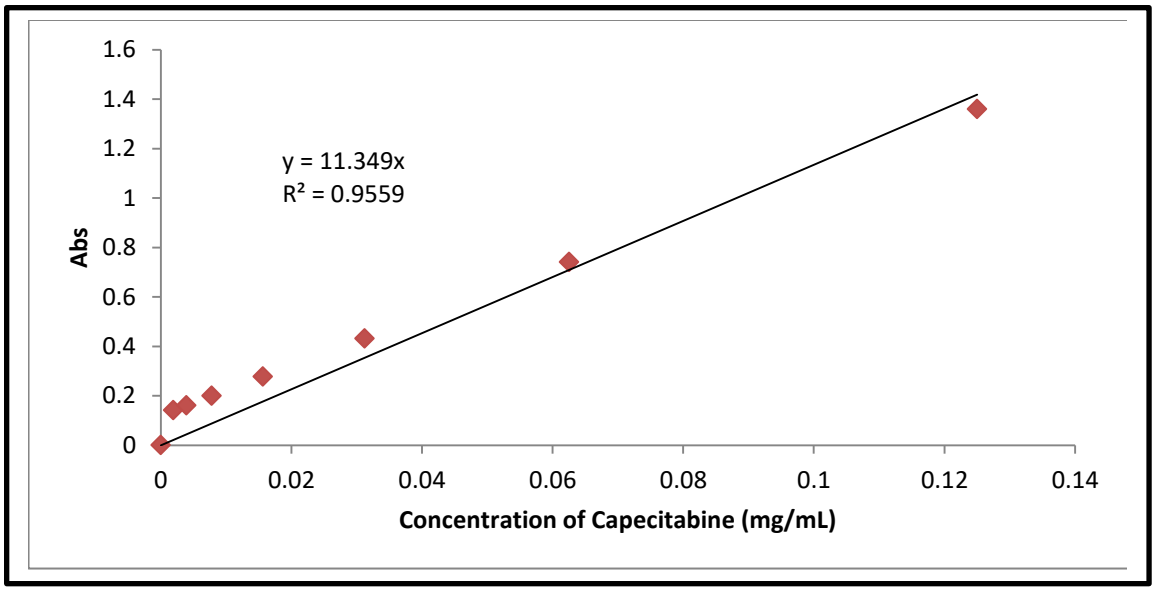

Figure (2.3). Calibration Curve for Capecitabine

2.5.3 In vitro Drugs loaded on hierarchical nanostructures released

The release of furosemide and capecitabine was studied for 12 hours, 24 hours, and 33 hours in a pH 2.8 glycine-HCl buffer solution and pH 7.4 PBS solution, respectively. Exact (10 mg) flower-like microspheres loaded with drugs were immersed in the appropriate (5 mL) buffer solutions while agitated on a shaker plate (500 rpm). At predetermined intervals, aliquots (1 mL) of the supernatant were withdrawn and mixed with the same volume of fresh buffer solution. The amount of drugs released was calculated using the UV/Vis absorbance of furosemide at 270 nm and capecitabine at 340 nm, respectively.

2.5.4 Study the percentage of drug release from hierarchical nanostructures

The percentage of drug release was followed up separately utilizing a UV-Vis spectrophotometry with changes in an hour, and by dividing the concentration at each time C_t extracted from the calibration curves by the total drug concentration and according to the following equation, the percentage of release is calculated[137,138].

$$Release\ \% = \frac{Wt\ of\ drug\ released(mg)}{Wnp * \%\ drug\ loading} \times 100 \qquad \ldots (2.4)$$

The emancipation path was studied to determine the order it would follow. If the aforementioned path is based on the pseudo first-order model, then it is subject to the following equation [139].

$$Log\left(1 - \frac{C_t}{C_T}\right) = \frac{k_1}{2.303}\ x\ t \qquad \ldots (2.5)$$

While in the case of his behavior of the second pseudo order, it is subject to the following equation [139].

$$\frac{t}{C_t} = \frac{1}{CT} x\ t + \frac{1}{k_2 x\ CT^2} \qquad \ldots (2.6)$$

Here:

t: time of release, C_t: releasing at time t, C_T: Total liberation in time ∞ , k_1: Rate constant for 1st order, and k_2: Rate constant for the 2nd order

Chapter Three
Results and Discussion

3.1 Characterizations of nanostructures before and after drug loading

In this work, the studied samples were determined by characterization such as employing XRD, SEM, FTIR, and Uv-Visible techniques.

3.1.1 X-Ray Diffraction (XRD)

XRD technique is the most widely used for characterizing materials. The X-ray diffraction pattrens of the hybrid nanostructure was measured before loading and after loading the drugs on it.

(Figure 3.1.a) shows the X-ray diffraction pattrens of the PTA and indicates the diffraction of the levels (hkl) are (222, 323, 701, 723), which appear at the angles (25.37°, 34.59°, 53.25°, 59.87°) respectively[140,141]. The mean crystal size (L) was calculated using Scherrer's equation and it was sized (87.944 nm). The inter-planar spacing (d) was calculated using Bragg's equation before incorporated PTA with dopamine (DA) as-prepared flowerlike hierarchical nanostructures, as shown in (table 3.1).

(Figure 3.1.b) explains the X-ray diffraction pattrens of the DA The mean crystal size (L) was calculated depending on the peaks of angles (25.45°, 34.18°, 52.36°, 25.93°), and found to be (68.56 nm). Well, using Bragg's equation to the same angles, the interplanar spacing (d) of DA was done in (table 3.1).

The X-ray diffraction of the PTA-DA flowerlike hierarchical nanostructures as drug carriers are shown in (Figure 3.1.c), and the mean crystal size was determined by basing on the peaks of the angles (9.80°,

13.82°, 16.70°, 25.13°), and gave the sized equal to (12.95 nm). Moreover, the interplanar spacing (d) at the same angles was listed in (table 3.1).

(Table3.1). The interplanar spacing (d) of PTA, DA, and flowerlike microspheres.

PTA		**DA**		**PTA-DA**	
2$\boldsymbol{\theta}$	**d-spacing [Å]**	2$\boldsymbol{\theta}$	**d-spacing [Å]**	2$\boldsymbol{\theta}$	**d-spacing [Å]**
25.37	**3.50**	**25.45**	**3.49**	**9.80**	**9.05**
34.59	**2.59**	**34.18**	**2.62**	**13.82**	**6.41**
53.25	**1.71**	**52.36**	**1.74**	**16.70**	**5.31**
59.87	**1.54**	**45.46**	**1.99**	**25.13**	**3.54**

The XRD pattern of PTA demonstrated several Keggin-type POM are known for their sharp Bragg reflections [142, 143]. In comparison, besides the characteristic peaks of PTA, there are two new peaks at 2$\boldsymbol{\theta}$=13.82° and 16.70° are visible for the flower-like nanostructures, which indicates the The complexation of DA and PTA through strong interactions results in the formation of a crystalline state, though the precise crystal structure needs to be investigated further flowerlike microspheres [140].

On the other side, the mean crystal size after incorporation of PTA with DA as nanostructure is very reduced in nanosize (12.95 nm), and with elevated the interplanar spacing value at 25^{o}, that may be to increase the repulsive force between the inter levels during decreasing the size to lower nanosize. This behavior is confirmed also in the production of PTA- DA nanostructure.

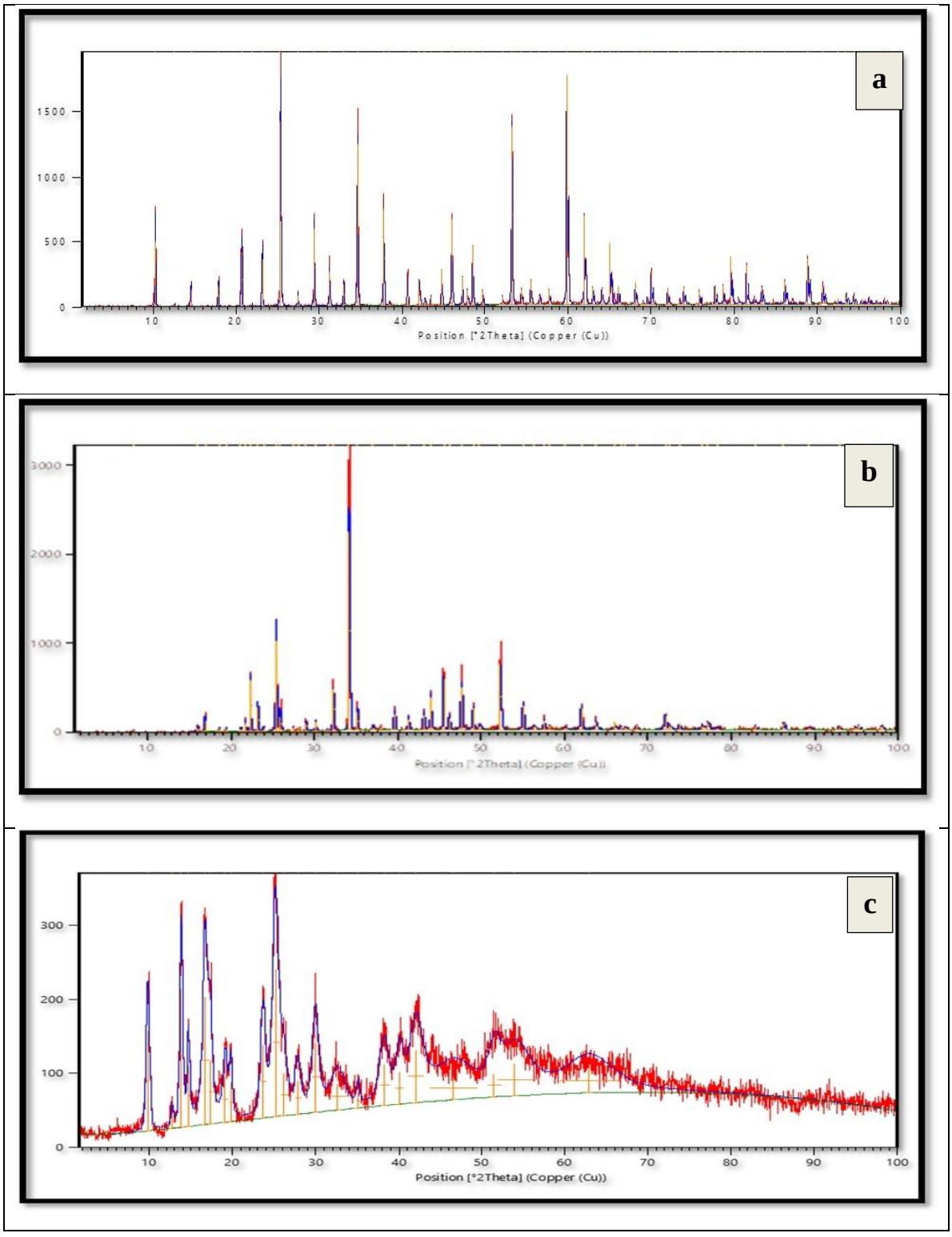

(Figure 3.1). XRD patterns of (a) PTA, (b) DA, (c) flower-like hierarchical nanostructures as prepared

Based on Figure(3.2.a), the mean crystal size of the pure Furosemide (L) was calculated through using the (XRD) patterns data with angles (6.00°, 18.11°, 22.89°, 24.78°) [144,145], which equal to (62.56 nm). The interplanar spacing (d) was predicted before loading of Furosemide in the table (3.2). Also, the mean crystal size for PTA-DA nanostructure after the Furosemide drug loading process in (Figure 3.2. b) is elevated from 12.95 nm to 66.17 nm. This case refers to Furosemide drug loading on PTA-DA nanostructure, and the angle after loading Furosemide drug is reduced from 13.82^{o} to 12.05^{o} as shown in (table 3.2).

(Table 3.2).The difference in the interplanar spacing (d) before the process of loading and after using for Furosemide.

Furosemide		**PTA-DA after loading Furosemide**	
2θ	**d-spacing [Å]**	**2θ**	**d-spacing [Å]**
6.00	**14.71**	**6.01**	**14.69**
18.11	**4.89**	**12.05**	**7.33**
22.89	**3.88**	**18.12**	**4.89**
24.78	**3.58**	**24.89**	**3.57**

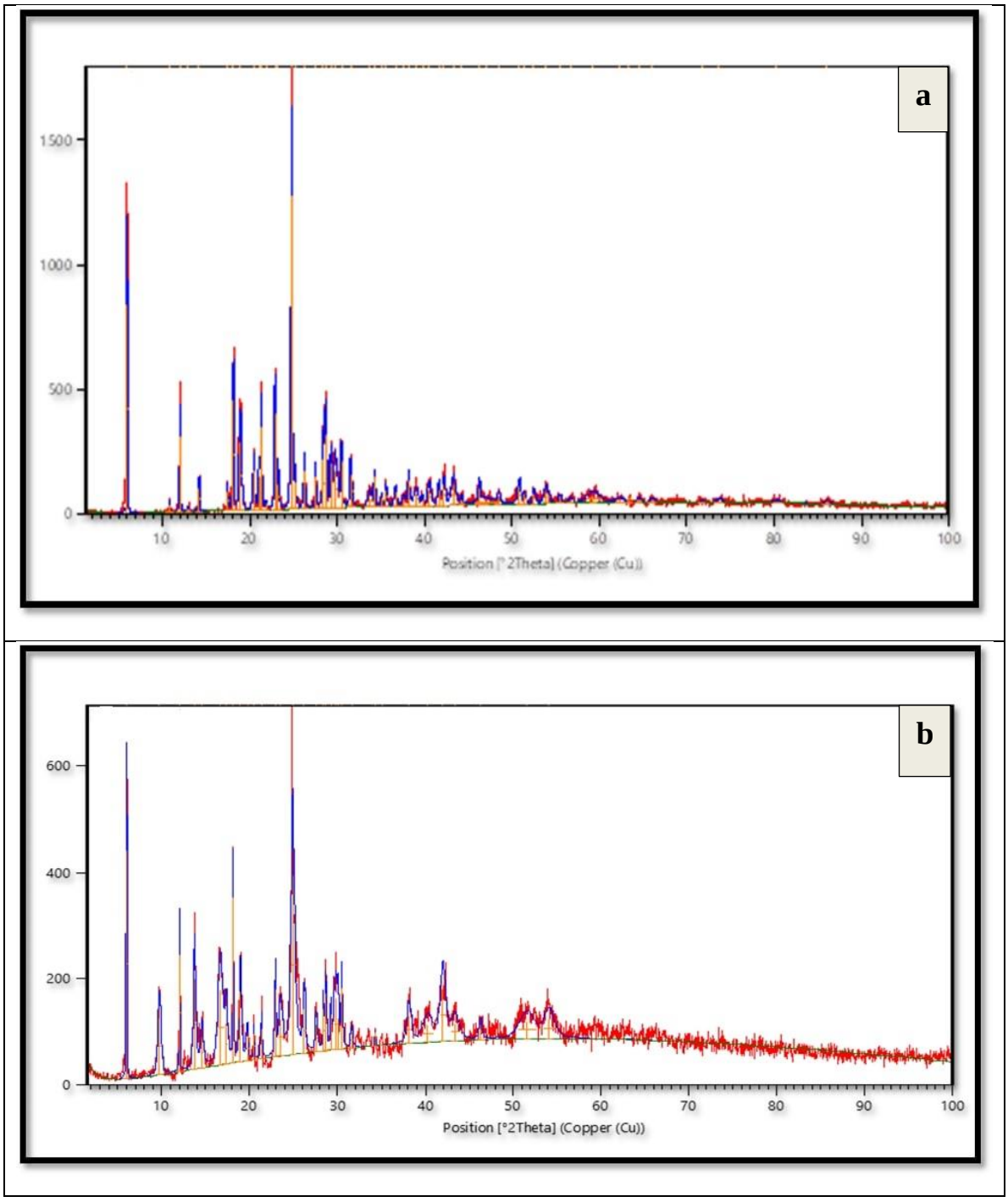

(Figure3.2). The X-ray diffraction (XRD) patterns of (a) the Furosemide pure (b) PTA-DA after loading Furosemide.

From the X-ray diffraction analysis in (Figure 3.3.a) found, the mean crystal size of the pure Capecitabine was calculated employing the peaks with the angles (5.03°, 4.86°, 20.04°, 20.34°) [146] and equal to (59.67 nm), and the interplanar spacing value before the process of drug loading using the Bragg's equation that was predicted in table variation (3.3). While after the loading process in (Figure 3.3 b), the mean crystal size for PTA-DA nanostructure is elevated from 12.95 nm to a size equal to (16.06 nm), that due to the Capecitabine drug is loaded on nanostructure with decreasing in interplanar spacing value from 4.36 Åfor drug to 3.54 Å at 25^{o} for PAT-DA. The stability of d-spacing values of pTA-DA after loading is observed in comparison with the values before loading in Table (3.1). This indicates that the drug did not change the crystal structure of the nanoparticles, this may be due to the fact that the drug remained adsorbed on the surface of the nanostructure and did not enter the nanostructure.

(Table 3.3).The difference in the interplanar spacing (d) before the process of loading and after using for Capecitabine.

Capecitabine		**PTA-DA after loading Capecitabine**	
2θ	**d-spacing [Å]**	**2θ**	**d-spacing [Å]**
5.03	**18.15**	**9.76**	**9.04**
4.86	**17.52**	**13.78**	**6.41**
20.04	**4.42**	**16.62**	**5.32**
20.34	**4.36**	**25.09**	**3.54**

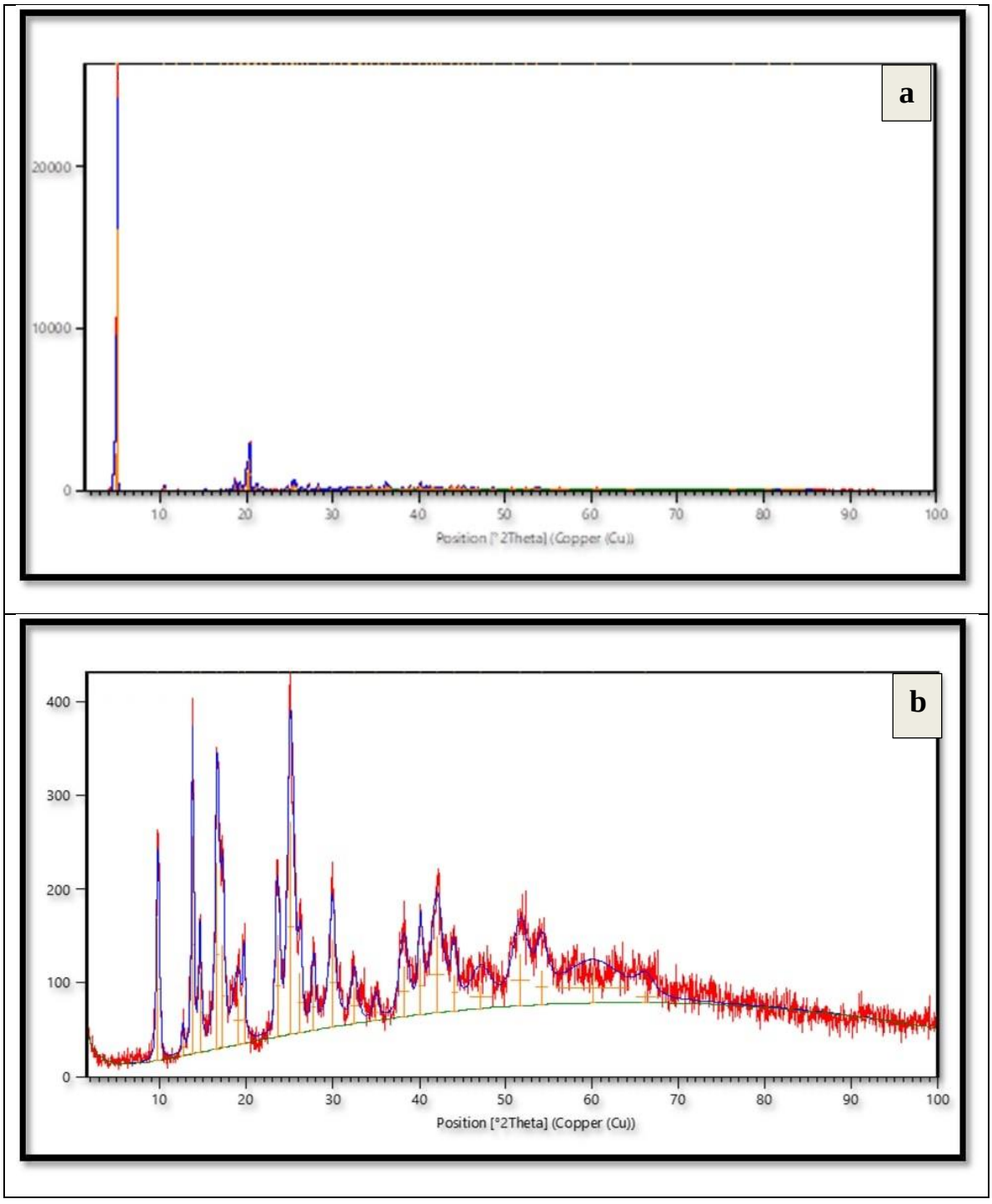

(Figure3.3). The X-ray diffraction (XRD) patterns of (a) the Capecitabine pure (b) PTA-DA after loading Capecitabine.

3.1.2 Scanning Electron Microscopy (SEM)

The surface shape of the individual materials (Dopamine and PTA) was studied before the preparation of the nanostructures, and notice the changes in surface shape after the preparation process. Figure (3.4.a,b) explains the morphology of the dopamine where the shape was in the form of irregular smooth sheets of thickness with a size (3,30)µm, while, the morphology of the PTA shows the semi-spherical agglomerated nanoparticles with high roughness in Figure (3.4.c,d).

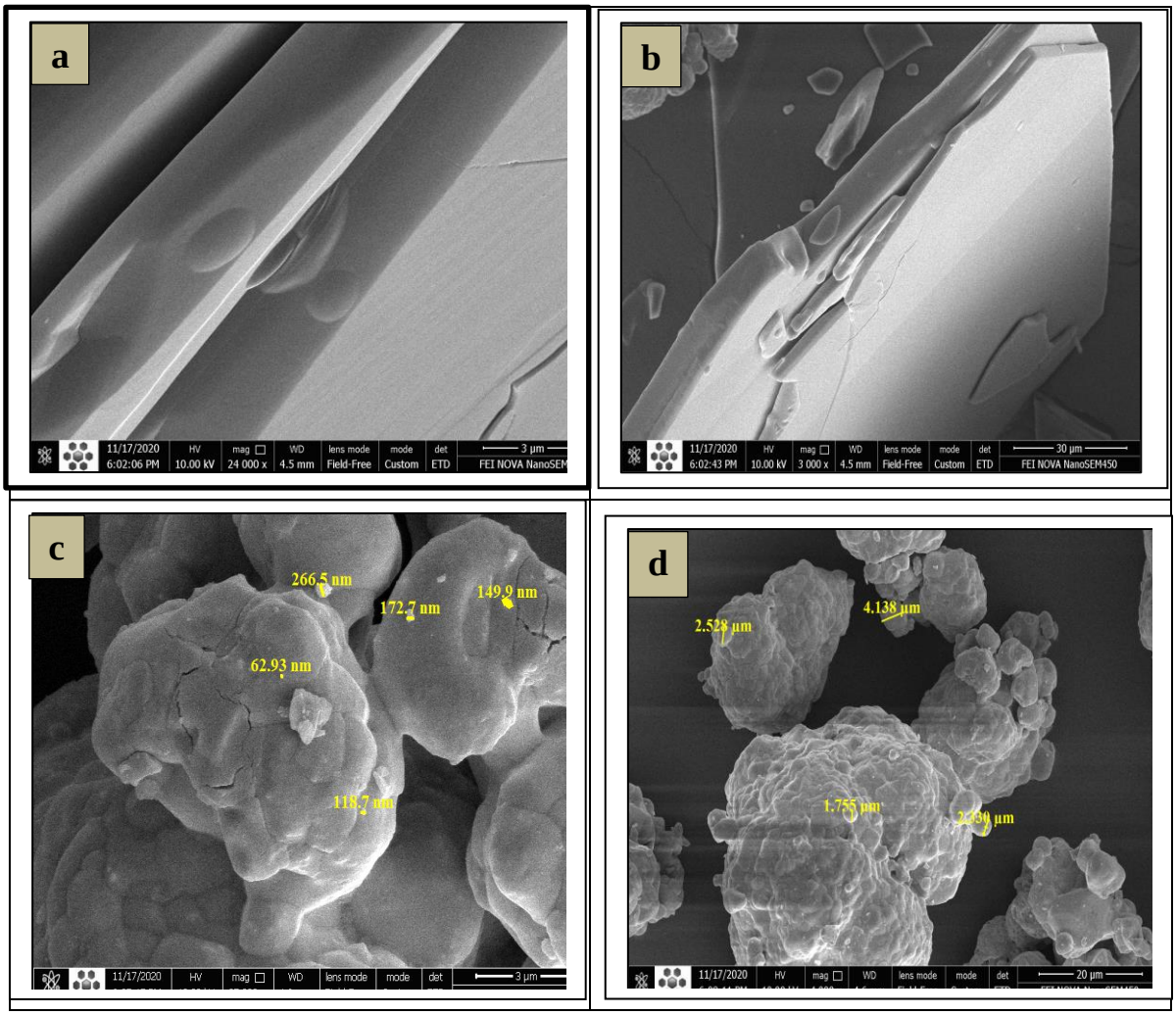

(Figure 3.4). SEM images of the individual materials (a,b) Dopamine (DA). (C,d) PTA

The outer surface of the nanostructure was studied before and after the drug loading process using a scanning electron microscopy, the SEM images in (Figure 3. 5.a) showed that the detailed morphology of the flower-like nanostructures which reveals that they are made up of a large number of nanopetals with smooth surfaces. The thickness of these nanopetals is around 21 nm, with a width of (300–500) nm, were linked by a central core to form three-dimensional flower-like hierarchical structures [147].The microspheres were well-defined, with many pores and hierarchical structures, and ranged in size from (2 to 6.5) micrometers, as shown in (Figure 3.5 b, c). Where proportion was used (1:1) weight ratio by the addition of a phosphotungstic acid(PTA) solution to Dopamine(DA) solution at 37 °C and the color is yellowing. This was consistent with the result obtained by Hong Li [140,148,149].

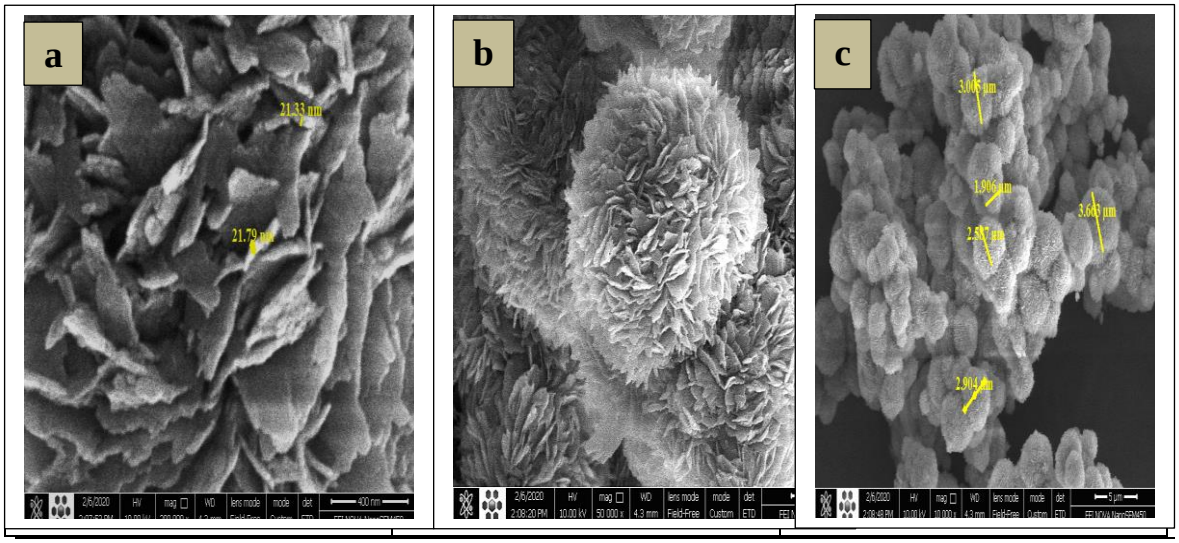

(Figure 3.5). SEM images of (a) a magnified region of the surface structure,(b) an individual flower-like hierarchical nanostructure in detail , c) the overall product morphology.

3.1.2.1 Study the influencing of some parameters on the size and morphology of the Nanostructures with 3D hierarchical structures

I. Different ratios: Drug carriers' sizes and morphologies have a big impact on their drug loading efficiencies and release kinetics. Various DA:PTA weight ratios, specifically (1:2, 1:3, 1:1, 2:1, 3:1)by using amino methane

(Tris) solution were investigated. From the results in (Figure 3.6.a,b) found, the large and compact superstructures of DA : PTA ratio were obtained at 1:2 ratio this proportion is thought to be ideal for DA and PTA interactions. Since each DA molecule has one positive charge and each PTA molecule has three negative charges, and thus the number of positive charges greatly outnumber the total amount of negative charges In these circumstances, other interactions between the two components, such as hydrogen bonds and van der Waals forces, could have occurred in addition to electrostatic interactions. Besides the size of the particle changed from the to (28.07-33.27) nm. As for the color, it remained yellow[150-152]. At a 1:3 ratio of DA to PTA, an clear distance was seen in each microsphere (Figure 3.6.c,d) indicating that the hierarchical nanostructures grew along an axle with high roughness under these conditions, where the size became (20.23-27.83)nm, and the yellow color was also observed. (1: 1) the ratio was seen in this (figure 3.5).

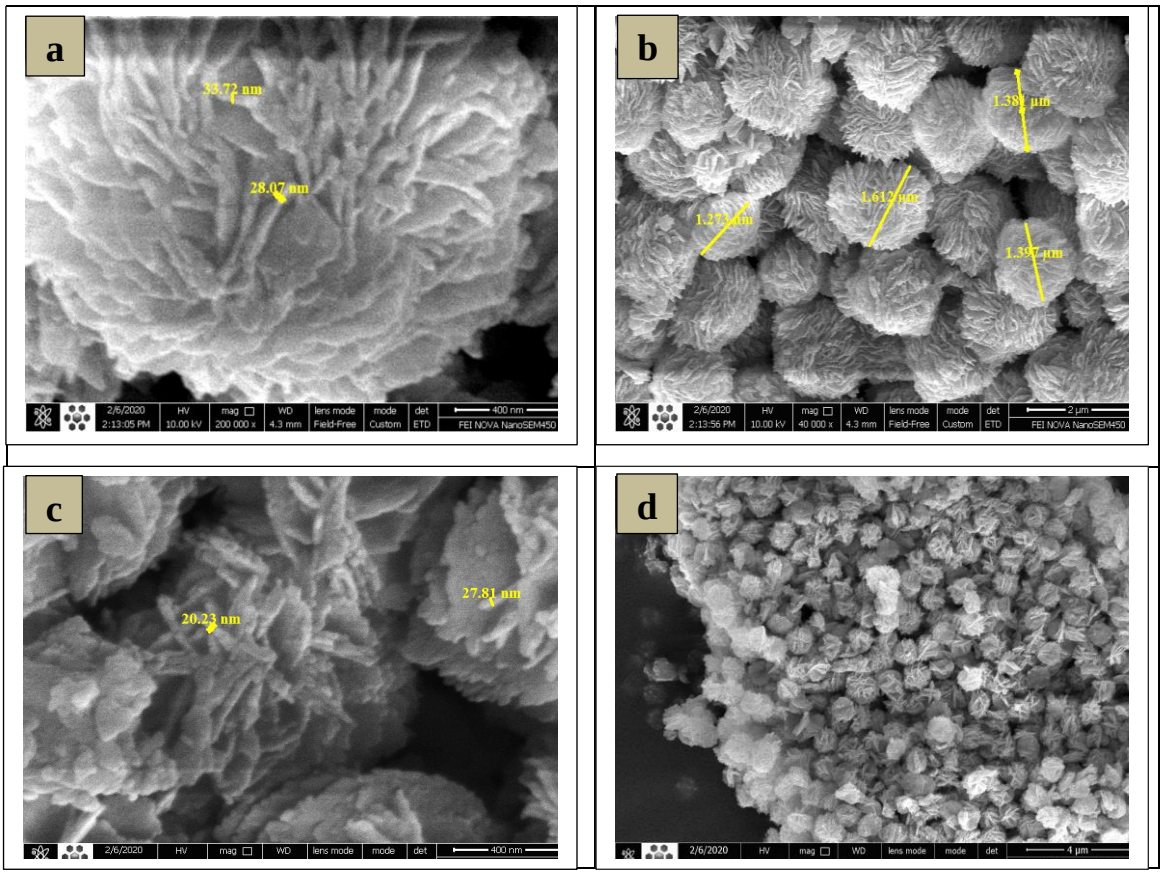

(Figure 3.6). SEM images of 3D hierarchical nanostructures made in a Tris-HCl solution (10 mM, pH 9.5) with different PTA/DA ratios , (a,b) 1:2 and c,d) 1:3, and DA is constant.

When the amount of DA is increased, the ratio of (2:1, 3:1) is compared with PTA, the color was turned greenish-yellow. In (Figure 3.7.a,b,c,d), the morphology of the flower-like microspheres did not change significantly, except that the product size distribution has been widened. Further research revealed that the morphological growth of these 3D hierarchical superstructures is concentration-dependent. By varying the concentrations of the two components, a variety of intriguing nanostructures could be created [153,154]. The range of sizes is found to be (23.21- 29.58) nm and (18.15-21.79) nm for DA: PTA ratio of (2:1 and 3:1), respectively. This reduced in size attitude to elevate the DA ratio that has less size (68.56 nm) than PTA (87.94 nm).

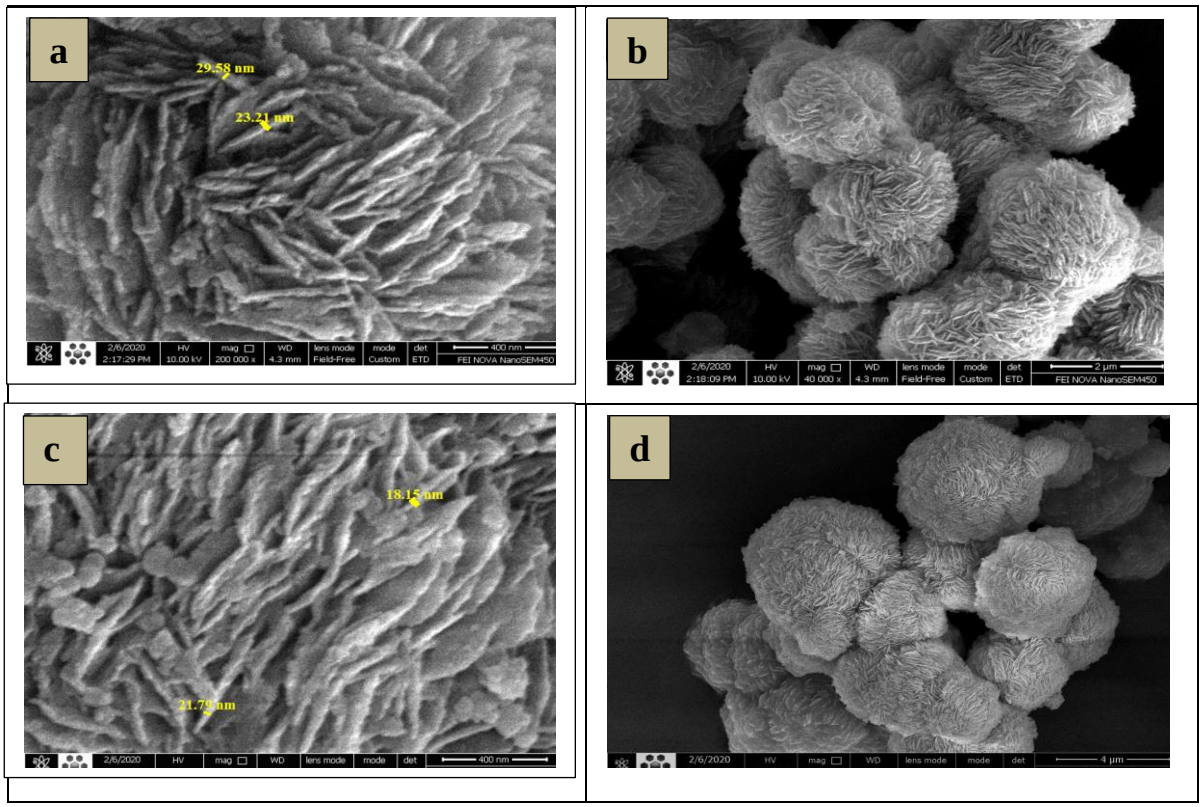

(Figure 3.7). SEM images of 3D hierarchical nanostructures made in a Tris-HCl solution (10 mM, pH 9.5) with different DA/PTA ratios, (a,b) 2:1 and (c,d) 3:1,and PTA is constant.

II. Different concentration of Tris-HCl:

The Tris-HCl concentration has been raised in the range of 10 mM, 20 mM, and 30 mM, with fixing the concentration of dopamine and PTA. In (Figure 3.8)the morphology of the flowerlike microspheres did not change significantly, when 20 mM concentration was used, except that the size became (21.33-21.79) nm (Figure 3.8.a,b).

When 30 mM of Tris-HCl solution was used, the morphology of the flowerlike microspheres changed to irregular shape, as well as the scale, which changed to sizes (47.81, 126.7, 112.4, and 121.5) nm in (Figure 3.8.c,d).

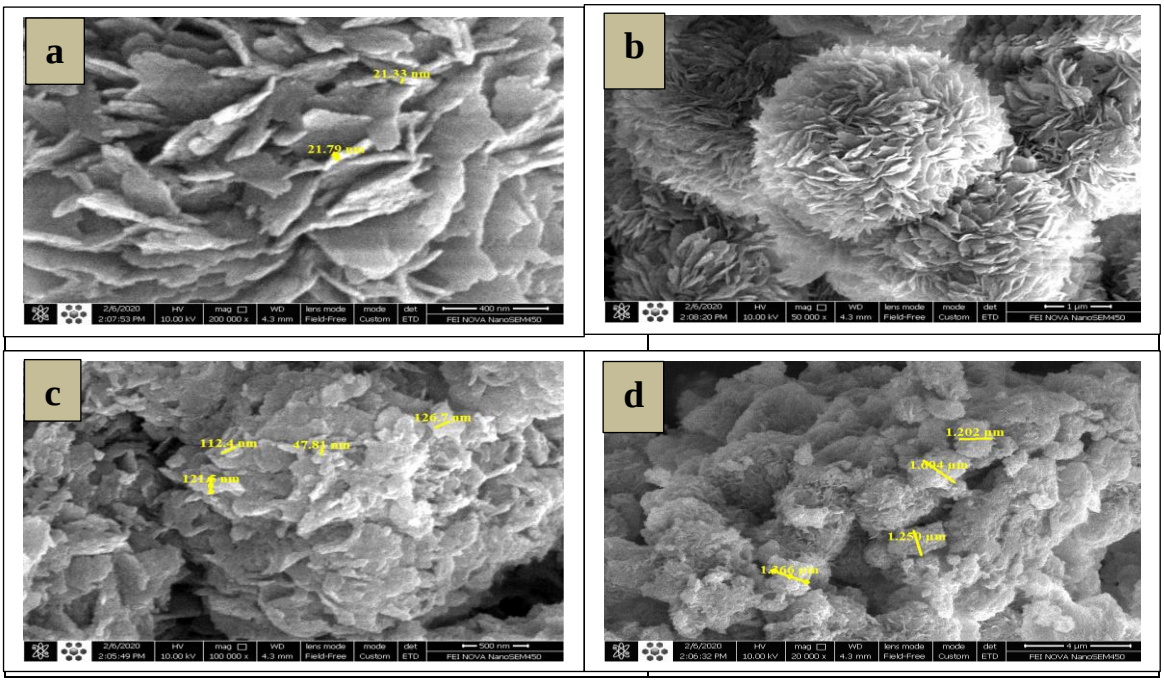

(Figure 3.8). SEM images of 3D hierarchical nanostructures prepared in Tris-HCl solution a,b)20 mM Tris-HCl , c,d)30 mM Tris-HCl. while remained the dopamine and PTA concentration constant.

III The changed in stirring time to (1:1) ratio from DA to PTA :

This influence investigated,that the morphology and structure evolved over time as microspheres aged at different rates, and as evidenced by SEM measurements. As can be seen in (Figure 3.9.a,b), at 30 minutes of stirring, diameters of about (26.19,22.97 and 36.30) nm were formed loosely aggregated together, as seen in (Figure 3.8.a,b). The microspheres' surfaces were rough, and short petals grew out of the primary aggregations as the self-assembly process progressed, eventually becoming ellipsoidal hierarchical nanostructures of size around(1-2)µm [155], The as prepared product grew into highly ordered, spherical, hierarchical nanostructures of size around (25, and 29)nm after 60 minutes of aging. The flower-like microspheres were made up of hundreds of nanopetals with relatively smooth surfaces as shown in (Figure 3.9.c,d). With longer aging times, the product's size and morphology remained the same [156,157]. Even after subjecting the as-obtained product to ultrasonication for 30 minutes, the architecture of the microspheres could not be destroyed or split into discrete individual nanopetals, implying high microspheres stability and good binding interactions between DA and PTA molecules, and the color for everything was yellow [158,159].

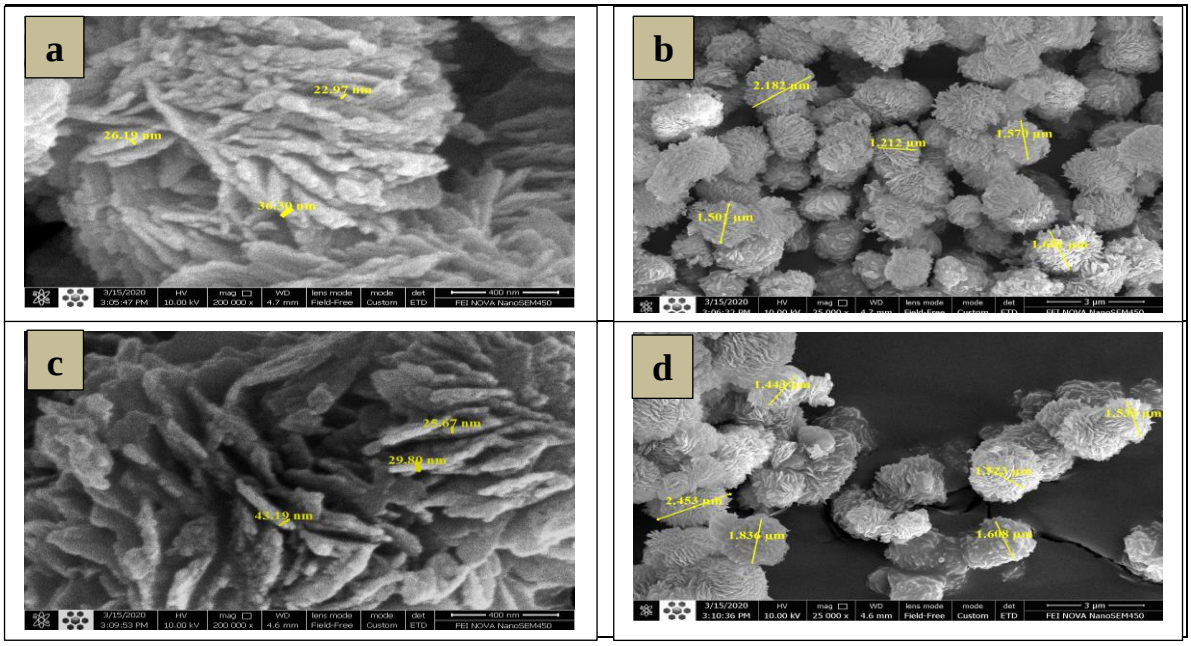

(Figure 3.9) SEM images of 3D hierarchical nanostructures for a,b) 30 minute c,d) 1 hour

IV. Synthesis by using the ultrasonication :

The ultrasonic waves were used instead of the magnetic stirrer at different times. At 15 minutes, the created diameters of around (35.92, 54.63, and 44.90) nm were thrown together in a haphazard manner, and the microspheres' surfaces were very rough .The microspheres' short petals grew in size as they expanded out of the primary aggregations, eventually forming ellipsoidal hierarchical nanostructures, as seen in (Figure 3.10.a,b). In (Figure 3.10.c,d) showed, the size of the microspheres short petals increased with diameters of around(49.23, 54.3, and 64.76) at 30 minutes. The microspheres' surfaces shrank after 60 minutes, and the microspheres narrow petals with diameters of around (31.61, 48.73, and 64.75) nm (Figure 3.10.e) revealed that [160]. Figure (3.10.f) depicts simple spherical shapes scattered and isolated from one another with a size of (3-5)µm, with the color greenish-yellow for all described.

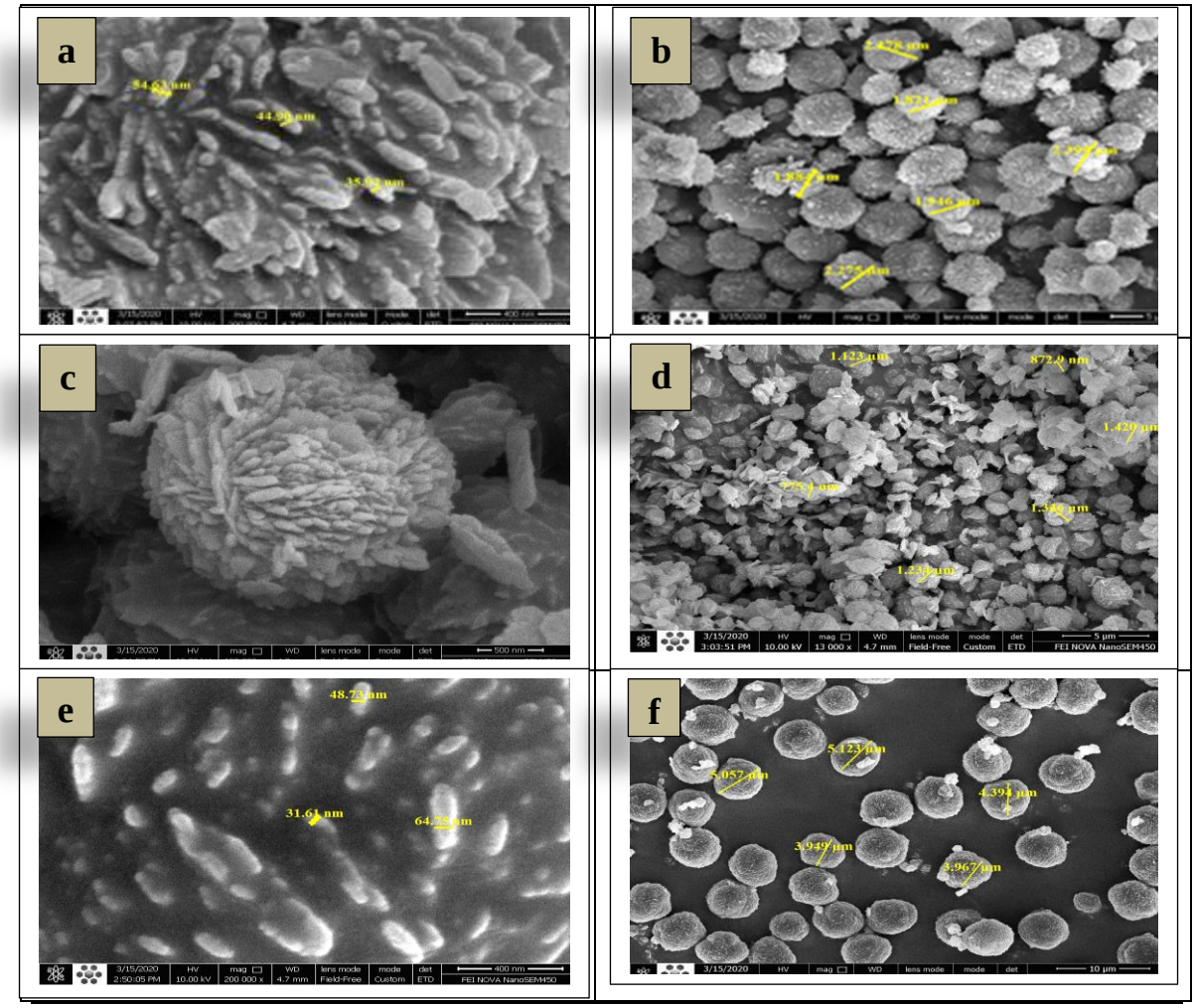

(Figure 3.10). SEM images of 3D hierarchical nanostructures when using ultrasonic at :(a,b) 15 min, (c,d) 30 min , (e,f) 60 min.

3.1.2.2 SEM of 3D hierarchical nanostructures after loading the drugs (Furosemide and Capecitabine)

The outer surface of the hierarchical nanostructures was studied after the loading process of Furosemide and Capecitabine by using the SEM analysis. (Figure 3.11.a, b, c,d) explains the appearance of overlapping leaflets of irregular sizes and in the form of spherical shapes spaced, which supports the results obtained with X-ray diffraction spectrum as well as FT-IR [161].

From the observation of the scanning electron microscope(SEM) images of theNanostructures with 3D hierarchical structures before the loading process Previously shown in (Figure 3.4), the presence of spherical shapes flowers-like with low porosity, while the SEM images of the hybrid nanostructure after the loading process showed the presence of structures with high porosity between the sheets they can store a greater amount of data due to their size as a result of the attraction between the drug and the hierarchical nanostructures, was the size of the microspheres short petals with diameters of around (60-100) nm [162].

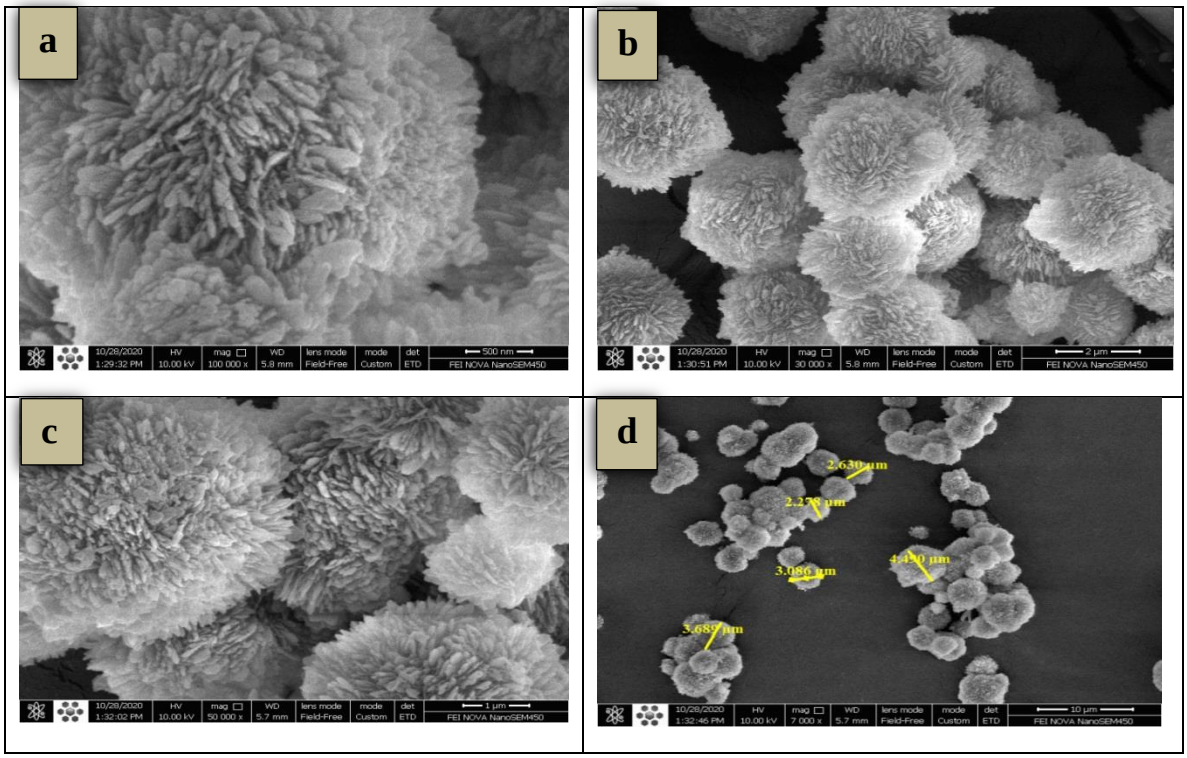

(Figure 3.11). SEM images of 3D hierarchical nanostructures after loading the drugs (a,b) Furosemide (c,d) Capecitabine

3.1.3 Fourier-transform infrared spectroscopy (FTIR)

FTIR technique was used to determine the functional group of solid materials such as Dopamine, PTA, POM- Dopamine, Furosemide drug, Capecitabine drug, and the drug loading process on the POM-Dopamine synthesis that diagnosed.

3.1.3.1 The Fourier transform infrared (FTIR) spectra of the flower-like microspheres, DA, and PTA.

(Figure 3.12.a) appears four main Keggin characteristic bands for PTA around 1082, 985, 891, and 800 cm^{-1}that are, respectively attributed to (P-O),(W-Ot), (W-Oc-W), and (W-Oe-W) stretching vibrations, wherein Ot, Oc, and Oe refer to the terminal, corner and edge oxygen‘s, respectively [24]. A strong and broadband appearing at 3281cm^{-1}corresponds to O–H stretching vibrations of the hydroxyl groups of PTA [163].

The Fourier transform infrared spectra of dopamine is depicted in (Figure 3.12.b), For dopamine, a wideband at low energy enclosing three important peaks has been observed, so the peaks at 3344 cm^{-1}, 3151 cm^{-1}, and 2960 cm^{-1} are assigned to stretching vibrations of the OH, CH aromatic NH groups of dopamine respectively. Other small peaks can be found in the range (2723–2642) cm^{-1}, which correspond to various CH vibrations in aryl or aliphatic CH bonds . At higher energies, significant bands can be seen at 1500 cm^{-1} and 1282 cm^{-1}, which correspond to CH's bending vibration and aryl oxygen's stretching vibration, respectively. The peak at 1348 cm^{-1} is attributed to the OH-groups of the dopamine(AD) molecule [164, 165].

After the incorporated DA with PTA, the ν(W-Oc-W) and ν(W-Oe-W) peaks shifted to 899 cm^{-1} and 823 cm^{-1}, respectively, suggesting strong hydrogen bonding or electrostatic interaction between the components[166,167]. Other absorption bands in the IR spectrum of the flower-like nanostructures were almost consistent with those of pure DA in (Figure3.12.c).

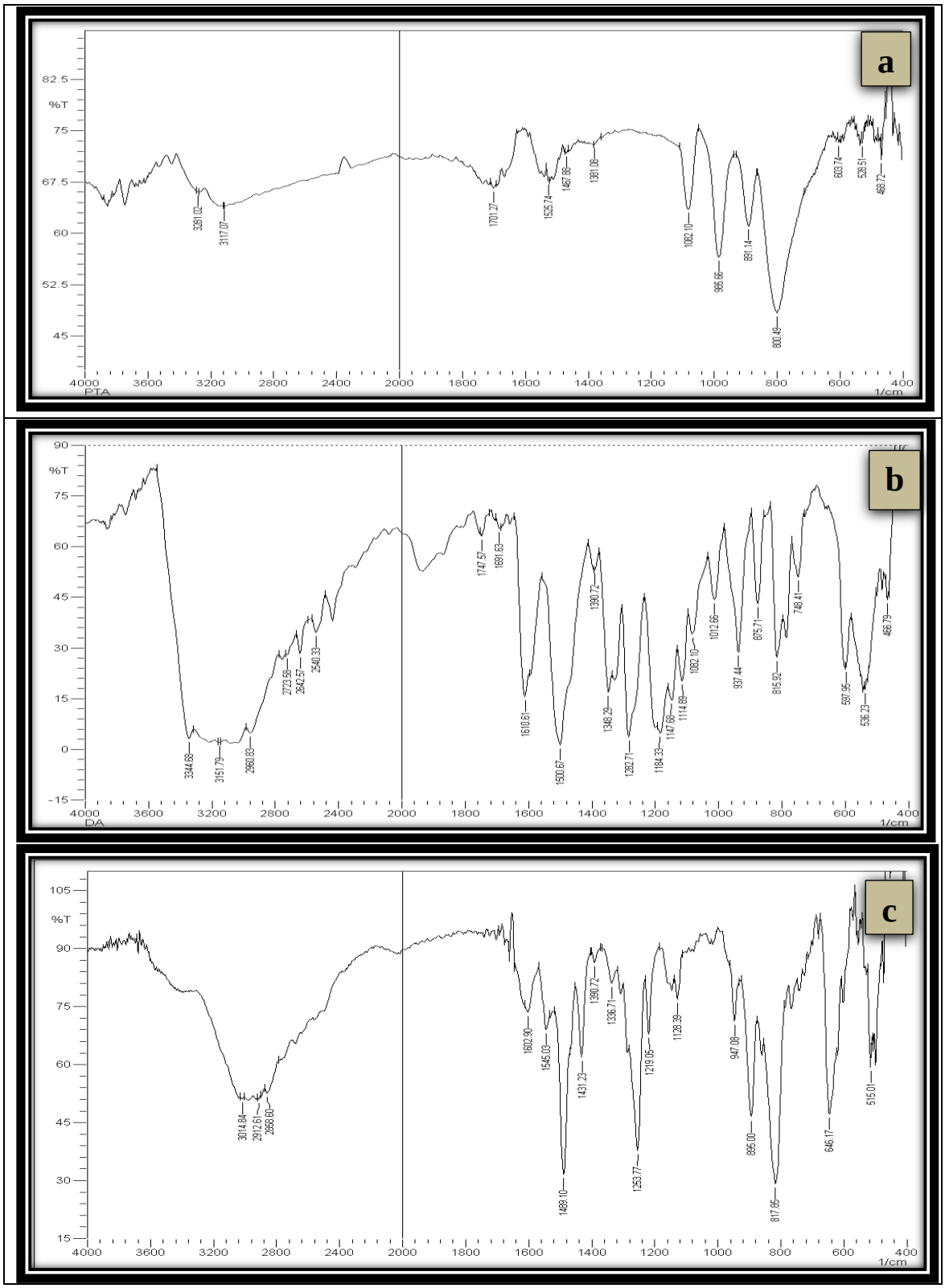

(Figure3.12). FTIR spectra of (a) PTA, (b) DA, and (C) The as-prepared flower-like hierarchical nanostructures.

3.1.3.2 The Fourier-transform infrared (FTIR) spectra of the two drugs (Furosemide, Capecitabine) pure and after loading on as-prepared flower-like hierarchical nanostructures

The FTIR spectrum of furosemide pure drug obtained in the solid phase, KBr pellets, shows well-defined bands with relatively high intensity in the (1800-400) cm^{-1} wavenumber range. In (Figure 3.13) the spectrum of pure furosemide appears the characteristic peaks at 3396.76 cm^{-1} for (O-H) stretch, 3350.46 cm^{-1} for (N-H) stretch, 3117.07 cm^{-1} for (C-H) stretch, 1564.32 cm^{-1} for (C=O) stretch, 1670.41 cm^{-1} for (N-H) bending, and 1242.20 cm^{-1} for (S=O) asymmetric stretch[168]. The (C-O-C) bond goes back to the furan ring [169-171].

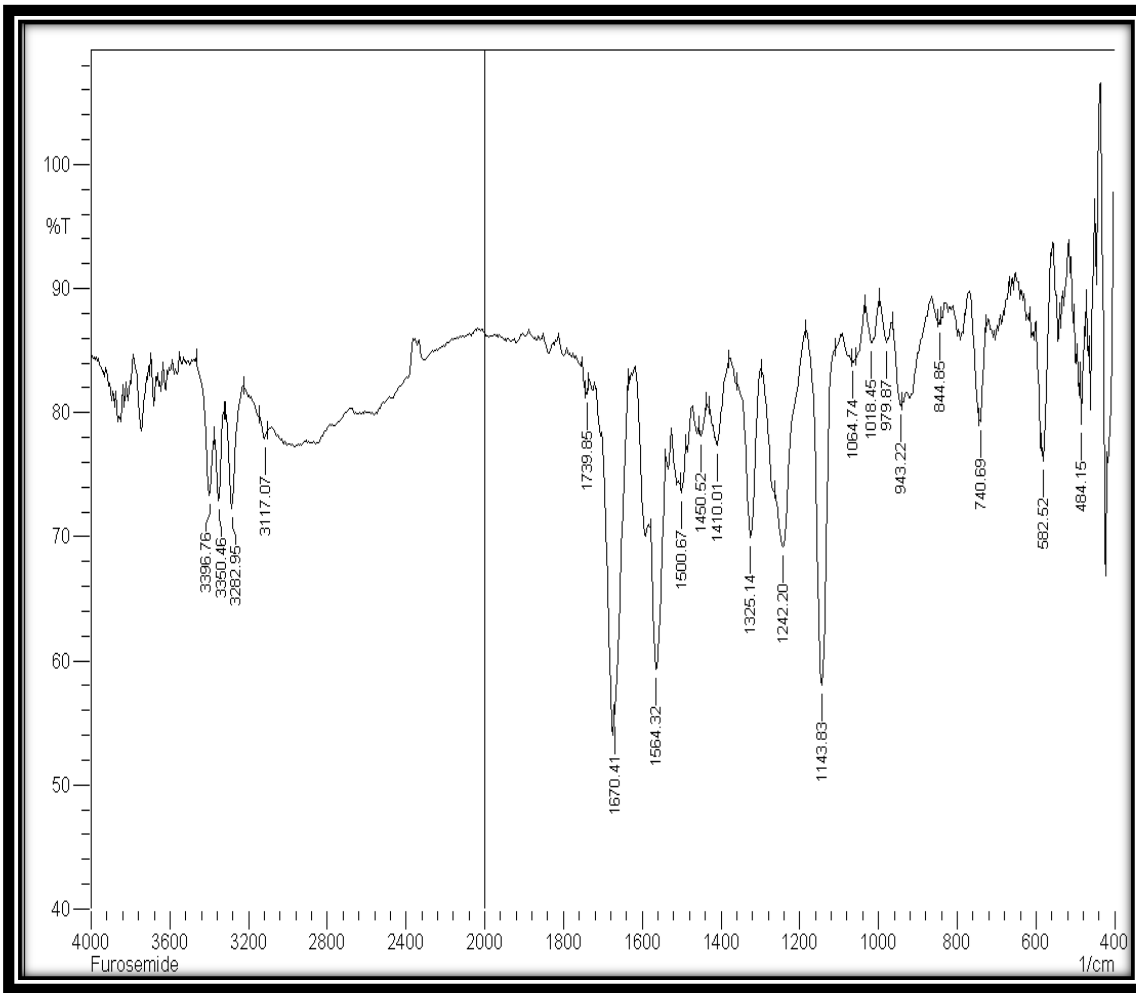

(Figure3.13). A spectrum of pure furosemide.

Figure (3.14) gave the as-prepared flower-like hierarchical nanostructures. Many new peaks suggested that the furosemide loading process on the hybrid nanostructure was effective. The presence of a peak with a frequency of 1672.34 cm^{-1} is related to (N-H bending) and 1564.32 cm^{-1} belongs to (C=O) stretch and 1143 cm^{-1} is related to(C-O-C) bond in the furan ring [172].

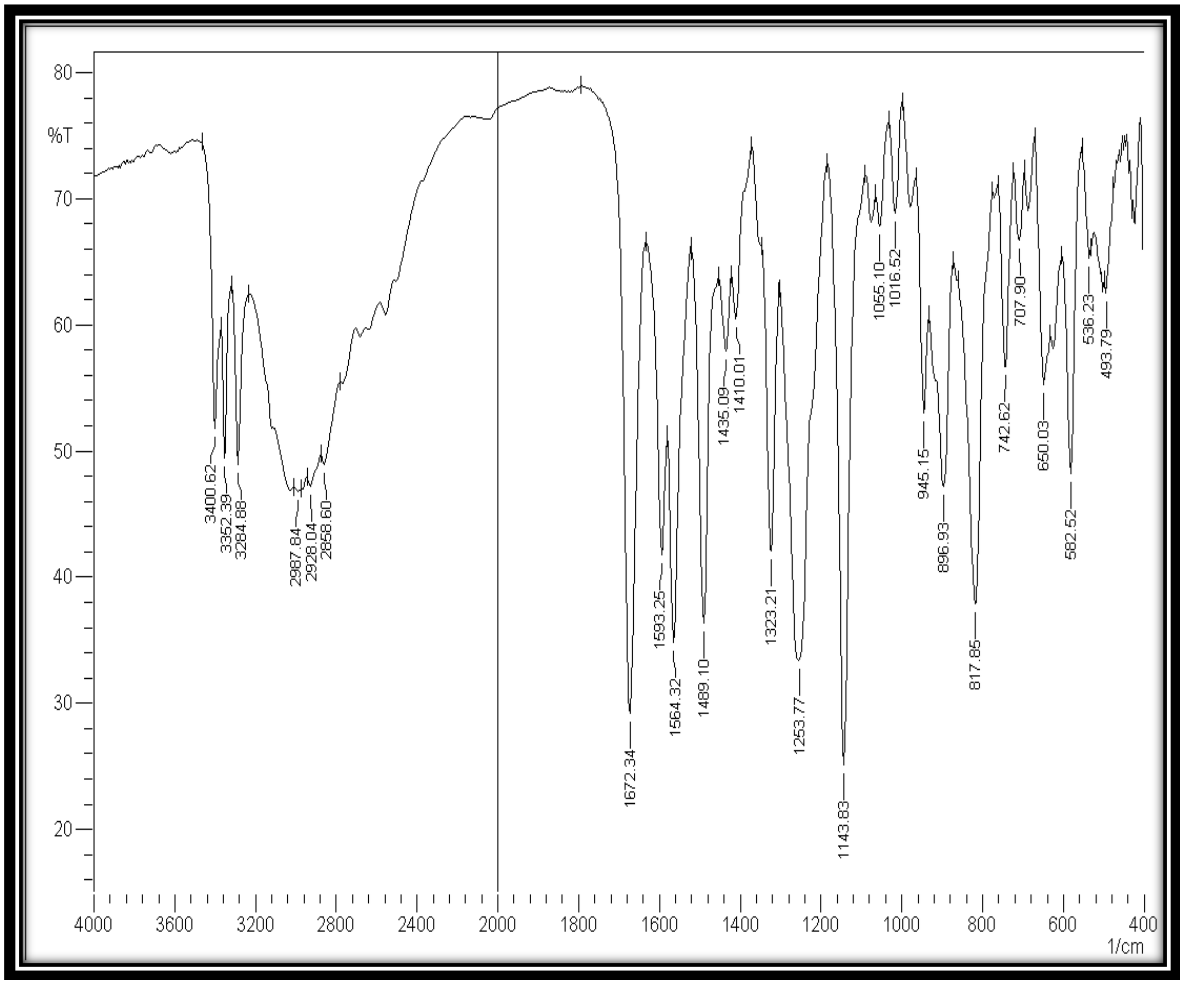

(Figure3.14). Spectrum of the as-prepared flowerlike hierarchical nanostructures after furosemide loading.

Different characteristic peaks were observed in Capecitabine in (Figure3.15) at 3520.21, 3161.43, 2960.83, 2870.17, 1716.70, 1647.26, 1612.54, and 1504.53cm^{-1}, which were assumed to be O-H stretch, CH-Stretch (alkane), CH stretch (aromatic), CH Stretch (alkene), C-O stretching from amide I, N-H bending and C-N stretching from amide II,-CH bending, -CH symmetrical deformation, and skeletal vibration of C-O stretching, respectively[173].

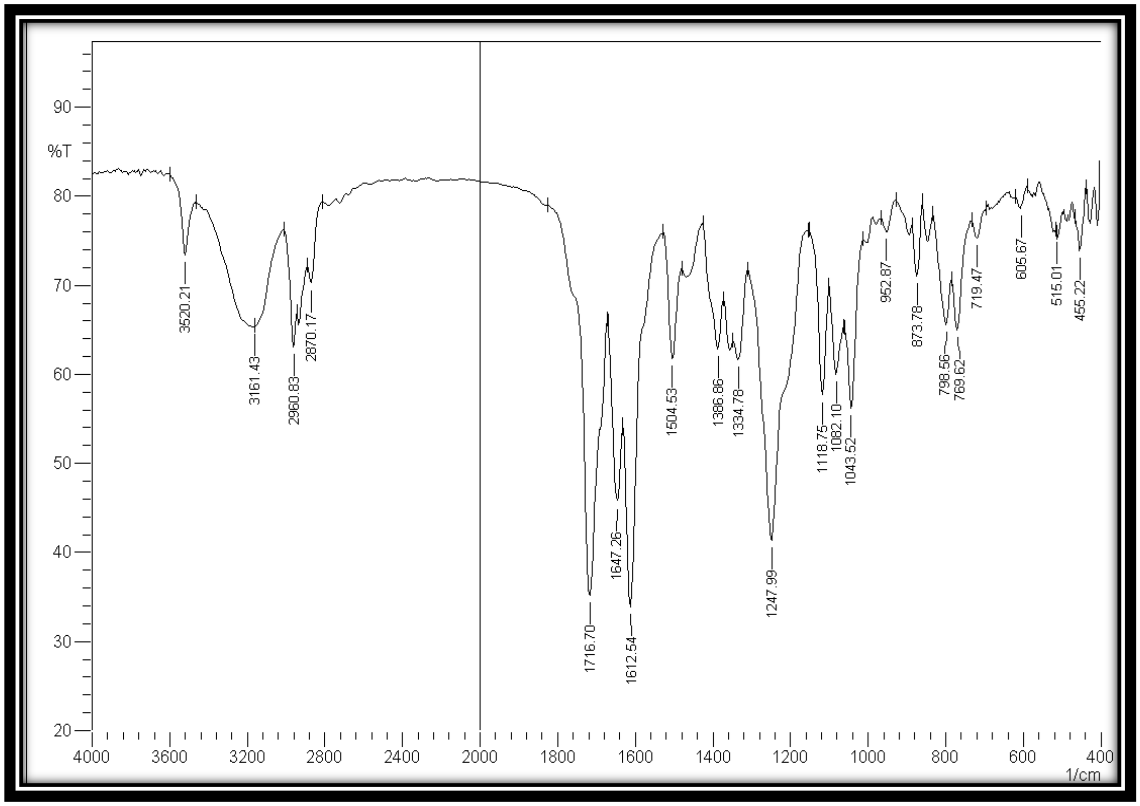

(Figure 3.15) the spectrum of pure Capecitabine

The as-prepared flower-like hierarchical nanostructures can be seen in Figure (3.16), which indicates to shift occur that due to its association with the metallic ion, after which the electrons are shifted towards a red offset, the peaks in flower-like hierarchical nanostructures are shifted from 3014.84 cm^{-1} to 3520.21cm^{-1} as (O-H stretch) and from 2912.61 cm^{-1} to 2985.91 cm^{-1} that belonging to CH-Stretch (alkane). While the 1716.70 cm^{-1} packages of the drug have disappeared belonging to C-O stretching from amide I and an indication of the occurrence of interdependence[174].

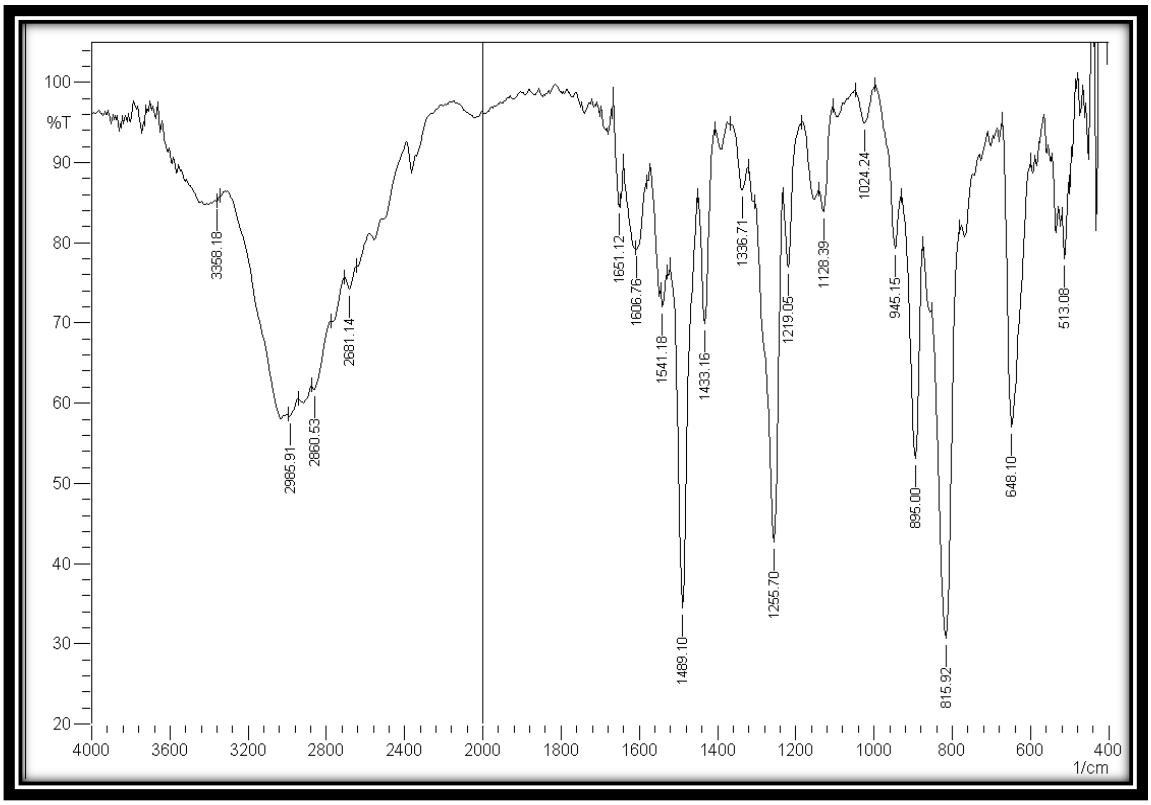

(Figure 3.16). The spectrum of the as-prepared flowerlike hierarchical nanostructures after Capecitabine loading.

3.1.4 Study the load ratios

The loading ratio of furosemide on the as-prepared flower-like hierarchical nanostructures in deionized water, at a temperature of 37°C, and during the different times (4, 6, 8, 10,12) hour. A powder of (10 mg) flower-like microspheres was immersed in an aqueous solution of (0.02 mg/mL) was done. The drug adsorbed amount on the flower-like microspheres was calculated by measuring the amount of supernatant that is absorbed on Synthesis of nano-PTA-D at 270 nm. (Figure 3.17) shows the relationship between the percentage of loading and time, as it is found that the lowest loading percentage is at four hours, and the highest loading rate occurred at 12 hours. The percentage of drug loading was calculated for each time using the equation (2.1).

Where the ratio of drug loading at (4, 6, 8, 10,12)hour was equal to (8% , 21% , 25% , 31% , 58%) respectively.

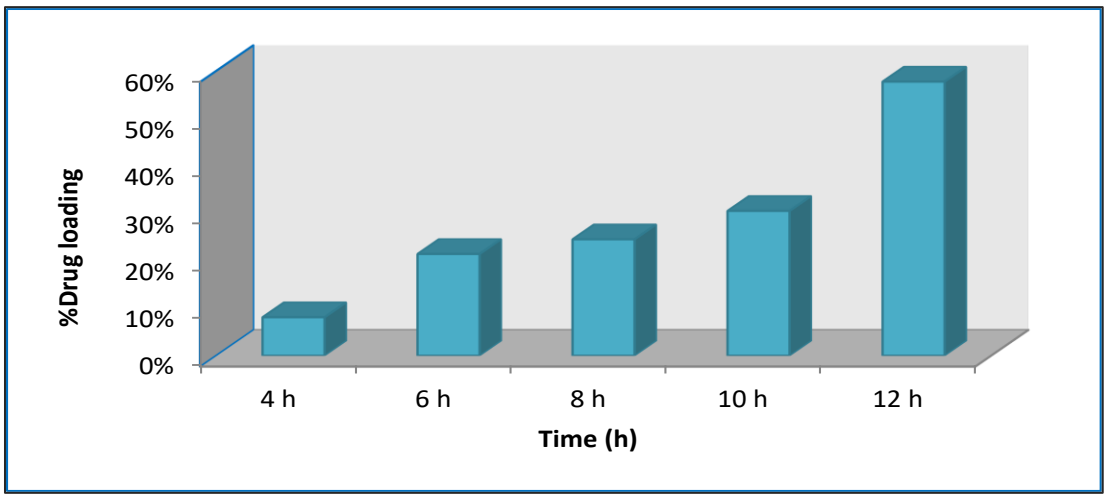

(Figure3.17).The relationship between time and the percentage of loading Furosemide on flowerlike microspheres

The loading ratio of Capecitabine was studied at the same mentioned conditions of furosemide drug. The exact (10 mg) of flowerlike microspheres powder was immersed in an aqueous solution of (1 mg/mL) drug. nm. (Figure 3.18) shows the relationship between the percentage of loading and time, as it is found that the lowest loading percentage is at four hours and the highest load rate occurred at 12 hours. The percentage of drug loading was calculated for each time using the equation (3.1). Where the ratio at (4, 6, 8, 10, 12) hour was equal to (3%,10%, 31%, 39%, 64%) respectively.

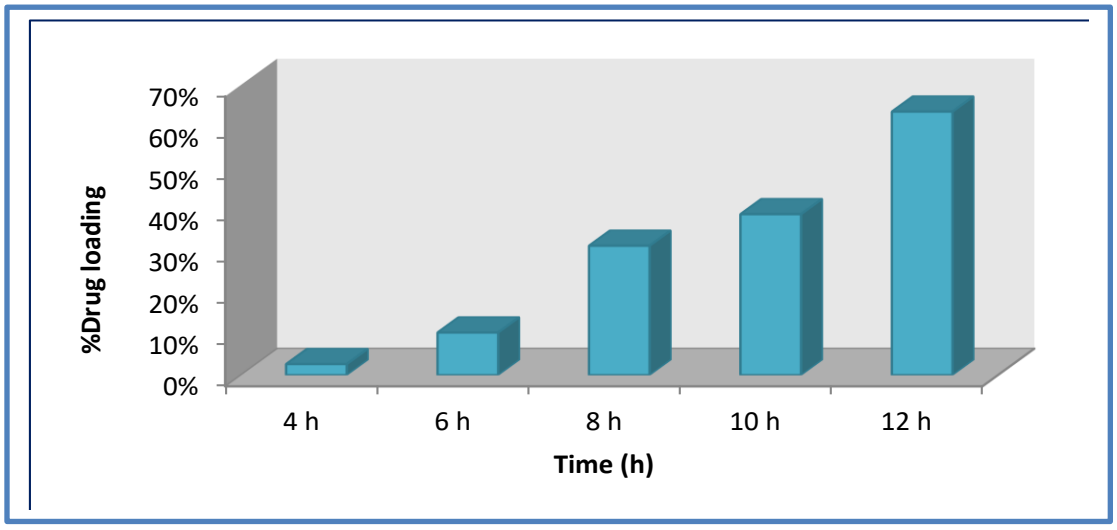

(Figure3.18). The relationship between time and the percentage of loading Capecitabine on flowerlike microspheres.

3.1.5 Study the percentage of Furosemide release

The percentage of Furosemide releasing from the flower-like microspheres, at the highest loading ratio (58%) was chosen, they have been carried out in pH (2.8) [glycine-HCl] buffer solution and pH (7.4) as Phosphate buffer saline (PBS) solution with a period of (1-33) hours. The amount of Furosemide released was determined based on the UV/Vis absorbance at 270 nm. With the passage of time, the absorbance increased. The amine groups of Furosemide are partially deprotonated at pH 7.4, but fully protonated at pH 2.8, according to (Figure 3.19) [174]. As a result, lower pH will favor protonated Furosemide adsorption. As a result, weaker electrostatic interactions between Furosemide and the flower-like microspheres could account for the higher release rate and cumulative release percentage at pH 7.4 compared to pH 2.8. The pH-responsive drug release behavior of the flower-like microspheres was demonstrated by the above results. Because the 3D hierarchical nanostructures could store drugs in acidic environments and then release them under basic conditions, they could be used to store and release drugs.

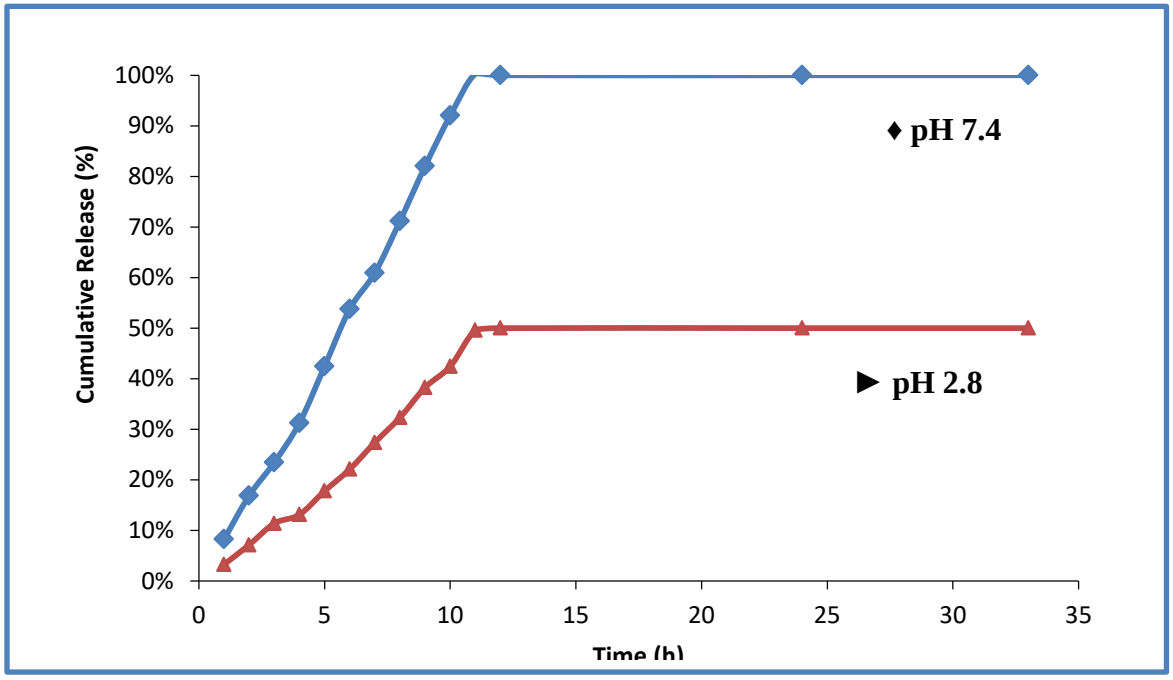

(Figure3.19). Profiles of drug release of Furosemide-loaded flower-like microspheres in pH (2.8) glycine-HCl buffer solution (►), and pH (7.4) phosphate buffered saline (PBS) solution (♦).

3.1.6 Study the percentage of Capecitabine release

The study of the percentage of Capecitabine release from the flower-like microspheres was chosen at the highest loading ratio 64%. The release

procedure was carried out in pH (2.8) as glycine-HCl buffer solution and pH (7.4) as Phosphate buffer saline (PBS) solution with the same previous time. The amount of Capecitabine released was measured based on the UV/Vis absorbance at 340 nm. In (Figure 3.20), the absorbance was increasing with increasing time, and note that the drug reached a 100% liberation rate in both acidic and neutral media with a slight advance in the neutral medium from the acid medium , and this could be attributed to the drug remaining adsorbed on the surface and did not enter the polyoxometalate.

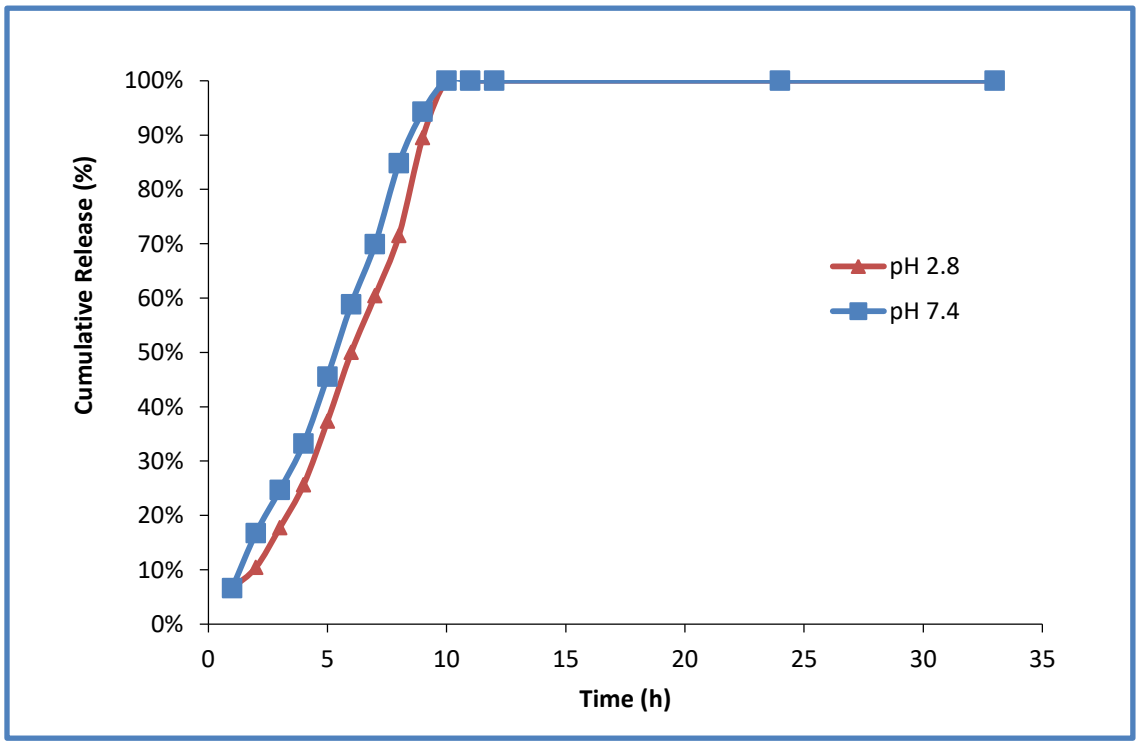

(Figure3.20). Profiles of drug release of Capecitabine-loaded flower-like microspheres in pH (2.8) glycine-HCl buffer solution (►), and pH (7.4) phosphate-buffered saline (PBS) solution (■).

3.1.7 Study of the release kinetics

The ion exchange kinetics of two drugs release in two buffer solutions glycine-HCl buffer solution in pH (2.8) and phosphate buffer saline in pH (7.4) have been studied by applying pseudo first-order and pseudo second-order equations. By applying the pseudo first-order equation as it was drawn [-log (1-Ct/CT)] against time (t), and the value of the coefficient of determination (R^2) was extracted[138]. Figures (3.21.a, 3.22.a, 3.23.a, 3.24.a) are shown that the mathematical model of the first pseudo-order is the most applicable to explain both drugs behavior for both buffer solutions under study. It reached the values of R^2 for Furosemide to (0.9141, 0.9311) and for Capecitabine to (0.8698, 0.8883) at buffer solutions glycine-HCl pH= 2.8 and PBS pH= 7.4, respectively.

The figure (3.21.b , 3.22.b , 3.23.b , 3.24.b) have shown the deviation of the values from the straight line, which indicates the non-compliance of the release process with the pseudo-second-order model this was shown by applying the pseudo-second-order equation, as it was drawn t/Ct against time (t). It reached the values of R^2 for Furosemide and Capecitabine as shown in table (3.4). Likewise, the reaction velocity constant for the first pseudo-order (k_1) and the second pseudo-second-order (k_2) were calculated [138], as shown in table (3.4).

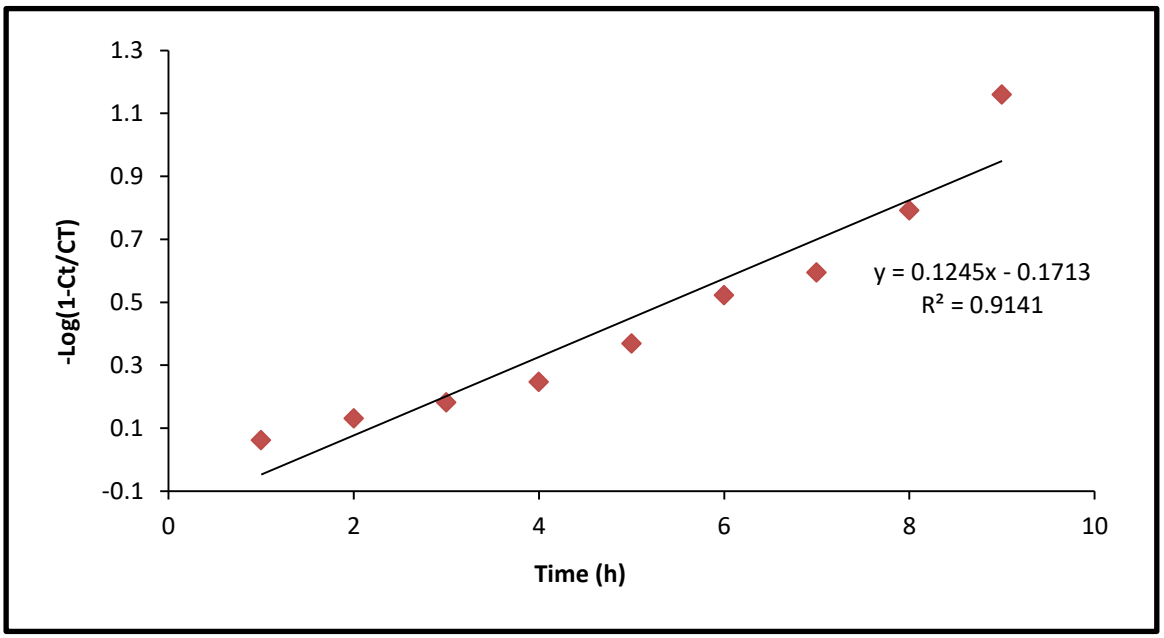

(a)

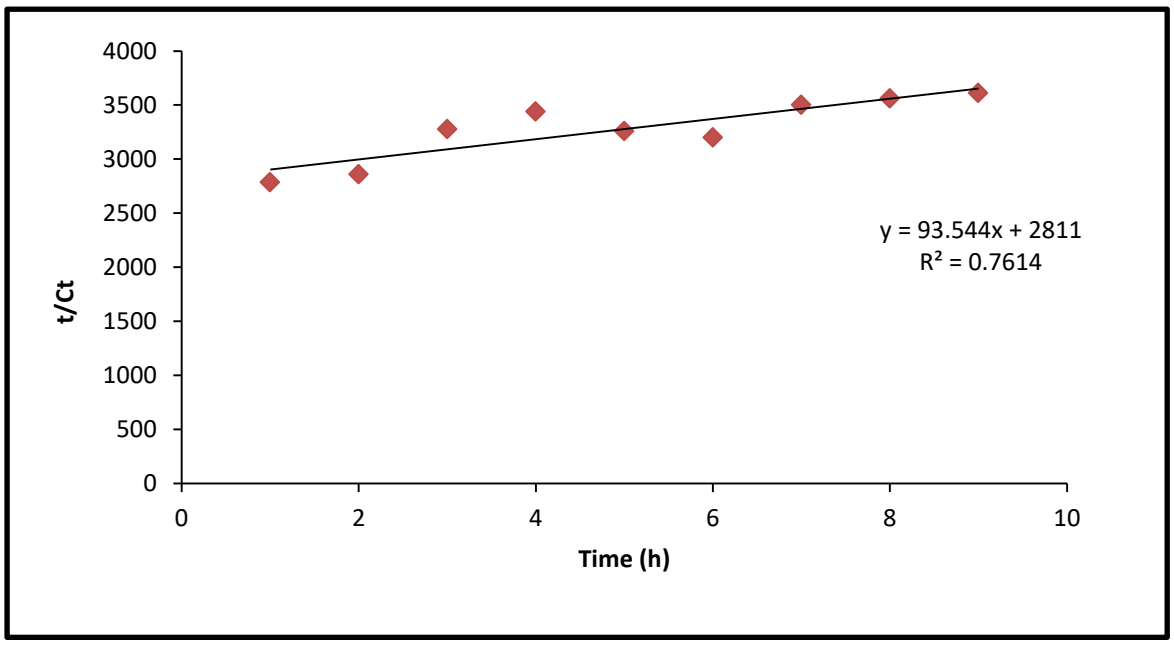

(b)

(Figure 3.21). (a)pseudo-first-order model of furosemide release, (b) pseudo-second-order model of furosemide release, in PBS solution pH 7.4.

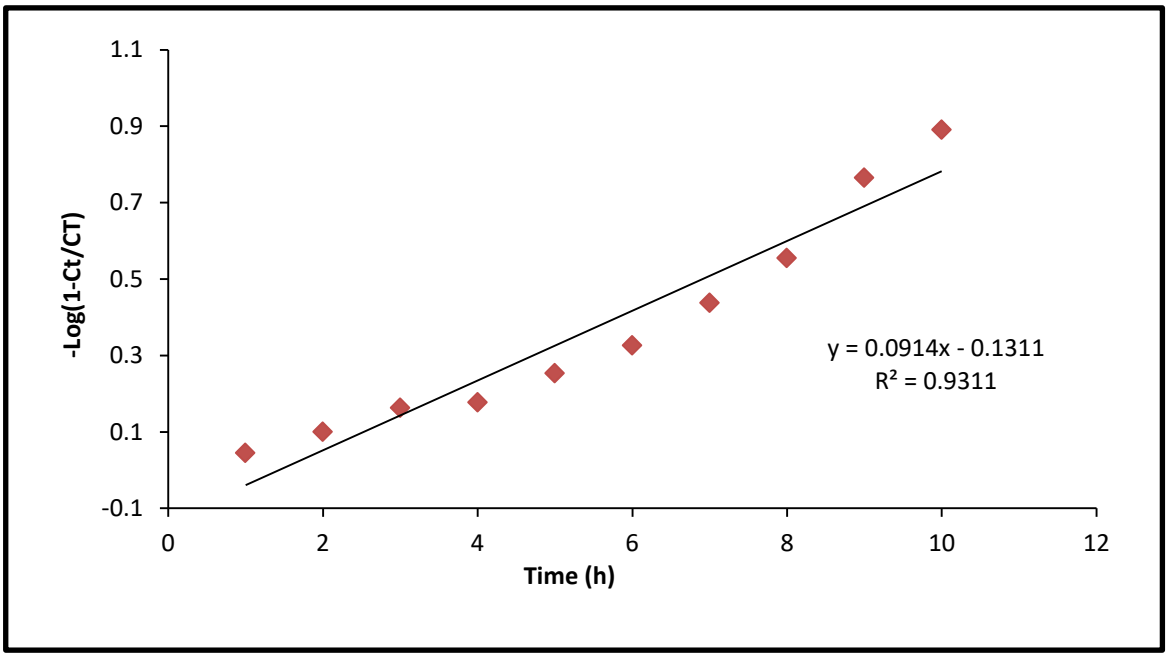

(a)

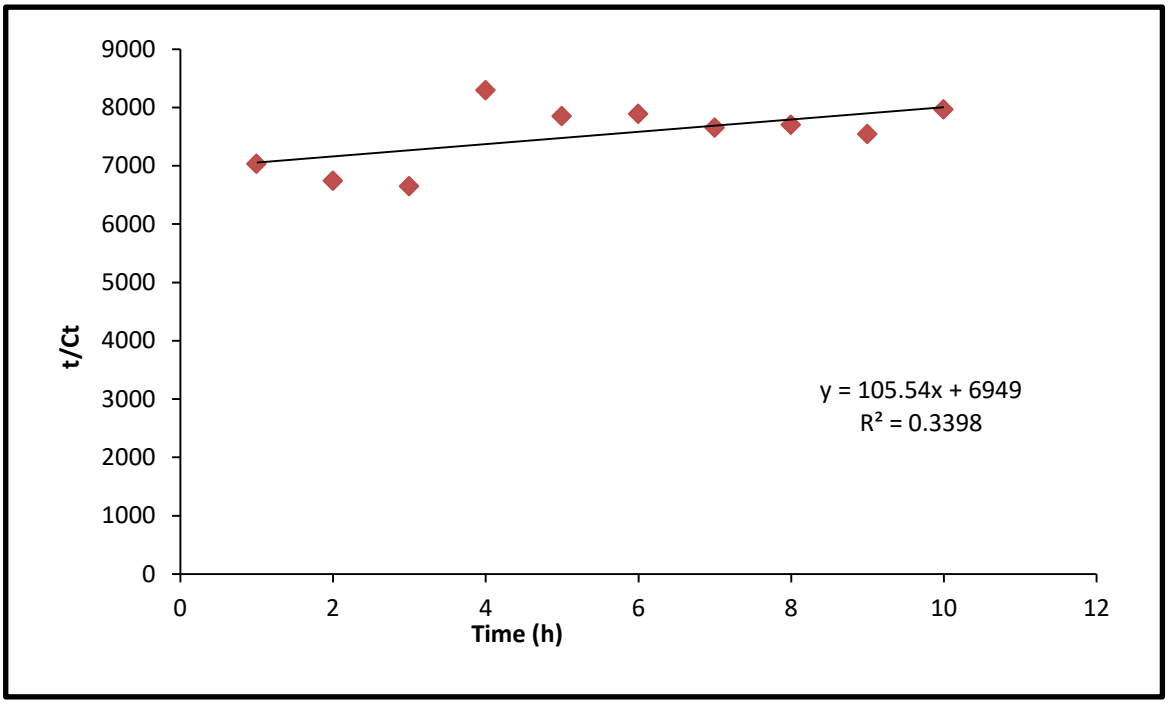

(b)

(Figure 3.22). (a) pseudo-first-order model of furosemide release, (b) pseudo-second-order model of furosemide release, in glycine-HCl buffer solution pH 2.8.

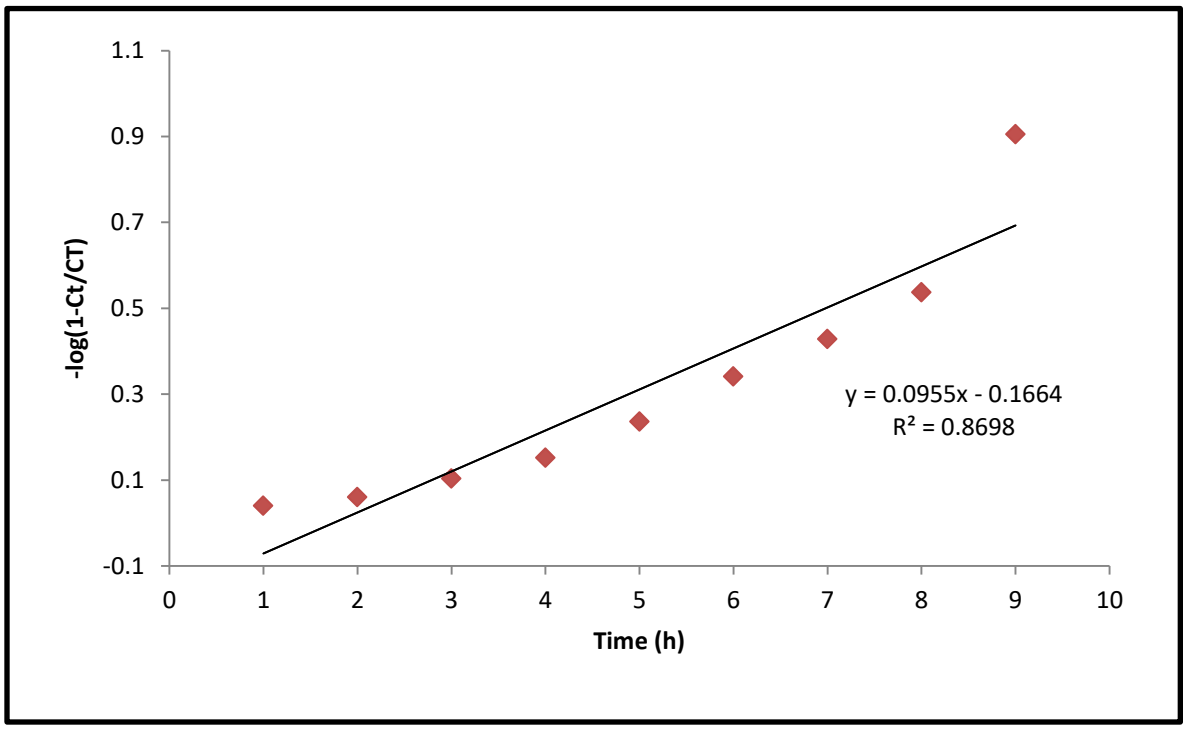

(a)

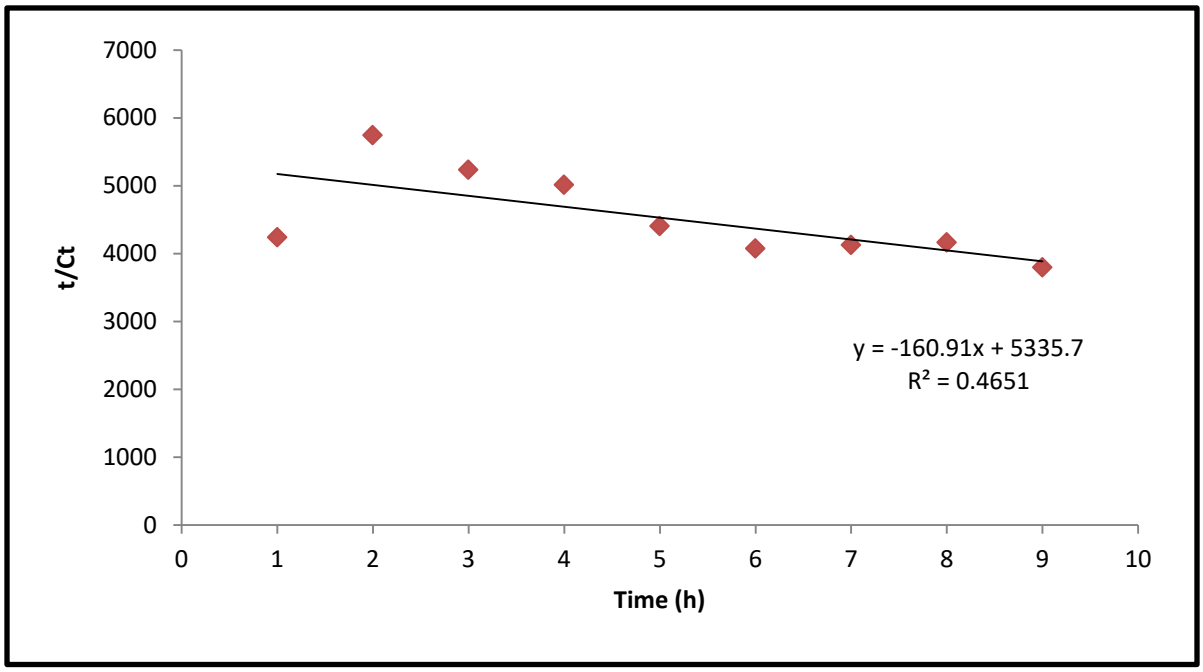

(b)

(Figure 3.23). (a)pseudo-first-order model of Capecitabine release, (b) pseudo-second-order model of Capecitabine release, in glycine-HCl buffer solution pH 2.8 .

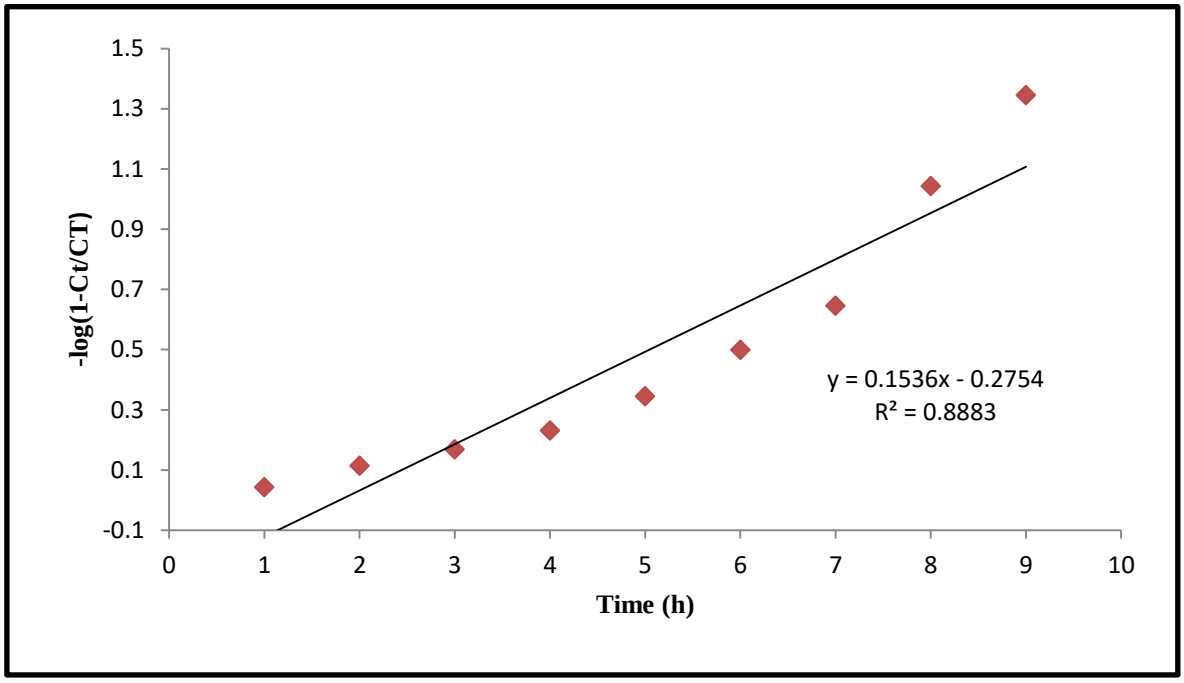

(a)

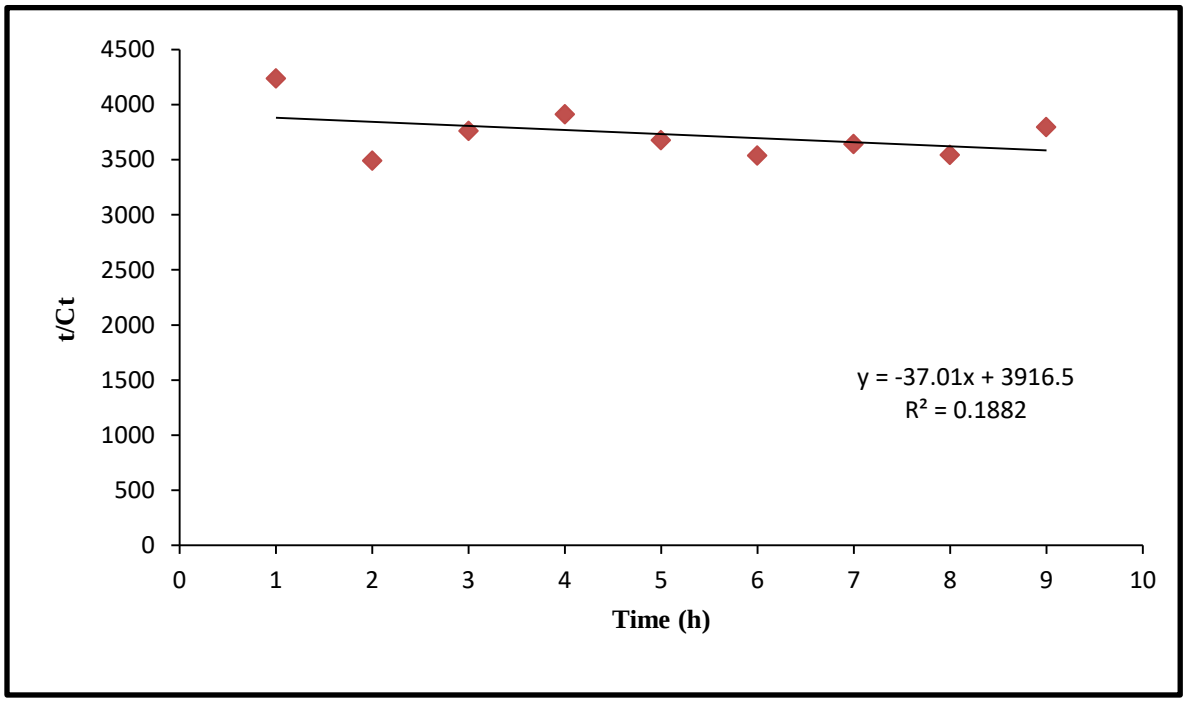

(b)

(Figure 3.24). (a)pseudo-first-order model of Capecitabine release, (b) pseudo-second-order model of Capecitabine release, in PBS solution pH 7.4.

(Table 3.4). The coefficient of determination and the constant velocity (k_1,k_2) of the releasing kinetics reaction for two drugs (Furosemide, Capecitabine).

NO.	The drugs	Type of buffer solution	The coefficient of determination(R^2)		reaction velocity constant(k)	
			Pseudo-first order	Pseudo-second order	k_1 h^{-1}	k_2 $L.h^{-1}$ mol^{-1}
1	Furosemide	PBS (pH 7.4)	0.9141	0.7614	0.2867	0.3212
		Glycine-HCl (pH 2.8)	0.9311	0.3398	0.2104	0.6238
2	Capecitabine	PBS (pH 7.4)	0.8883	0.1882	0.3537	2.8593
		Glycine-HCl (pH 2.8)	0.8698	0.4651	0.2199	2.8593

3.2 Conclusions

1. The 3D hierarchical nanostructures are successfully prepared and proved using XRD data, and the Sherrer equation. Co-assembly of a cationic bioactive component Dopamine (DA) and a Keggin type polyoxometalate(POM) phosphotungstic acid(PTA) is used to create the nanostructure , which is predominantly driven by hydrogen bonds and electrostatic interaction.
2. The 3D nano-structures shapes of different sizes can be obtained simply by controlling the ratio of the two building blocks by varying their concentrations of precursor materials, and the best ratio was (1:1), or the concentration of Tris-HCl solution or Changing the stirring time (using a magnetic stirrer or ultrasonic waves or microwave energy) and confirmed by SEM analysis, as a flowerlike hierarchical nanostructure and microstructure.
3. Two-stages 3D nanostructures were discovered by controlling the temporal evolution of the process of building nanostructures.
4. The as prepared flower-like hierarchical nanostructures demonstrated an excellent pH responsive release of Furosemide and Capecitabine in acidic medium and neutral media.
5. The kinetic study for releasing both drugs is found to be pseudo-first-order kinetics in acidic medium and neutral media. Moreover, the maximum releasing of both drugs was demonstrated in neutral media.

3.3 Recommendations

Several recommendations can be outlined in the future:

1. Further characterization for 3D hierarchical nanostructures using various techniques such as Energy-dispersive X-ray (EDX), transmission electron microscope (TEM), X-ray photoelectron spectra (XPS), Zeta potentials, and Confocal laser scanning microscopy (CLSM).
2. Preparation 3D hierarchical nanostructures using a various methodology like the Microwave technique.
3. Use another metal instead of tungsten, such as molybdenum or mixture from both to prepare another POM.
4. Using other medicines, such as (Paclitaxel, Temozolomide).

References

References

1. X. Huang, and C.S. Brazel, "On the importance and mechanisms of burst release in matrix-controlled drug delivery systems", *Journal of controlled release*, Vol. 73, no. (2-3), pp. 121-136, (2001).

2. A. A. Deshpande, C. T. Rhodes, N. H Shah, and, A. W. Malick,"Controlled-release drug delivery systems for prolonged gastric residence: an overview", *Drug development and industrial pharmacy*, Vol. 22, no. 6, pp.531-539, (1996).

3. S. Zhang, R. Geryak, J. Geldmeier, S. Kim and V. V. Tsukruk ,"Synthesis, assembly, and applications of hybrid nanostructures for biosensing", *Chem. Rev.* ,Vol. 117, no. 20, pp.12942-13038, (2017).

4. J. Jeevanandam, A. Barhoum, Y. S. Chan, A. Dufresne and M. K. Danquah, "Review on nanoparticles and nanostructured materials: history, sources, toxicity and regulations", *Beilstein Journal of Nanotechnology* Vol. 9, pp. 1050-1074, (2018).

5. N. A. Ochekpe, P. O. Olorunfemi, and N. C. Ngwuluka, "Nanotechnology and drug delivery part 2: nanostructures for drug delivery", *Tropical Journal of Pharmaceutical Research*, Vol. 8, no.3, pp. 275-287, (2009).

6. X. Huang, M. Li, D. C. Green, D. S. Williams, A. J. Patil, and S. Mann, "Interfacial assembly of protein–polymer nano-conjugates into stimulus-responsive biomimetic protocells", *Nature communications*, Vol. 4, no. 1, pp.1-9, (2013).

7. Y. Huang, X. Ran, Y. Lin, J. Ren, and X. Qu, "Self-assembly of an organic–inorganic hybrid nanoflower as an efficient biomimetic catalyst for self-activated tandem reactions", *Chemical Communications*, Vol. 51, no. 21, pp. 4386-4389, (2015).

8. B. J. Zern, H.Chu, A. O.Osunkoya, J. Gao, and Y. Wang, "A biocompatible arginine-based polycation", *Advanced functional materials*,Vol. 21, no.3, pp. 434-440, (2011).

9. Y.Gong, Q. Hu, N.Cheng, T.Wang, W. Xu, Y.Bi, and L. Yu, "Fabrication of pH- and temperature-directed supramolecular materials from 1D fibers to exclusively 2D planar structures using an ionic self-assembly approach" *Journal of Materials Chemistry C*, Vol. 3, no.14, pp.3273-3279, (2015).

10. Y. Huang, Y.Yan, B. M. Smarsly, Z.Wei, and C. F. Faul, "Helical supramolecular aggregates, mesoscopic organisation and nanofibers of a perylenebisimide–chiral surfactant complex via ionic self-assembly", *Journal of Materials Chemistry*, Vol.19, no.16, pp.2356-2362, (2009).

11. K.. Liu, R.Xing, C.Chen, G.Shen, L.Yan, Q. Zou, and X. Yan, "Peptide-Induced Hierarchical Long-Range Order and Photocatalytic Activity of Porphyrin Assemblies", *Angewandte Chemie International Edition*, Vol. 54, no.2, pp. 500-505, (2015).

12. J. T. Rhule, C. L. Hill, D. A. Judd, and R. F. Schinazi, "Polyoxometalates in medicine",*Chemical Reviews,*Vol. 98, no.1, pp. 327-358, (1998).

13. A. Al-Yasari, and J. Fielden, "Polyoxometalates in visible-light photocatalysis and solar energy conversion", *Reviews in Advanced Sciences and Engineering*, Vol. 3, no.4, pp. 304-319, (2014).

14. N. A. Peppas, "Intelligent biomaterials as pharmaceutical carriers in microfabricated and nanoscale devices", *MRS bulletin*, Vol. 31, no. 11, pp. 888-893, (2006).

15. C. Demetzos, and N. Pippa, "Advanced drug delivery nanosystems (aDDnSs): a mini-review",*Drug Delivery*, Vol. 21, no. 4, pp. 250-257, (2014).

16. A.Ganesan, "The impact of natural products upon modern drug discovery", *Current opinion in chemical biology*, Vol12, no.3, pp. 306-317, (2008).

17. Y. H. Yun, , B. K..Lee, and K. Park, "Controlled Drug Delivery: Historical perspective for the next generation", *Journal of Controlled Release*, Vol. 219, pp. 2-7, (2015).

18. K. Park, "Drug delivery research: the invention cycle", *Molecular pharmaceutics*, Vol.13,no. 7, pp.2143-2147, (2016).

19. A.Salimi, B. S. Makhmalzadeh, and G.Esfahani, "Polymeric micelle as a new carrier in oral drug delivery systems". *Asian J. Pharm*, Vol. 11, no. 4, pp. 704-711,(2017).

20. G. Esfahani, "Polymeric Micelle as a New Carrier in Oral Drug Delivery Systems", *Asian Journal of Pharmaceutics (AJP): Free full text articles from Asian J Pharm*, Vol.11, no. 04, (2018).

21. K.Park, "Drug delivery of the future: Chasing the invisible gorilla", *Journal of Controlled Release*, Vol. 240, pp. 2-8, (2016).

22. J. B. Dressman, G. L. Amidon, C. Reppas, and V. P. Shah, "Dissolution testing as a prognostic tool for oral drug absorption: immediate release dosage forms", *Pharmaceutical research*, Vol. 15, no. 1, pp. 11-22, (1998).

23. A.Maroni, A. Melocchi, L.Zema, A. Foppoli, and A.Gazzaniga, "Retentive drug delivery systems based on shape memory materials", *Journal of Applied Polymer Science*, Vol.137,no. 25, pp.48798, (2020).

24. J.Stockwell, N. Abdi, X. Lu, O. Maheshwari, and C.Taghibiglou, "Novel central nervous system drug delivery systems", *Chemical biology & drug design*, Vol.83, no.5, pp.507-520, (2014).

25. B. S. Dave, A. F. Amin, and M. M. Patel, "Gastroretentive drug delivery system of ranitidine hydrochloride: formulation and in vitro evaluation", *Aaps PharmSciTech*, Vol. 5, no.2, pp.77-82, (2004).

26. S. A. Stewart, J. Domínguez-Robles, V. J. McIlorum, , E. Mancuso, D. A. Lamprou, R. F. Donnelly, and E. Larrañeta, "Development of a biodegradable subcutaneous implant for prolonged drug delivery using 3D printing", Pharmaceutics, Vol.12, no.2, pp.105, (2020).

27. S. H.Lim, H.Kathuria, J. J. Y.Tan, and L.Kang, "3D printed drug delivery and testing systems—a passing fad or the future?", *Advanced drug delivery reviews*, Vol. 132, pp.139-168,(2018).

28. S. Hossen, M. K.Hossain, M. K.Basher, M. N. H. Mia, M. T. Rahman, and M. J. Uddin, "Smart nanocarrier-based drug delivery systems for cancer therapy and

toxicity studies: A review", *Journal of advanced research*, Vol. 15, pp. 1-18, (2019).

29. O.Tacar, P. Sriamornsak, and C. R. Dass, "Doxorubicin: an update on anticancer molecular action, toxicity and novel drug delivery systems", *Journal of pharmacy and pharmacology*, Vol. 65, no.2, pp. 157-170, (2013).

30. A. Misra, S.Ganesh, A.Shahiwala, and S. P. Shah, "Drug delivery to the central nervous system: a review", *J Pharm Pharm Sci*, Vol. 6, no. 2, pp. 252-273,(2003).

31. G.Vilar, J.Tulla-Puche, and F. Albericio, "Polymers and drug delivery systems", *Current drug delivery*, Vol. 9, no.4, pp.367-394., (2012).

32. S.Parveen, R. Misra, and S. K. Sahoo, "Nanoparticles: a boon to drug delivery, therapeutics, diagnostics and imaging", *Nanomedicine: Nanotechnology, Biology and Medicine*, Vol. 8, no.2, pp.147-166, (2012).

33. R. Mara Mainardes, M. Cristina Cocenza Urban, P.Oliveira Cinto, M.Vinicius Chaud, R.Cesar Evangelista, and M.Palmira Daflon Gremiao,"Liposomes and micro/nanoparticles as colloidal carriers for nasal drug delivery", *Current drug delivery*, Vol. 3, no.3, pp.275-285,(2006).

34. V. J. Mohanraj, and Y. Chen, "Nanoparticles-a review", *Tropical journal of pharmaceutical research*, Vol. 5, no. 1, pp. 561-573, (2006).

35. B. Kumar, K. Jalodia, P. Kumar, and H. K. Gautam, "Recent advances in nanoparticle-mediated drug delivery", *Journal of Drug Delivery Science and Technology*, Vol. 41, pp. 260-268. (2017).

36. S. Shen, Y. Wu, Y. Liu, and D. Wu, "High drug-loading nanomedicines: progress, current status, and prospects", *International journal of nanomedicine*, Vol. 12, pp. 4085, (2017).

37. A. J. Gavasane, and H. A. Pawar, "Synthetic biodegradable polymers used in controlled drug delivery system: an overview", *Clin Pharmacol Biopharm*, Vol. 3, no. 2, pp. 1-7, (2014).

38. M. R. Shaik, M. Korsapati, and D. Panati, "Polymers in controlled drug delivery systems", *International journal of pharma sciences*, Vol. 2, no.4, pp.112-116, (2012).

39. N. Kamaly, B. Yameen, J. Wu, and O. C. Farokhzad, "Degradable controlled-release polymers and polymeric nanoparticles: mechanisms of controlling drug release", *Chemical reviews*, Vol. 116, no. 4, pp.2602-2663, (2016).

40. D. Bennet, and S. Kim, "Polymer nanoparticles for smart drug delivery", *Application of nanotechnology in drug delivery*, pp. 257-310, (2014).

41. Z. Cao, W. Li, R. Liu, X. Li, H. Li, L. Liu, Y. Liu, "pH-and enzyme-triggered drug release as an important process in the design of anti-tumor drug delivery systems", *Biomedicine & Pharmacotherapy*, Vol. 118, pp.109340, (2019).

42. Y. Lu, and S. C. Chen, "Micro and nano-fabrication of biodegradable polymers for drug delivery", *Advanced drug delivery reviews*, Vol. 56, no. 11, pp.1621-1633, (2004).

43. Y. Hayashi, J. M. Harris, and A. S. Hoffman, "Delivery of PEGylated drugs from mucoadhesive formulations by pH-induced disruption of H-bonded complexes of PEG-drug with poly (acrylic acid)", *Reactive and Functional Polymers*, Vol. 67, no. 11, pp.1330-1337, (2007).

44. M. Sowjanya, S. Debnath, P. Lavanya, "Thejovathi, R., & Babu, M. N. Polymers used in the Designing of Controlled Drug Delivery System", *Research Journal of Pharmacy and Technology*, Vol. 10, no. 3, pp. 903-912, (2017).

45. D. Singh Malik, N. Mital, and G. Kaur, "Topical drug delivery systems: a patent review", *Expert opinion on therapeutic patents*, Vol. 26, no. 2, pp. 213-228, (2016).

46. L. Brannon-Peppas, "Polymers in controlled drug delivery", *Medical Plastic and Biomaterials*, Vol. 4, pp.34-45, (1997).

47. M.Goldberg, R. Langer, and X.Jia, "Nanostructured materials for applications in drug delivery and tissue engineering", *Journal of Biomaterials Science, Polymer Edition*, Vol.18, no.3, pp. 241-268, (2007).

48. G.Adlakha-Hutcheon, R.Khaydarov, R.Korenstein, R.Varma, A.Vaseashta, H.Stamm, and M.Abdel-Mottaleb, "Nanomaterials, nanotechnology. In Nanomaterials: Risks and Benefits", *Springer, Dordrecht*, pp. 195-207, (2009).

49. H.Cui, M. J.Webber, and S. I. Stupp, "Self-assembly of peptide amphiphiles: From molecules to nanostructures to biomaterials", *Peptide Science: Original Research on Biomolecules*, Vol. 94, no.1, pp.1-18,(2010).

50. D. Kanjana, "Advancement of nanotechnology applications on plant nutrients management and soil improvement". *In Nanotechnology Springer*, pp. 209-234, (2017).

51. W.Zhang, and Z. Hu, "Recent advances in sample preparation methods for elemental and isotopic analysis of geological samples", *Spectrochimica Acta Part B: Atomic Spectroscopy*, Vol.160, pp.105690, (2019).

52. R. Ravichandran, "Nanotechnology applications in food and food processing: innovative green approaches, opportunities and uncertainties for global market", *International Journal of Green Nanotechnology: Physics and Chemistry*, Vol.1, no.2, P72-P96, (2010).

53. X. F. Zhang, Z. G. Liu, W.Shen, and S.Gurunathan, "Silver nanoparticles: synthesis, characterization, properties, applications, and therapeutic approaches", *International journal of molecular sciences*, Vol.17, no.9, pp. 1534, (2016).

54. A.De, R.Bose, A.Kumar, and S. Mozumdar, "Targeted delivery of pesticides using biodegradable polymeric nanoparticles", *New Delhi: Springer India*, pp. 59-81, (2014).

55. I.Ghiuţă, D.Cristea, and D.Munteanu, "Synthesis methods of metallic nanoparticles-An overview", Bulletin of the Transilvania University of Brasov. Engineering Sciences. Series I, Vol. 10, no.2, pp.133-140, (2017).

56. K. Jain, N. K. Mehra, and N. K. Jain, "Potentials and emerging trends in nanopharmacology", *Current opinion in pharmacology*, Vol.15, pp. 97-106, (2014).

57. M. A. Robles-García, F. Rodriguez-Felix, , E.Marquez-Rios, , J. A. Aguilar, A.Barrera-Rodriguez, J.Aguilar, and C. L. Del-Toro-Sánchez, "Applications of nanotechnology in the agriculture, food, and pharmaceuticals", *Journal of Nanoscience and Nanotechnology*, Vol.16, no.8, pp. 8188-8207, (2016).

58. A.Pudlarz, and J.Szemraj, "Nanoparticles as carriers of proteins, peptides and other therapeutic molecules", *Open Life Sciences*, Vol. 13, no.1, pp.285-298, (2018).

59. F. ud Din, W.Aman, I.Ullah, O. S.Qureshi, O. Mustapha, S.Shafique, and A. Zeb, "Effective use of nanocarriers as drug delivery systems for the treatment of selected tumors", *International journal of nanomedicine*, Vol.12, pp.7291, (2017).

60. B. H. Rehm, "Biogenesis of microbial polyhydroxyalkanoate granules: a platform technology for the production of tailor-made bioparticles", *Current issues in molecular biology*, Vol. 9, no.1, pp. 41, (2007).

61. A. Z.Wilczewska, K. Niemirowicz, K. H. Markiewicz, and H.Car, "Nanoparticles as drug delivery systems", *Pharmacological reports*, Vol. 64, no.5, pp.1020-1037, (2012).

62. A.Baeza, M.Colilla, and M.Vallet-Regí, "Advances in mesoporous silica nanoparticles for targeted stimuli-responsive drug delivery", *Expert opinion on drug delivery*, Vol.12, no.2, pp. 319-337, (2015).

63. M. A.Ghaz-Jahanian, F. Abbaspour-Aghdam, N.Anarjan, A.Berenjian, and H.Jafarizadeh-Malmiri, "Application of chitosan-based nanocarriers in tumor-targeted drug delivery", *Molecular biotechnology*, Vol.57, no.3, pp.201-218, (2015).

64. Y. Yun, , Y. W. Cho, and K. Park, "Nanoparticles for oral delivery: targeted nanoparticles with peptidic ligands for oral protein delivery", *Advanced drug delivery reviews*, Vol. 65, no. 6, pp. 822-832, (2013).

65. D. Nevozhay, U. Kańska, R. Budzyńska, and J.Boratyński, "Current status of research on conjugates and related drug delivery systems in the treatment of cancer and other diseases", *Postepy higieny i medycyny doswiadczalnej (Online)*, Vol.61, pp. 350-360,(2007).

66. M. Malamatari, K. M.Taylor, S. Malamataris, D. Douroumis, and K. Kachrimanis, "Pharmaceutical nanocrystals: production by wet milling and applications", *Drug Discovery Today*, Vol. 23, no. 3, pp. 534-547,(2018).

67. R. Shegokar, R. H. Müller, "Nanocrystals: industrially feasible multifunctional formulation technology for poorly soluble actives", *International journal of pharmaceutics*, Vol.399, no.1-2, pp. 129-139, (2010).

68. C. M. Keck, and R. H. Müller, "Drug nanocrystals of poorly soluble drugs produced by high pressure homogenization", *European journal of pharmaceutics and biopharmaceutics*, Vol. 62, no.1, pp. 3-16, (2006).

69. C. Brough, and R. O. Williams Iii, "Amorphous solid dispersions and nano-crystal technologies for poorly water-soluble drug delivery", *International journal of pharmaceutics*, Vol. 453, no.1, pp. 157-166, (2013).

70. A. de la Escosura-Muñiz, A. Ambrosi, and A. Merkoçi, "Electrochemical analysis with nanoparticle-based Biosystems", *TrAC Trends in Analytical Chemistry*, Vol. 27, no.7, pp.568-584, (2008).

71. S. Ranghar, P. Sirohi, P.Verma, and V. Agarwal, "Nanoparticle-based drug delivery systems: promising approaches against infections", *Brazilian Archives of Biology and Technology*, Vol.57, no.2, pp. 209-222, (2014).

72. J. Leleux, and R. O. Williams, "Recent advancements in mechanical reduction methods: particulate systems", *Drug development and industrial pharmacy*, Vol. 40, no. 3, pp. 289-300, (2014).

73. H. K. Chan, and P. C. L. Kwok, "Production methods for nanodrug particles using the bottom-up approach", *Advanced drug delivery reviews*, Vol. 63, no. 6, pp. 406-416, (2011).

74. J. Hu, , K. P. Johnston, and R. O. Williams III, "Nanoparticle engineering processes for enhancing the dissolution rates of poorly water soluble drugs", *Drug development and industrial pharmacy*, Vol. 30, no. 3, pp. 233-245. (2004).

75. K. T. Savjani, A. K. Gajjar, and J. K. Savjani, "Drug solubility: importance and enhancement techniques", *ISRN pharmaceutics*, Vol. 2012, pp. 10 (2012).

76. R. Sheikh, N. Walsh, M. Clynes, R. O'Connor, and R. McDermott, "Challenges of drug resistance in the management of pancreatic cancer", *Expert review of anticancer therapy*, Vol. 10, no.10, pp.1647-1661, (2010).

77. C. M. Walko, and C. Lindley, "Capecitabine: a review", *Clinical therapeutics*, Vol. 27, no. 1, pp. 23-44, (2005).

78. D. R. Budman, N. J. Meropol, B. Reigner, P. J. Creaven, S. M. Lichtman, , E. Berghorn, , and T. Griffin, "Preliminary studies of a novel oral fluoropyrimidine

carbamate: capecitabine", *Journal of clinical oncology*, Vol. 16, no. 5, pp.1795-1802, (1998).

79. N. Shimma, I. Umeda, M. Arasaki, C. Murasaki, K. Masubuchi, Y. Kohchi, and H. Ishitsuka, "The design and synthesis of a new tumor-selective fluoropyrimidine carbamate, capecitabine", *Bioorganic & medicinal chemistry*, Vol. 8, no. 7, pp. 1697-1706, (2000).

80. M. Miwa, M. Ura, M. Nishida, N. Sawada, T. Ishikawa, K. Mori, H. Ishitsuka, "Design of a novel oral fluoropyrimidine carbamate, capecitabine, which generates 5-fluorouracil selectively in tumours by enzymes concentrated in human liver and cancer tissue", *European journal of cancer*, Vol. 34, no. 8, pp.1274-1281, (1998).

81. B. R. Hirsch, and S. Y. Zafar, "Capecitabine in the management of colorectal cancer", *Cancer management and research*, Vol. 3, no. 79, (2011).

82. T O. H. emmink, T. Emura, M. De Bruin, M. Fukushima, and G. J. Peters, "Therapeutic potential of the dual-targeted TAS-102 formulation in the treatment of gastrointestinal malignancies", *Cancer science*, Vol. 98, no. 6, pp.779-789, (2007).

83. S. A. Qureshi, and I. J. McGilveray, "Assessment of pharmaceutical quality of furosemide tablets from multinational markets", *Drug development and industrial pharmacy*, Vol. 24, no. 11, pp. 995-1005, (1998).

84. S. Herrmann, New Synthetic Routes to Polyoxometalate Containing Ionic Liquids-An Investigation of their Properties, 1st ed., Springer Fachmedien Wiesbaden, Germany, p. 6, (2015).

85. M. José Ruiz-Angel, A. Berthod, S. Carda-Broch, and M.Celia García-Álvarez-Coque, "Analytical techniques for furosemide determination", *Separation & Purification Reviews*, Vol. 35, no. 02, pp.39-58, (2006).

86. M. Zilker, F. Sörgel, and U. Holzgrabe, "A systematic review of the stability of finished pharmaceutical products and drug substances beyond their labeled expiry dates", *Journal of Pharmaceutical and Biomedical Analysis*, Vol. 166, pp. 222-235, (2019).

87. K. M. Ho, and B. M. Power, Benefits and risks of furosemide in acute kidney injury. *Anaesthesia*, Vol. 65, no. 3, pp. 283-293, (2010).

88. F. A. Finnerty Jr, "Advantages and disadvantages of furosemide in the edematous states of pregnancy", *American journal of obstetrics and gynecology*, Vol. 105, no.7, pp. 1022-1027, (1969).

89. G. M. Pacifici, "Clinical pharmacology of the loop diuretics furosemide and bumetanide in neonates and infants", *Pediatric Drugs*, Vol. 14, no. 4, pp.233-246, (2012).

90. R. Lombardi, A. Ferreiro, and C. Servetto, "Renal function after cardiac surgery: adverse effect of furosemide", *Renal failure*, Vol. 25, no. 5, pp.775-786, (2003).

91. P. S. Eid, D. A. Ibrahim, A. H. Zayan, M. M. Abd Elrahman, M. A. A. Shehata, H. Kandil, N. T. Huy, "Comparative effects of furosemide and other diuretics in the treatment of heart failure: a systematic review and combined meta-analysis of randomized controlled trials", *Heart Failure Reviews*, pp. 1-10, (2020).

92. S. Herrmann, New Synthetic Routes to Polyoxometalate Containing Ionic Liquids-An Investigation of their Properties, 1st ed., Springer Fachmedien Wiesbaden, Germany, p. 6, (2015).

93. M. T. Pope, Heteropoly and Isopoly Oxometalates,1st ed, Springer-Verlag Berlin, Heidelberg, pp.1-2, (1983).

94. N. I. Gumerova and A. Rompel, "Synthesis, structures, and applications of electron-rich polyoxometalates", *Nature Reviews Chemistry*, Vol. 2, no. 2, pp. 1-20, (2018).

95. R. V. Eldik and L.Cronin, Advances in Inorganic Chemistry 69, Polyoxometalate Chemistry-Academic Press , First edition, Elsevier Inc, pp. 2-3, (2017).

96. D-L. Long, E. Burkholder and L. Cronin, "Polyoxometalate clusters, nanostructures and materials: From self-assembly to designer materials and devices", *Chem. Soc. Rev*, Vol. 36, pp. 105-121, (2007).

97. H. Zhang, L. Y. Guo, J. Jiao, X. Xin, D. Sun, and S. Yuan, "Ionic self-assembly of polyoxometalate–dopamine hybrid nanoflowers with excellent catalytic activity for dyes", *ACS Sustainable Chemistry & Engineering*, Vol. 5, no. 2, pp. 1358-1367, (2017).

98. C. Sanchez, G. D. A. Soler-Illia, F. Ribot, T. Lalot, C. R. Mayer, and V.Cabuil, "Designed hybrid organic− inorganic nanocomposites from functional nanobuilding blocks", Chemistry of Materials, Vol. 13, no. 10, pp. 3061-3083, (2001).

99. C. P. Pradeep, D. L.Long, G. N. Newton, Y. F. Song, and L.Cronin, "Supramolecular metal oxides: programmed hierarchical assembly of a protein-sized 21 kDa [(C16H36N) 19 {H2NC (CH2O) 3P2V3W15O59} 4] 5− polyoxometalate assembly", Angewandte Chemie, Vol. 120, no.23, pp. 4460-4463, (2008).

100. S. F. Pirdosti, R. Khoshnavazi, and E. Naseri, "Solid-state rearrangement of sandwich-type polyoxometalate-dopamine nanohybrid to the nanoflower Keggin polyoxometalate: synthesis, characterization, and catalytic efficiency", *Journal of Coordination Chemistry*, Vol. 73, no. 5, pp. 723-736, (2020).

101. R. J. Hickey, A. S. Haynes, J. M. Kikkawa, and S. J. Park,"Controlling the self-assembly structure of magnetic nanoparticles and amphiphilic block-copolymers: from micelles to vesicles", *Journal of the American Chemical Society*, Vol. 133, no. 5, pp. 1517-1525, (2011).

102. M. Husein, "Preparation of nanoscale organosols and hydrosols via the phase transfer route", *Journal of Nanoparticle Research*, Vol. 19, no. 12, PP. 405, (2017).

103. Y. Huang, X. Ran, Y. Lin, J. Ren, X. Qu, "Self-assembly of an organic–inorganic hybrid nanoflower as an efficient biomimetic catalyst for self-activated tandem reactions", *Chemical Communications*, Vol. 51, no. 21, pp. 4386-4389, (2015).

104. G. M. Whitesides, and B. Grzybowski, "Self-assembly at all scales", *Science*, Vol. 295, no. 5564, pp.2418-2421, (2002).

105. G. R. Desiraju, Crystal Engineering: The Design of Organic Solids Elsevier, New York, (1989).

106. N. Ban, P. Nissen, J. Hansen, P. B. Moore, and T. A. Steitz, "The complete atomic structure of the large ribosomal subunit at 2.4 Å resolution", *Science*, Vol. 289, no. 5481, pp. 905-920, (2000).

107. S. I. Stupp, J. D. Hartgerink, and E. Beniash, "Self-assembly and mineralization of peptide-amphiphile nanofibers", *Northwestern University (Evanston, IL)* , no. 7,838,491, (2010).

108. O. D. Lavrentovich, " Transport of particles in liquid crystals", *Soft Matter*, Vol. 10, no. 9, pp.1264-1283, (2014).

109. T. D. Clark, J. Tien, D. C. Duffy, K. E. Paul, and G. M. Whitesides, "Self-assembly of 10-μm-sized objects into ordered three-dimensional arrays", *Journal of the American Chemical Society*, Vol. 123, no. 31, pp. 7677-7682, (2001).

110. A. L. Morais, P. Rijo, B. Hernán, M. Nicolai, "Biomolecules and Electrochemical Tools in Chronic Non-Communicable Disease Surveillance: A Systematic Review", *Biosensors*, Vol. 10, no.9, pp. 121, (2020).

111. N. Xiao, and B. J. Venton, "Rapid, "sensitive detection of neurotransmitters at microelectrodes modified with self-assembled SWCNT forests", *Analytical chemistry*, Vol. 84, no.18, pp. 7, (2012).

112. L. Zhang, J. Wu, Y. Wang, Y. Long, N. Zhao, and J. Xu, "Combination of bioinspiration: a general route to superhydrophobic particles", *Journal of the American Chemical Society*, Vol.134, no. 24, pp. 9879-9881, (2012).

113. H. Zhang, L. Y. Guo, J. Jiao, X. Xin, D. Sun, and S. Yuan, "Ionic self-assembly of polyoxometalate–dopamine hybrid nanoflowers with excellent catalytic activity for dyes", *ACS Sustainable Chemistry & Engineering*, Vol. 5, no. 2, pp. 1358-1367, (2017).

114. R. Dong, Y. Zhou, X. Huang, X. Zhu, Y. Lu, and J. Shen, "Functional supramolecular polymers for biomedical applications", *Advanced Materials*, Vol. 27, no.3, pp. 498-526, (2015).

115. W. S. Smith, G. Sung, S. Starkman, J. L. Saver, C. S. Kidwell, Y. P. Gobin, and M. P. Marks, "Safety and efficacy of mechanical embolectomy in acute ischemic stroke: results of the MERCI trial", *Stroke*, Vol. 36, no. 7, pp. 1432-1438, (2005).

116. X. López, J. J. Carbó, C. Bo, and J. M. Poblet, "Structure, properties and reactivity of polyoxometalates: a theoretical perspective", *Chemical Society Reviews*, Vol. 41, no. 22, pp. 7537-7571, (2012).

117. S. A. Qureshi, and I. J. McGilveray, "Assessment of pharmaceutical quality of furosemide tablets from multinational markets", *Drug development and industrial pharmacy*, Vol. 24, no. 11, pp. 995-1005, (1998).

118. E. Taghizadeh Davoudi, M. Ibrahim Noordin, A. Kadivar, B. Kamalidehghan, A. S. H. Farjam, Akbari Javar, "Preparation and characterization of a gastric floating dosage form of capecitabine", *BioMed research international*, Vol. *2013*, (2013).

119. N. I. Hammadi, Y. Abba, M. N. M. Hezmee, I. S. A. Razak, A. Z. Jaji, T. Isa, and M. Z. A. B. Zakaria, "Formulation of a sustained release docetaxel loaded cockle shell-derived calcium carbonate nanoparticles against breast cancer", *Pharmaceutical research*, Vol. 34, no. 6, pp. 1193-1203, (2017).

120. S. A. Khan, S. Rehman, B. Nabi, A. Iqubal, N. Nehal, U. A. Fahmy, S. Kotta, S. Baboota, S. Md and J. Ali, "Boosting the Brain Delivery of Atazanavir through Nanostructured Lipid Carrier-Based Approach for Mitigating NeuroAIDS", *Pharmaceutics*, Vol. 12, no. 1059, pp. 1-26, (2020).

121. C. Domingo, and J. Saurina, "An overview of the analytical characterization of nanostructured drug delivery systems: Towards green and sustainable pharmaceuticals: A review", *Analytica chimica acta*, Vol. 744, pp. 8-22, (2012).

122. M. Mohammadian, T. S. J. Kashi, M. Erfan, and F. P. Soorbaghi, "Synthesis and characterization of silica aerogel as a promising drug carrier system", *Journal of Drug Delivery Science and Technology*, Vol. 44, pp. 205-212, (2018).

123. H.Zhang, L.Guo, Z. Xie, X. Xin, D.Sun, and S. Yuan, "Tunable aggregation-induced emission of polyoxometalates via amino acid-directed self-assembly and their application in detecting dopamine", *Langmuir*, Vol. 32, no.51, pp. 13736-13745, (2016).

124. H. Lee, S. M. Dellatore, W. M. Miller, and P. B. Messersmith, Mussel-inspired surface chemistry for multifunctional coatings. science, Vol. 318, no. 5849, pp. 426-430. (2007).

125. H. Zhang, L. Y. Guo, J.Jiao, X. Xin, D.Sun, and S.Yuan, "Ionic self-assembly of polyoxometalate–dopamine hybrid nanoflowers with excellent catalytic activity for dyes", *ACS Sustainable Chemistry & Engineering*, Vol. 5, no.2, pp. 1358-1367,(2017).

126. H. Li, Y. Jia, H. Peng, amd J. Li, "Recent developments in dopamine-based materials for cancer diagnosis and therapy", *Advances in colloid and interface science*, Vol. 252, pp.1-20,(2018).

127. A. Al-Yasari, H. F. Alesary, H. Alghurabi, M. M. M. A. Alali, L. M. Ahmed, and R. Alasadi, "METHOTREXATE pH-RESPONSIVE RELEASE FROM NANOSTRUCTURES OF DOPAMINE AND POLYOXOMETALATE", *Biochemical and Cellular Archives*, Vol. 19, no. 2, pp.3675-3680 (2019).

128. H. Li, Z. Xiong, X.Shi, F. Gao, H. Peng, and Y. Jia, "Controllable ionic self-assembl of polyoxometalate and melamine for synthesis of nanostructured Ag", *Colloids and Surfaces A: Physicochemical and Engineering Aspects*, Vol.623, pp. 126732, (2021).

129. S. F. Pirdosti, R. Khoshnavazi, and E. Naseri, "Solid-state rearrangement of sandwich-type polyoxometalate-dopamine nanohybrid to the nanoflower Keggin polyoxometalate: synthesis, characterization, and catalytic efficiency", *Journal of Coordination Chemistry*, Vol. 73, no. 5, pp. 723-736, (2020).

130. Y. Huang, Y. Yan, B. M. Smarsly, Z. Wei, and C. F. Faul, Helical supramolecular aggregates, mesoscopic organisation and nanofibers of a perylenebisimide–chiral surfactant complex via ionic self-assembly. Journal of Materials Chemistry, 19(16), 2356-2362,(2009).

131. K. Liu, R. Xing, C. Chen, G. Shen, L.Yan, Q. Zou, G. Ma, H. Möhwald, X. Yan, "Peptide-Induced Hierarchical Long-Range Order and Photocatalytic Activity of Porphyrin Assemblies", *Angew. Chem. Int. Edit*, Vol.127, pp.510-515, (2015).

132. S. Kuśnieruk, J. Wojnarowicz, A. Chodara, T. Chudoba, S. Gierlotka, and W. Lojkowski, "Influence of hydrothermal synthesis parameters on the properties of hydroxyapatite nanoparticles", *Beilstein journal of nanotechnology*, Vol. 7, no.1, pp. 1586-1601, (2016).

133. N. Xiao, and B. J. Venton, "Rapid, "sensitive detection of neurotransmitters at microelectrodes modified with self-assembled SWCNT forests", *Analytical chemistry*, Vol. 84, no.18, pp. 7, (2012).

134. L. Zhang, J. Wu, Y. Wang, Y. Long, N. Zhao, and J. Xu, "Combination of bioinspiration: a general route to superhydrophobic particles", *Journal of the American Chemical Society*, Vol.134, no. 24, pp. 9879-9881, (2012).

135. H. Zhang, L. Y. Guo, J. Jiao, X. Xin, D. Sun, and S. Yuan, "Ionic self-assembly of polyoxometalate–dopamine hybrid nanoflowers with excellent catalytic activity for dyes", *ACS Sustainable Chemistry & Engineering*, Vol. 5, no. 2, pp. 1358-1367, (2017).

136. S. M. Kang, S. Park, D. Kim, S. Y. Park, R. S. Ruoff, and H. Lee, "Simultaneous reduction and surface functionalization of graphene oxide by mussel-inspired chemistry", *Advanced Functional Materials*, Vol. 21, no. 1, pp. 108-112, (2011).

137. K. Moothi, S. G. Nyembe, S. P. Malinga, "Zinc oxide nanostructures with carbon nanotube and gold additives for co gas sensing application", Msc thesis, (2019).

138. S. Govender, V. Pillay, D. J. Chetty, S. Y. Essack, C. M. Dangor, T. Govender, "Optimisation and characterisation of bioadhesive controlled release tetracycline microspheres", *International journal of pharmaceutics*, Vol. 306, no. 1-2, pp. 24-40, (2005).

139. Y. C. Hacene, A. Singh, and G. Van den Mooter, "Drug loaded and ethylcellulose coated mesoporous silica for controlled drug release prepared using a pilot scale fluid bed system", *International journal of pharmaceutics*, Vol. 506, no. 1-2, pp. 138-147, (2016).

140. Z. Sh. M. Ali, “Preparation of Nanocompounds from some antibiotics and studying their inhibitory effect on some microorganisms”, Msc thesis, (2007).

141. M. Kooti and M. Afshari, " Phosphotungstic acid supported on magnetic nanoparticles as an efficient reusable catalyst for epoxidation of alkenes", *Materials Research Bulletin*, Vol .47, no. 11, pp. 3473-3478, (2012).

142. X. Yan, P. Mei, J. Lei, Y. Mi, L. Xiong, and L. Guo," Synthesis and characterization of mesoporous phosphotungstic acid/TiO2 nanocomposite as a novel oxidative desulfurization catalyst", *Journal of Molecular Catalysis A: Chemical*, vol. 30, no. 1-2, pp. 52-57, (2009).

143. L. Pérez-Maqueda, and E. Matijević, "Preparation of uniform colloidal particles of salts of tungstophosphoric acid", *Chemistry of materials*, vol.10, no. 5, pp. 1430-1435, (1998).

144. Y. Ogasawara, S. Uchida, T. Maruichi, R. Ishikawa, N. Shibata, Y. Ikuhara, and N. Mizuno, "Cubic cesium hydrogen silicododecatungstate with anisotropic morphology and polyoxometalate vacancies exhibiting selective water sorption and cation-exchange properties", *Chemistry of Materials*, vol. 25, no. 6, pp. 905-911, (2013).

145. N. Goud, S. Gangavaram, K. Suresh, S. Pal, S. Manjunatha, S. Nambiar, and A. Nangia, "Novel furosemide cocrystals and selection of high solubility drug forms", *Journal of pharmaceutical* sciences", vol. 101, no. 2, pp.664-680, (2021).

146. G. Chaulang, P. Patel, S. Hardikar, M. Kelkar, A. Bhosale, and S. Bhise, " Formulation and evaluation of solid dispersions of furosemide in sodium starch glycolate", *Tropical Journal of Pharmaceutical Research*, vol.8, no. 1,pp. 43-51, (2009).

147. S. Sun, P. Liu, F. Shao, and Q. Miao, "Formulation and evaluation of PLGA nanoparticles loaded capecitabine for prostate cancer", *International journal of clinical and experimental medicine*, vol. 8, no.10, pp.19670, (2015).

148. A. Kousalya, S. Carbon-based nanostructured surfaces for enhanced phase-change cooling (Doctoral dissertation, Purdue University), (2014).

149. Z. Lin, "Evaporative self-assembly of ordered complex structures", *World Scientific*, British, 2012.

150. S. Wu, X. Liu, K. Yeung, C. Liu, and X. Yang, "Biomimetic porous scaffolds for bone tissue engineering", *Materials Science and Engineering: R: Reports*, vol. 80, pp. 1-36, (2014).

151. X. Yan, P. Zhu, J. Fei, and J. Li, "Self-assembly of peptide-inorganic hybrid spheres for adaptive encapsulation of guests", *Advanced Materials*, vol.22, no. 11, pp.1283-1287, (2010).

152. Y. Jia, Q. Li, and J. Li, "Assembly and application of diphenylalanine dipeptide nanostructures", *Chinese Science Bulletin*, vol.62, no. 6, pp. 469-477, (2017).

153. Y. Zhang, B. Yang, X. Zhang, L. Xu, L. Tao, S. Li, and Y. Wei, "A magnetic self-healing hydrogel", *Chemical Communications*, vol. 48, no. 74, pp.9305-9307, (2012).

154. Y. Yin, and A. Yin, "Colloidal nanocrystal synthesis and the organic–inorganic interface. Nature", vol. 437, no. 7059, pp. 664-670, (2005).

155. C. Altavilla, and E. Ciliberto, "Inorganic nanoparticles: synthesis, applications, and perspectives", *CRC Press*, (2017).

156. C. Burda, X. Chen, R. Narayanan, and M. El-Sayed, "Chemistry and properties of nanocrystals of different shapes", *Chemical reviews*, vol.105, no. 4, pp. 1025-1102, (2005).

157. W. Bu, H. Li, H. Sun, S. Yin, and L. Wu, "Polyoxometalate-based vesicle and its honeycomb architectures on solid surfaces", *Journal of the American Chemical Society*, vol.127, no. 22, pp. 8016-8017, (2005).

158. R. Penn, "Kinetics of oriented aggregation", *The Journal of Physical Chemistry B*, vol.108, no. 34, pp. 12707-12712, (2004).

159. L. Zhong, J. Hu, H. Liang, A. Cao, W. Song, and L. Wan, "Self-Assembled 3D flowerlike iron oxide nanostructures and their application in water treatment.", *Advanced Materials*, vol.18, no. 18, pp.2426-2431, (2006).

160. A. R. D. Silva, M. E. D. Zaniquelli, M. O. Baratti, and R. A. Jorge, "Drug release from microspheres and nanospheres of poly (lactide-co-glycolide) without sphere separation from the release medium", *Journal Of The Brazilian Chemical Society*, vol. 21, no. 2, pp. 214-225, (2010).

161. S. Q. Liu, S. W. Wu, M. R. Gao, M. S. Li, X. Z. Fu, and J. L. Luo, "Hollow porous Ag spherical catalysts for highly efficient and selective electrocatalytic reduction of CO2 to CO", *ACS Sustainable Chemistry & Engineering*, vol. 7, no. 17, pp.14443-14450, (2019).

162. M. Bilal, M. Asgher, S. Z. H. Shah, and H. M. Iqbal, "Engineering enzyme-coupled hybrid nanoflowers: The quest for optimum performance to meet biocatalytic challenges and opportunities", *International journal of biological macromolecules*, vol. 135, pp. 677-690, (2019).

163. Z. Cui, C. Liu, T. Lu, and W. Xing, "Polyelectrolyte complexes of chitosan and phosphotungstic acid as proton-conducting membranes for direct methanol fuel cells", *Journal of Power Sources*, vol. 167, no. 1, pp. 94-99, (2007).

164. U. S. Rao, K. V. Sekharnath, H. Sudhakar, K. C. Rao, and M. C. Subha, "Mixed Matrix Membranes Of Sodium Alginate And Hydroxy Propyl Cellulose Loaded With Phosphotungstic Heteropolyacid For The Pervaporation Separation Of Water–Isopropanol Mixtures At 30 0 C", *International Journal Of Scientific & Technology Research*, vol. 3, pp.129-137, (2014).

165. I. M. Khalid, S. E. Abu Sharkh, H. Samamarh, R. Alfaqeeh, M. M. Abuteir, and S. M. Darwish, "Spectroscopic Characterization of the Interaction between Dopamine and Human Serum Albumin", (2019).

166. C. V. Durgadas, C. P. Sharma, and K. Sreenivasan, "Fluorescent and superparamagnetic hybrid quantum clusters for magnetic separation and imaging of cancer cells from blood", *Nanoscale*, vol. 3, no. 11, pp. 4780-4787, (2011).

167. H. K. Daima, P. R. Selvakannan, A. E. Kandjani, R. Shukla, S. K. Bhargava, and V. Bansal, "Synergistic influence of polyoxometalate surface corona towards enhancing the antibacterial performance of tyrosine-capped Ag nanoparticles", *Nanoscale*, vol. 6, no. 2, pp. 758-765, (2011).

168. A. Sanyal, S. Mandal, and M. Sastry, "Synthesis and assembly of gold nanoparticles in quasi-linear Lysine–Keggin-ion colloidal particles", *Advanced functional materials*, vol. 15, no. 2, pp. 273-280, (2005).

169. J. F. Alopaeus, E. Hagesæther, and I. Tho, "Micellisation mechanism and behaviour of Soluplus®–furosemide micelles: preformulation studies of an oral nanocarrier-based system", *Pharmaceuticals*, vol. 12, no. 1, pp. 15, (2019).

170. L. Perioli, V. Ambrogi, M. Nocchetti, M. Sisani, and C. Pagano, "Preformulation studies on host–guest composites for oral administration of BCS class IV drugs: HTlc and furosemide", *Applied clay science*, vol. 53, no.4, pp. 696-703, (2011).

171. A. Kovács, B. Démuth, A. Meskó, and R. Zelkó, " Preformulation studies of furosemide-loaded electrospun nanofibrous systems for buccal administration", *Polymers*, vol. 9, no. 12, pp. 643, (2017).

172. G. Z. Papageorgiou, S. Papadimitriou, E. Karavas, E. Georgarakis, A. Docoslis, and D. Bikiaris, " Improvement in chemical and physical stability of fluvastatin drug through hydrogen bonding interactions with different polymer matrices", *Current drug delivery*, vol. 6, no. 1, pp. 101-112,(2009).

173. P. Kathiravan, and V. Pandey, "Selection of excipients for polymer coated capsule of Capecitabine through drug-excipient compatability testing", *International Journal of PharmTech Research,* vol. 6, no. 5, pp.1633-1639, (2014).

174. S. Tan, A. Ebrahimi, and T. Langrish, "Controlled release of caffeine from tablets of spray-dried casein gels", *Food Hydrocolloids,* vol. 88, pp. 13-20, (2019).

175. S. Tan, A. Ebrahimi, and T. Langrish, "Smart release-control of microencapsulated ingredients from milk protein tablets using spray drying and heating" , *Food Hydrocolloids*, vol. 92, pp. 181-188, (2019).

176. Z. Sh. M. Ali, “Preparation of Nanocompounds from some antibiotics and studying their inhibitory effect on some microorganisms”, Msc thesis, (2007).

الخلاصة

تكون هذا العمل من ثلاثة اجزاء عملية. يهتم الجزء الأول بتشكيل الهياكل النانوية ثلاثية الأبعاد عبر إستراتيجية بسيطة ومتعددة الاستخدامات للتجميع الذاتي لمركبين (حامض الفوسفوتنكستن و الدوبامين) بهياة هجين عضوي ـغير عضوي , والتي يمكن التحكم في شكلها و حجمها عن طريق تغير نسبة المكونين المتفاعلين , حامظية الوسط , وتغير تركيز المحلول المنظم الترس اميناوميثان , وايضا طريقة التنوية ومدتها. تم استخدام المجهر الالكتروني الماسح لتشخيص البنية النانوية المذكورة اعلاه، وكان الشكل عبارة عن هياكل نانوية هرمية شبيهة بالزهور. وأيضًا من خلال استخدام تحليل حيود الاشعة السينية تم تم التأكيد على أن الأبعاد ضمن المقياس النانوي ، وعن طريق تشخيص طيف الاشعة تحت الحمراء تم التاكد من حدوث الارتباط بين الدوبامين و حامض الفوسفو تنكستن.

الجزء الثاني يتعامل مع الهياكل النانوية الهرمية المعدة لتحميل دوائين (الفوروسيميد والكابسيتابين) ، وقد تم تحديد كمية الأدوية المحملة في البنية النانوية من خلال استخدام التحليل الطيفي للأشعة المرئية / فوق البنفسجية, حيث تم تحميل كلا الدوائين على سطحه خلال فترات وتم حساب كمية الدواء المحملة خلال فترات زمنية مختلفة هي (2 , 4 , 6 , 8 , 10 , 12) ساعة وكانت نسب تحميل الفيروسمايد تساوي 8٪ ، 21٪ ، 25٪ ، 31٪ ، 58٪ على التوالي . بينما الكابسيتابين تساوي 3٪ ، 10٪ ، 31٪ ، 39٪ ، 64٪ على التوالي.

درس الجزء الثالث عملية إطلاق العقارين من الهياكل النانوية الهرمية إلى محلولين منظمين باستخدام درجة حموضة مختلفة عند درجة حموضة 7.4 لمحلول الفوسفات بفر سيلان و 2.8 لمحلول المنظم الكلاسين،وتم التحقق من نجاح عملية الإطلاق باستخدام التحليل الطيفي للأشعة المرئية/ فوق البنفسجية، كما اظهرت البنية النانوية المعدة الشبيه بالزهورالمحملة بالفيروسمايد سلوك إطلاق واعد يعتمد على الأس الهيدروجيني، مما يشير إلى أن البنية النانوية هي مرشح جيد للإيصال الفموي للفوروسيميد. أظهر سلوك الإطلاق للبنية النانوية الشبيهة بالزهور المحملة بالفوروسيميد عند درجة الحموضة 7.4 صورة إطلاق أعلى من الرقم الهيدروجيني 2.8. في حين أن البنية النانوية المحملة بالكابسيتابين اظهرت صورة تحرر متقاربة في كلا الوسطين. وعليه أظهرت الهياكل النانوية سلوك إطلاق مثير للفضول يعتمد على الأس الهيدروجيني، مما يجعلها واعدة للتطبيقات في العلوم الطبية الحيوية. تم دراسة حركية تفاعل تحررکلا الدوائين من البنية النانوية الهرمية الشبيهة بالزهور في كلا المحلولين المنظمين ووجد انها تخضع الى الرتبة الاولى الكاذبة .

جمهورية العراق
وزارة التعليم العالي والبحث العلمي
جامعة كربلاء-كلية العلوم-قسم الكيمياء

تحضير و تشخيص المركبات النانوية الهجينة من البولي اوكسوموليت(POM) والدوبامين كأنظمة توصيل دوائية

رسالة مقدمة الى
مجلس كلية العلوم- جامعة كربلاء
كجزء من استكمال متطلبات نيل درجة الماجستير في علوم الكيمياء

تقدمت بها
سجى محمد حسين علي
بكلوريوس علوم كيمياء (2016) / جامعة كربلاء

بأشراف
أ.د.لمى مجيد احمد
م.د. مقدام مهدي محمد علي

2021م 1442هـ